FINAL REPORT

for

U.S. Department of Energy

Plutonium Chemistry in the UREX+ Separation Processes

Principal Investigator: Alena Paulenova
Institution: Oregon State University

Collaborators: George F. Vandegrift, III, Argonne National Laboratory
Kenneth R. Czerwinski, University of Nevada, Las Vegas

PROJECT TITLE: PLUTONIUM CHEMISTRY IN THE UREX+ SEPARATION PROCESSES

AWARD NUMBER: **DE-FC07-05ID14652**
AWARDEE NAME: **Oregon State University**
Period covered: **April 10/2005 – April 10/2009**
Report: **Final Report**

PRINCIPAL INVESTIGATORS: **Alena PAULENOVA**
Radiation Center, Oregon State University
Corvallis, OR 97331
Phone: (541) 737-70707, Fax: (541) 737-0480
E-mail: paulenoa@engr.orst.edu
Congressional District: 5th

COLLABORATORS:

George F. Vandegrift, III
Argonne National Laboratory
Chemical Engineering Division
9700 South Cass Avenue
Argonne, IL 60439
Phone: 630-252-4513; Fax: 630-252-4771
E-mail: vandegrift@cmt.anl.gov
Congressional District: 13th

Kenneth R. Czerwinski
Department of Chemistry
University of Nevada, Las Vegas
4505 Maryland Parkway, Box 454003
Las Vegas, Nevada 89154-4003
Phone: (541) 737-70707, Fax: (541) 737-0480
E-mail: czerwin@unlv.nevada.edu
Congressional District: 1st

PROJECT OBJECTIVES

The project "Plutonium Chemistry in the UREX+ Separation Processes" is led by Dr. Alena Paulenova of Oregon State University under collaboration with Dr. George Vandegrift of ANL and Dr. Ken Czerwinski of the University of Nevada at Las Vegas. The objective of the project is to examine the chemical speciation of plutonium in UREX+ (uranium/tributylphosphate) extraction processes for advanced fuel technology. Researchers will analyze the change in speciation using existing thermodynamics and kinetic computer codes to examine the speciation of plutonium in aqueous and organic phases. They will examine the different oxidation states of plutonium to find the relative distribution between the aqueous and organic phases under various conditions such as different concentrations of nitric acid, total nitrates, or actinide ions. They will also utilize techniques such as X-ray absorbance spectroscopy and small-angle neutron scattering for determining plutonium and uranium speciation in all separation stages. The project started in April 2005 and is scheduled for completion in March 2008.

Contents

Captions to Figures

Figure 1.1 Structure of acetohydroxamic acid

Figure 1.2 Isomers of acetohydroxamic acid

Figure 1.3 Distribution ratios of acetohydroxamic acid by 30 % TBP in n-dodecane

Figure 1.4 FT-IR spectra for the hydroxyl band (A), and the carbonyl band (B) for 0.023, 0.030, 0.045, 0.068, 0.090 and 0.135 M AHA in 100% TBP

Figure 2.1 Degradation of AHA in 2.5 M HNO_3 or $HClO_4$ as a function of the initial AHA concentration and time: $[AHA]_{initial}$ = 0.35-2.5 mM

Figure 2.2 Degradation of AHA as a function of the mineral acid concentration and time: $[AHA]_{initial} = 2.5\times10^{-3}$M

Figure 2.3 A half-life of AHA (T½, min) measured as temperature dependence for 2.5×10^{-3}M AHA

Figure 2.4 The Arrenius plot of the rate constant measured for AHA in three nitric acid concentrations (1.5; 2 and 2.5M) at three temperatures.

Figure 3.1 Extraction of uranium from nitric acid with and without presence of AHA and $LiNO_3$. Concentration of U(VI): A= 0.043 M, B = 0.176 M

Figure 3.2 UV-VIS spectra of uranium(VI)-AHA complexes in aqueous solutions of nitric acid.

Figure 3.3 Oscilation oxidation-reduction reaction of U(VI) and U(IV) in TBP

Figure 3.4 Uranium solids containing acetohydroxamic acid produced at low nitric acid concentration

Figure 3.5 Spectra of uranium in organic phases: A: UN in TBP, B: UN-AHA -TBP complex prepared by combination of UN and AHA in TBP, C: Extraction organic phase agitated for

several days. Initial concentrations in aqueous phase: 0.2 M UN; 0.1 M HNO_3 and 0.7 M AHA. Inset: Spectrum of AHA in 30% TBP/n-dodecane.

Figure 3.6 Absorbance of uranium-AHA complex in TBP at 485 nm as a function of molar fraction of acetohydroxamic acid.

Figure 3.7 The FT-IR spectra of the 0.0675M AHA solution in TBP (spectrum 1) and the 0.0675M AHA and 0.045M $UO_2(NO_3)_2$ in TBP (spectrum 2): region of hydroxyl band of AHA (A); region of carbonyl band of AHA (B).

Figure 3.8 The FT-IR spectra of the organic extraction phase (D) of 30% TBP equilibrated with the $UO_2(NO_3)_2$/AHA/HNO_3 aqueous phase, compared with the spectra of 30% TBP (A); 0.1M AHA in 30%TBP (B); 0.045M $UO_2(NO_3)_2$ in 30% TBP (C).

Figure 3.9 The proposed structure of the solvated complex of $UO_2(AHA)(NO_3).2TBP$

Figure 4.1 Distribution ratio of Pu(IV) from various range of nitric acid and $LiNO_3$: (■) 0.1-12M HNO_3; (●) 1M $LiNO_3$ and 0.1-12M HNO_3; (▲) data from ref. [Petrich & Kolarik, 1998]; (+) data from ref [Karraker 2002].

Figure 4.2 Distribution ratio of Pu(IV) from HNO_3 and various addition of nitrate in the absence (open symbols) and presence (full symbols) of acetohydroxamic acid (0.4M) and addition of $LiNO_3$. HNO_3 concentration: (●○) 0.5M; (■□) 1M; (▲△) 2M; (◆) data from ref. [Karraker 2002], 0.5M HNO_3, addition of $NaNO_3$ and 0.3M HAHA

Figure 4.3 Distribution ratio of Pu(IV) from various range of nitric acid in the presence of HAHA (●) 0.1-6M HNO_3 + 0.4M HAHA; (▲) data from ref. [Carrott et al., 2007], 0.5M HAHA; (●) data from ref. [Karraker 2002] 0.1M HAHA; (▲) data from ref. [Karraker 2002], 0.3M HAHA.

Figure 4.4 Distribution ratio of Pu(IV) from 1M HNO_3 and various concentration of acetohydroxamic acid: (●) 8×10^{-4} - 8.8×10^{-1} M HAHA; (▲) data from ref. [Carrott et al., 2007], 0.05-2M HAHA;(◆) no AHA.

Figure 4.5 The effect of agitation on the distribution of plutonium at 294 K: (♦) 7*M* HNO_3; (■) 1*M* HNO_3; (▲) 0.1*M* HNO_3.

Figure 4.6 The distribution of plutonium at various temperatures for a system containing nitric acid: T = (♦) 294 K; (■) 303 K; (▲) 313 K.

Figure 4.7 Van't Hoff plots for systems containing (▲) nitric acid: slope = 6.99, y-intercept = -13.6; (●) 2*M* HNO3 + LiNO3: slope = 7.56, y-intercept = -15.4; (line) average linear regression.

Figure 4.8 The equilibrium constants at various temperatures calculated by Eq. (11) for a system containing 2*M* HNO_3 and $LiNO_3$. Values for $\ln K_{ex}^{0}(T)$ were found at the extrapolated point $[NO_3^-] = 0M$. T = (♦) 294 K; (●) 303 K; (▲) 313 K.

Figure 5.1 The speciation distribution diagram of Pu(IV) in aqueous solution containing: a) (0.1 to 2) mol·L^{-1} HNO_3, b) 1 mol·L^{-1} $LiNO_3$ and various HNO_3 concentration. – ·· – Pu^{4+}; – – – $Pu(OH)^{3+}$; ····· $Pu(OH)_2^{2+}$; —— $Pu(NO_3)^{3+}$; ── $Pu(NO_3)_2^{2+}$.

Figure 5.2 Plot of experimental vs. calculated data for Pu(IV) distribution ratio determined using Equation 13 and a value of $K_1=1.77\times10^5$. The line represents theoretical correlation between experimental and calculated data. (◆) 0.2 to 4 mol·L^{-1} HNO_3; (▲) 0.5 mol·L^{-1} HNO_3, various $LiNO_3$; (■) 1 mol·L^{-1} HNO_3, various $LiNO_3$; (+) 2 mol·L^{-1} HNO_3, various $LiNO_3$; (●) 1 mol·L^{-1} $LiNO_3$, various HNO_3; (○) 0.2 to 4.2 mol·L^{-1} HNO_3, [Petrich & Kolarik, 1981]; (□) 0.5 to 4 mol·L^{-1} HNO_3, [Karraker, 2001].

Figure 5.3 Plot of experimental vs. calculated data for Pu(IV) distribution ratio determined using Equation 15 and values of $K_1=1.06\times10^5$ and $K_2=2.12\times10^4$. The line represents theoretical correlation between experimental and calculated data. (◆) 0.2 to 4 mol·L^{-1} HNO_3; (▲) 0.5 mol·L^{-1} HNO_3, various $LiNO_3$; (■) 1 mol·L^{-1} HNO_3, various $LiNO_3$; (+) 2 mol·L^{-1} HNO_3, various $LiNO_3$; (●) 1 mol·L^{-1} $LiNO_3$, various HNO_3; (○) 0.2 to 4.2 mol·L^{-1} HNO_3, [Petrich & Kolarik, 1981]; (□) 0.5 to 4 mol·L^{-1} HNO_3, [Karraker, 2001].

Abbreviations and Acronym List

A	frequency factor
A	absorbance
AHA/HAHA	Acetohydroxamic acid/protonated
AMUSE	Argonne Model for Universal Solvent Extraction
CCD-PEG	chlorinated cobalt dicarbollide-polyethylene glycol
D	distribution ratio
Ea	Activation energy
EXAFS	Extended X-ray Absorption Fine Structure
FHA	Formohydroxamic acid
FITEQL	a computer program for determination of chemical equilibrium constants from experimental data
FT-IR	Fourier Transformed Infrared Spectroscopy
Gy	Gray
h	Planck constant
HAN	hydroxylamine
HySS	Hyperquad simulation and speciation
ICP-OES	Inductively Coupled Plasma Atomic Emission Spectroscopy
IS	Ionic Strength
J	
k, K	
K_H	hydrolysis constant
LSC	liquid scintillation counting
NMR	Nuclear Magnetic Resonance
PUREX	Plutoniun and Uranium Recovery by Extraction
R	gas constant
SIT	Specific Ion Interaction Theory
SXLSQI	equilibrium modeling program
SX Solver	a computer program for analyzing solvent- extraction equilibria
T	absolute temperature
TALSPEAK	Trivalent Actinide - Lanthanide Separation by Phosphorous reagent Extraction from Aqueous Complexes
TRUEX	Trans Uranic Extraction process
TBP	tri-*n*-butyl phosphate
TTA	1-(2-thenoyl)-3,3,3-trifluoracetate
UN/UNH	Uranyl Nitrate/Uranyl Nitrate Hexahydrate
UREX	URanium Extraction
UV-Vis-NIR	Ultra Violet – Visible – Near Infrared Spectroscopy
z_{eff}	effective charge
ΔH	enthalpy
ΔS	entropy
β	stability constant
ε	interaction parameter
ε	molar absorptivity (extinction coefficient)
λ	wavelength, nm
{}	chemical activities
°C	Celsius

References

Abu-Dari K., Raymond K. N., 1980 Coordination chemistry of microbial iron transport compounds. 20. Crystal and molecular structures of two salts of cis- and trans-tris(benzohydroximato)chromate(III). *Inorg. Chem*. **19**, 2034-2040.

Alderighi L., Gans P., Ienco A., Peters D., Sabatini A., Vacca A. 1999 Hyperquad simulation and speciation (HySS): a utility program for the investigation of equilibria involving soluble and partially soluble species. *Coord. Chem. Rev.* **184**, 311–318. (http://www.hyperquad.co.uk/hyss.htm).

Allen P. G., Veirs D. K., Conradson S. D., Smith C. A., Marsh S. F. 1996 Characterization of aqueous plutonium(IV) nitrate complexes by extended X-ray absorption fine structure spectroscopy. *Inorg. Chem*. **35**, 2841-2845

Artemenko A. I., Tikunova I. V., Anufriev E. K., 1976 IR spectra of some O-acyl derivatives of hydroxamic acids *J. Appl. Spec*. **24** (3), 344-347.

Artemenko A. I., Anufriev E. K., Tikunova I. V., Eksner O., 1980 Tauterism of hydroxamic acids and their derivates. *J. Appl. Spec*. **33**, 758-761.

Baqawde S. V., Ramkrishna V. V., Patil S. K., 1976 Complexing of tetravalent plutonium in aqueous solutions. *J. Inorg. Nucl. Chem*. **38** 1339.

Barocas A., Baroncelli F., Biondi G. B., Grossi G., 1966 The complexing power of hydroxamic acids and its effect on behaviour of organic extractants in the reprocessing of irradiated fuels--II : The complexes between benzohydroxamic acid and thorium, uranium (IV) and plutonium (IV). *J. Inorg. Nucl. Chem*., **28(12)** 2961-2967.

Baroncelli F., Grossi G., 1965 The complexing power of hydroxamic acids and its effect on the behaviour of organic extractants in the reprocessing of irradiated fuels--I the complexes between benzohydroxamic acid and zirconium, iron (III) and uranium (VI) *J. Inorg. Nucl. Chem.*, **27**(5) 1085-1092

Berg J. M., Veirs D. K. Vaughn R. B., Cisneros M. A., Smith C. A., 1998 Plutonium(IV) mononitrate and dinitrate complex formation in acid solutions as a function of ionic strength. *J. Radioanal. Nucl. Chem.* **235** 25-29.

Berg J. M., Veirs D. K., Vaughn R. B., Cisneros M. R., Smith C. A., 2000 Speciation model selection by monte carlo analysis of optical absorption spectra: plutonium(IV) nitrate complexes. *Applied Spec*. **54** 812-823.

Berndt D. C., Sharp J. K., 1973 Reactivity of hydroxamic acids. Correlation with the twoparameter Taft equation. *J. Org. Chem*. **38**(2) 396- 397.

Berndt D. C., Ward I. E., 1974 Proximity Effects. Correlation of ortho-Substituted benzohydroxmic Acid reactivities. *J. Org. Chem*. **39**(6) 841-843.

Borkowski M., Ferraro J. R., Chiarizia R., McAlister D. R., 2002 FT-IR study of third phase formation in the U(VI) or Th(IV)/HNO3, TBP/alkane systems *Solvent Extr. Ion Exch*. **20**, 313-330.

Bromley L A., 1973 Thermodynamic properties of strong electrolytes in aqueous solutions. *AIChE J.* **19** 313-320.

Burger L. L., 1984 Physical Properties, in *Science and Technology of Tributyl Phosphate* vol. 1; W. W. Schulz and J. D. Navratil, Eds. (CRC Press: Boca Raton, FL, 1984), Chap. 3, p.26.

Carrott M. J., Fox O. D., Jones C. J., Mason C., Taylor R. J., Sinkov S. I., Choppin G. R., 2007 Solvent extraction behaviour of plutonium ions in the presence of simple hydroxamic acids. *Solv. Extr. Ion Exch*., **25**(6) 723-745.

Connors K.A., 1990 *Chemical Kinetics*. Chapter I-II, VCH Publishers, NY 1990.

Chaiko D. J., Vandegrift G. F., 1988 A thermodynamic model of nitric acid extraction by tri-n-butyl phosphate. *Nucl. Technol.* **82** 52-59.

Chiarizia R., Jensen M. P., Borkowski M., Ferraro J. R., Thiyagarajan P., Littrell K. C., 2003 Third Phase Revisited: the U(VI),HNO_3- TBP, *n*-Dodecane System *Solv. Extr. Ion Exch*. **21** 1-27.

Chiarizia R., Briand R., 2007 Third Phase Formation in the Extraction of Inorganic Acids by TBP in *n*-Octane. *Solv. Ex. Ion Exch*. **25** 351-371.

Choppin G. R., Rao L. F., 1984 Complexation of Pentavalent and Hexavalent Actinides by Fluoride. *Radiochim. Acta* **37** 143-146.

Cleveland J. M., 1968 Sulfamate complexes of plutonium(IV). *Inorg. Chem*. **7** 874-878.

Danesi P. R., Orlandini F., Scibona G., 1965 The Effect of Temperature on the Extraction of Nitric Acid, Uranyl, and Plutonium Nitrates by Long Chain Amines. *Radiochim. Acta*, **4** 9-12.

Danesi P.R., Orlandini F., Scibona G., 1966 Aqueous chemistry of actinide elements : Determination of the stability constant of nitrate, chloride and bromide complexes of Pu(IV). J. *Inorg. Nucl. Chem*. **28** 1047.

Ferraro J. R., Borkowski M., Chiarizia R., McAlister D. R., 2001 FT-IR spectroscopy of nitric acid in TBP/octane solution *Solv. Extr. Ion Exch*. **19**(6) 981-992.

Garcia B., Ibeas S., Leal J. M., Senent M. L., Nino A., Munoz-Caro C., 2000 Theoretical and Experimental Study of the Acetohydroxamic Acid Protonation: The Solvent Effect. *Chem. Eur. J*. **6** 2644-2652.

Gez S., Luxenhofer R., Levina A., Codd R., Lay P. A., 2005 Chromium(V) Complexes of Hydroxamic Acids: Formation, Structures, and Reactivities. *Inorg. Chem*. **44** 2934-2943.

Ghosh K. K., 1997 Kinetic and mechanistic aspects of acid-catalysed hydrolysis of hydroxamic acids. *Indian J. Chem.* **36B** 1089-1102.

Ghosh K. K., Patle S. K., Sharma P., Rajpur S. K., 2003 A comparison between the acid-catalysed reactions of some dihydroxamic acids, monohydroxamic acids and desferal. *Bull.Chem.Soc. Jpn*., **76** (2) 283-290.

Ghosh K. K., Vaidya J., Sinha D., 2004 *Zeitschrift fur Physikalische Chemie - Int. J. Res. In Phys. Chem. & Chem. Phys*. **218**(5), 563-573.

Grenthe I., Noren B., 1960 On the Stability of Nitrate and Chloride Complexes of Plutonium (IV). *Acta Chem. Scand.* **14** 2216.

Grenthe I., Puigdomènech I., 1997 *Modelling in aquatic chemistry*, OECD Nuclear Energy Agency Publication, France, Paris, 1997.

Guillaumont R., Fanghanel T., Fuger J., Grenthe I., Neck N., Palmer D. A., Rand M. H., 2003 (*OECD, NEA-TDB*). *Chemical thermodynamics vol.* 5. *Update on the chemical thermodynamics of uranium, neptunium, plutonium, americium and technetium.* Elsevier, North-Holland, Amsterdam, 2003.

Herbelin A. L., Westall J. C., 1999 *FITEQL 4.0: A computer program for determination of chemical equilibrium constants from experimental data*, Department of Chemistry, Oregon State University, Report 99-01, 1999.

Higgins F. S., Magliocco L. G., Colthup N. B., 2006 Infrared and Raman spectroscopy study of alkyl hydroxamic acid and alkyl hydroxamate isomers. *Appl. Spec*. **60**(3) 279-287.

Johnson G. L., Toth L. M. 1978 *Plutonium(IV) and Thorium(IV) Hydrous Polymer Chemistry* Report ORNUrM-6365, Oak Ridge National Laboratory, Tennessee.

Kang H. A., Engle N. L., Bonnesen P. V., Delmau L. H., Haverlock T. J., Moyer B. A., 2005 An equilibrium model of pseudo-hydroxide extraction in the separation of sodium hydroxide from aqueous solutions using lipophilic fluorinated alcohols and phenols. *Sep. Sci. Technol.* **40**(1-2) 725-738.

Karraker G., Rudisill T. S., Thompson M. C., 2001 *Studies of the Effect of Acetohydroxamic Acid on Distribution of Plutonium and Neptunium by 30 Vol % Tributyl Phosphate*, Westinghouse Savannah River Company, WSRC-TR-2001-00509.

Karraker G., 2002 *Radiation chemistry of acetohydroxamic acid in the UREX process*, Westinghouse Savannah River Company, WSRC-TR-2002-00283.

Kim J. I., Kanellakopulos B., 1989 Solubility products of plutonium(IV) oxide and hydroxide. *Radiochim. Acta* **48** 145-150.

Knopp R., Neck V., Kim J. I., 1999 Solubility, hydrolysis and colloid formation of plutonium(IV). *Radiochim. Acta* **86** 101-108.

Koide Y., Uchino M., Shosenji H., Yamada K., *Bull. Chem. Soc. Jap.*, 62 (1989) 3714

Kolarik Z., 1984 The Effect of Temperature on the Extraction of Plutonium(IV) Nitrate and Nitric Acid by 30 vol.% Tributyl Phosphate (TBP). *Solv. Ex. Ion Exch.* **2** 621-633.

Kraus K. A., Nelson F. Hydrolytic behavior of metal ions. I. The acid constants of uranium(IV) and plutonium(IV). *J. Am. Chem. Soc.* **1950**, *72*, 3901-3906.

Laximinarayanan T. S., Patil S. K., Scibona G., 1964 Stability constants of nitrate and sulphate complexes of plutonium(IV). *J. Inorg. Nucl. Chem*. **26** 1001.

Lahr H., Knock W., 1970 Bestimmung von Stabilitätskonstanten einiger Aktinidenkomplexe. II. Nitrat- und Chloridkomplexe von Uran, Neptunium, Plutonium und Americium. *Radiochim. Acta*. **13** 1.

Lemire R. J., Fuger J., Nitsche H., Potter P., Rand M. H., Rydberg J., Spahiu K., Sullivan J. C., Ullman W. J., Vitorge P., Wanner H., 2001 *(OECD, NEA-TDB). Chemical thermodynamics vol. 4. Chemical thermodynamics of neptunium and plutonium.* Elsevier, North-Holland, Amsterdam.

Lin-Vien D., Colthup N. B., Fately W. G., Grasselli J. G., 1991 *The handbook of Infrared and Raman Characteristic Frequencies of Organic Molecules*, Academic Press, New York.

Lumetta G. J., 2002 *The SX Solver*: *a computer program for analyzing solvent extraction equilibria: version 3.0*, PNNL-13760, Pacific Northwest National Laboratory, Richland, Washington.

Martell A. E., Smith R. M., 2001 *Critically Selected Stability Constants of Metal Complexes*, National Institute of Standards and Technology, Standard Reference Database 46 Version 6.0.

May I., Taylor R. J., Dennis I.S., Brown G., Wallwork A. L., Hill N. J., Rawson J. M., Less R., 1998 Neptunium(IV) and uranium(VI) complexation by hydroxamic acids**.** *J. All. Comp.* **275-277** 769-772

McKay H. A. C., 1956 *Tri-n-butyl Phosphate as an Extracting Agent for the Nitrates of the Actinide Elements*, Proceedings of the International Conference on the Peaceful Uses of Atomic Energy **7**, 314-317.

Marmion C. J., Nolan K. B., 2002 Hydroxamic Acids – Iron chelators, aspirin analogues, nitric oxide donors and structurally diverse metal complexes. ***The Irish Scientist*** 10 173.

Marmion C. J., Murphy T., Docherty J. R., Nolan K. B., 2000 Hydroxamic acids are nitric oxide donors. Facile formation of ruthenium(II)-nitrosyls and NO-mediated activation of guanylate cyclase by hydroxamic acids. ***Chem. Commun***. **13** 1153-1154.

Meloan C. E., Holkeboer P., Brandt W. W., 1960 Spectrophotometric determination of uranium with benzohydroxamic acid in 1-hexanol. *Anal. Chem.* **32** 791-793.

Metivier H., Guilaumont R., 1972 Hydrolyse du plutonium tetravalent. *Radiochem. Radioanal. Lett.* **10** 27-35.

Moiseenko E. I., Rozen A. M., 1960 Distribution of plutonium on extraction with tributyl phosphate. *Radiochem.* **2** 11-17.

Moskvin A. I., 1969 Complexing of the actinides with anions of acids in aqueous solutions. *Soviet Radiochem*. **11** 447.

Moskvin A. I., 1971 Complexing of neptunium(IV) and plutonium(IV) in nitrate solutions. Russ. *J. Inorg. Chem*. **16** 405.

Moskvin A. I., 1973 Thermodynamic characteristics of the formation of actinide ions in aqueous solutions. *Soviet Radiochem*. **15** 504.

Munson J. W., 1982 *Chemistry and biology of hydroxamic acids - an overview*", in *Chemistry and Biology of Hydroxamic Acids*, H. Kehl, Ed., Karger, New York, p. 1.

Musikas C., Condamines N., Cuillerdier C., 1991 Separation chemistry for the nuclear industry. *Anal. Sci*. **7** 11-16.

Naganawa H., Tachimori S., 1993 *Solvent extraction of nitric acid by tri-n-butyl phosphate in dodecane and hydration of the extracts*. *Solvent extraction in the process industries*, *vol. 3.*, Elsevier, London, 1538-1545.

Neck V., Kim J. I., 2001 Solubility and hydrolysis of tetravalent actinides. *Radiochim. Acta* **89** 1-16.

Neck V., Altmaier M., Fanghänel Th., 2006 Ion interaction (SIT) coefficients for the Th^{4+} ion and trace activity coefficients in $NaClO_4$, $NaNO_3$ and NaCI solution determined by solvent extraction with TBP. *Radiochim. Acta* **94** 501-507.

Nukada K., Naito K., Maeda U., 1960 Mechanism of the extraction of uranyl nitrate by tributyl phosphate. II. Infrared study. *Bull. Chem. Soc. Jap.* **33** 894-898.

Petrich G., Kolarik Z., 1981 *The 1981 Purex Distribution Data Index*; KfK: 3080; Kernforschungszentrum Karlsruhe.

Rabideau S. W., Lemons J. E., 1951 The Potential of the Pu(III)-Pu(IV) couple and the equilibrium constants for some complex ions of Pu(IV). *J. Am. Chem. Soc.* **73** 2895-2899.

Rabideau S. W. 1953 Equilibria and Reaction Rates in the Disproportionation of Pu(IV). *J. Am. Chem. Soc.* **75**(4) 798-801.

Rabideau S. W., 1957 The hydrolysis of plutonium(IV). *J. Am. Chem. Soc.* **79** 3675-3677.

Rabideau S., Kline R. J., 1960 A Spectrophotometric study of the hydrolysis of plutonium(IV). *J. Phys. Chem.* **64** 680-682.

Ramanujan A., Ramakrishna V. V., Patil S. K., 1978 The Effect of Temperature on the Extraction of Plutonium(IV) by Tri-N-Butyl Phosphate. *J. Inorg. Nucl. Chem* **40** 1167.

Rubisov V. N., Solovkin S. E., 1982 Calculation of steady-state regimes of technological extraction processes from data on the thermodynamics of Pu (IV) extraction with tri-n-butyl phosphate (TBP) from nitrate solutions. *Atomic Energy* **52**(6) 400-403.

Rudisill T. S., Crooks III W. J., 2001 *Thermal stability of acetohydroxamic acid/nitric acid solutions*, Report WSRC-TR-2001-00306, Westinghouse Savannah River Company Aiken, SC 29808, 2001, www.osti.gov/bridge/servlets/purl/799683-9ICZfS/native/799683.html

Ryan J. L., 1960 Species involved in the anion-exchange absorptions of quadrivalent actinide nitrates *J. Phys. Chem*. **64**(10) 1375-1385.

Rydberg Jan., Cox M., Musikas C., Choppin G. R., 2004a *Solvent Extraction Principles and Practice*. Danbury, Marcel Dekker Incorporated.

Saha B., Venkatesan K. A., Natarajan R., Antony M. P., Rao P. R., 2002 Studies on the extraction of uranium by N-octanoyl-N-phenylhydroxamic acid. *Radiochim. Acta* **90** 455-459.

Sajun M. S., Ramakrishna V. V., Patil S. K., 1981 The Effect of Temperature on the Extraction of Plutonium(VI) from Nitric Acid by Tri-n-butyl Phosphate. *Thermochim. Acta*, **47** 277-286.

Schroeder N. C., Attrep Jr. M., Marrero T., 2001 *Technetium and Iodine Separations in the UREX Process*, Los Alamos National Laboratory (C-INC), Final Report for WBS 1.24.01.01.

Schulz W. W., Navratil J. D., 1984 *Science and Technology of Tributyl Phosphate. Vol. II Selected technical and industrial uses*, CRC Press, Inc., Boca Raton, FL, USA.

Schulz W. W., Burger L. L., Navratil J. D., Bender K. P., 1984 *Science and technology of tributyl phosphate. Vol. III Application of tributyl phosphate in nuclear fuel reprocessing.*, CRC Press, Inc., Boca Raton, FL, USA.

Shilin I. V., Nazarov V. K., 1966 Complex formation of neptunium(IV) with nitrate and chloride ions. *Soviet Radiochem* **8** 447.

Smirnov-Averin A. P., Kovalenko G. S., Krot N. N., 1963 Extraction of uranium(IV) from nitric acid solutions with tributylphosphate. *Russ. J. Inorg. Chem*. **8** 1257-1260.

Soderholm L., Almond P. M., Skanthakumar S., Wilson R. E., Burns P. C. 2008 The Structure of the Plutonium Oxide Nanocluster $[Pu_{38}O_{56}Cl_{54}(H_2O)_8]^{14-}$ *Angew. Chem. Int. Ed*. **47** 298-302.

Solovkin A. S. 1971 Thermodynamics of plutonium(IV) extraction from nitric acid solutions by tri-n-butyl phosphate. *Atomic Energy* **30**(6) 673-675.

Sinkov S. I., Choppin G. R., Taylor R. J., 2006 Complexation and redox chemistry of U(VI) , Np(V) and Pu(VI) with acetohydroxamic acid. In *American Chemical Society 232nd National Meeting & Exposition*, September 10-14, 2006, San Francisco, CA, USA, I&EC 173.

Spahiu K., Puigdomenech I., 1998 On weak complex formation: re-interpretation of literature data on the Np and Pu nitrate complexation. *Radiochim. Acta* **82** 413-419.

Stas J., Dahdouh A., Shlewit H., 2005 Extraction of uranium(VI) from nitric acid and nitrate solutions by tributylphosphate/kerosene. *Periodica Polytechnica Ser. Chem. Eng*. **49** 3-18.

Taylor R. J., May I., Dennis I. S., Wallwork A.L., Hunt G., Hutchison S., Richards V., Hill N. J., 1998a *The development of chemical separation technology for an advanced PUREX process*. RECOD 98, European nuclear Society, Nice, Acroplic, France October 25-28, p.417.

Taylor R. J., May I., Wallwork A. L., Denniss I. S., Hill N. J., Galkin B. Ya., Zilberman B. Ya., Fedorov Yu. S., 1998b The applications of formo and aceto-hydroxamic acids in nuclear fuel reprocessing, *J. All. Comp.* **271–273** 534–537.

Taylor R. J., Dennis I. S., May I., 2000 *Hydroxamic Acids – Novel Agents for Advanced Purex Process*, Atalante 2000, Avignon, France, P2-15.

Tomaselli V. L., Zarrabi H., Moller K. D., 1980 Quantitative Infrared Absorption Measurements on Tri-*n*-Butyl Phosphate. *Appl. Spec*. **34** 415-417.

Tkac P., Matteson B., Bruso J., Paulenova A., 2008 Complexation of Uranium (VI) with Acetohydroxamic Acid, *J. Radioanal. Nucl. Chem*. **277** 31-36.

Tkac P., Paulenova A., 2008 Speciation of Molybdenum (VI) in Aqueous and Organic Phases of Selected Extraction Systems, *Sep. Sci. Technol*. **43** 2641-2657.

Tkac P., Paulenova A., Vandegrift G. F., Krebs J. F. 2009 Modeling of Pu(IV) Extraction from Acidic Nitrate Media by Tri-n-butyl Phosphate. *J. Chem. Eng. Data*, ACS ASAP DOI: 10.1021/je800904t (http://pubs.acs.org/doi/abs/10.1021/je800904t)

Veirs K., Smith C. A., Berg J. M., Zwick B. D., Marsh S. F., Allen P., 1994 Conradson, S. D. Characterization of the nitrate complexes of Pu(IV) using absorption spectroscopy, 15N NMR, and EXAFS. *J. All. Comp.* **213/214** 328-332.

Walther C., Cho H. R., Marquardt C. M., Neck V., Seibert A., Yun J. I., Fanghanel Th., 2007 Hydrolysis of plutonium(IV) in acidic solutions: no effect of hydrolysis on absorption spectra of mononuclear hydroxide complexes. *Radiochim. Acta* **95** 7-16.

Weigel F., Katz J. J., Seaborg G. T. 1986 *The Chemistry of the Actinide Elements*, Vol. 1, Ed. J. J. Katz, G. T. Seaborg, L. R. Morss, Chapman and Hall, New York, 704.

Woodhead J. L. 1964 Nitrates of uranium (IV), plutonium (IV) and uranium (VI) in tri-n-butyl phosphate solutions. *J. Inorg. Nucl. Chem*. **26** 1472-1473.

Woodhead J. L., McKay H. A. C. 1965 Uranium (IV) nitrate and perchlorate species in tri-n-butyl phosphate solutions *J. Inorg. Nucl. Chem.* **27** 2247-2254.

Yang Y. Z., 1996 *Gao Deng Xue Xiao Hua Xue Bao* (*Chemical Journal of Chinese Universities*) **17** 515.

Yusov A. B., Fedosseev A. M., Delegard C. H. 2004 Hydrolysis of Np(IV) and Pu(IV) and their complexation by aqueous $Si(OH)_4$. *Radiochim. Acta* **92** 869-881.

Summary

This project "Plutonium Chemistry in the UREX+ Separation Processes" was performed at TRUELAB at the Radiation Center of Oregon State University (OSU) under direction of Dr. Alena Paulenova, Director of the Laboratory of Transuranic Elements (TRUELAB) at Oregon State University.

The research work was focused on solution chemistry of plutonium in both the aqueous and organic phases of the solvent extraction separation process UREX. UREX is an advanced PUREX process based on extraction of metals from nitric acid solutions (aqueous phase) with tributylphosphate diluted with n-dodecane (organic phase) to 30% by volume. Since the hydroxamic acids, particularly acetohydroxamic acid $CH_3CONHOH$ (AHA) has been proposed as a salt-free reagent for a separation of Pu and Np from U-product, experimental work was focused mainly on the interactions of hydroxamic acids with actinides and fission products (molybdenum). AHA is used in the scrub section of the UREX separation process, and the complexation and reduction capability of AHA can affect a behavior of actinides in this complex extraction process significantly. Research project data include investigation of solubility, kinetics of acidic hydrolysis, and radiation stability of AHA in the one and/or two-phase system containing nitric acid and tri-*n*-butyl phosphate, as well as the characterization of the complexation and reduction ability towards Pu, Np and U.

Studying the chemistry of plutonium under UREX-process relevant conditions, over 400 distribution ratios in total were collected and the main trends in the concentration effects on the extraction and stripping of plutonium for a wide range of the HNO_3, AHA and additional nitrate concentrations were determined. Working on this project, we had a great opportunity to work closely with George Vandegrift of Argonne National Laboratory. The data experimentally collected at our Laboratory of Transuranic Elements at OSU led to improved understanding of behavior of Pu and AHA in the UREX demonstration experiments at ANL, and the generated database was incorporated into AMUSE program.

The uranyl cation forms a strong complex with ATA with five-membered two-oxygen chelate ring with the –CONHO– group of acetohydroxamic acid. The extraction yields of

uranium(VI) with TBP are not affected by the presence of AHA in the aqueous phase; however, after a prolonged contact with TBP, the typically yellow organic phase turns orange. This is due to presence of the ternary $UO_2(NO_3)$(AHA) complex in the organic phase, which was confirmed by UV-Vis spectroscopy, and later identified by FT-IR as $UO_2(NO_3)$(AHA)·2TBP. Another successful outcome from this project was the development of an experimental method for easy determination of low concentrations of AHA in TBP and the distribution ratio of 0.01 was found for distribution of AHA between aqueous and organic phases of the UREX extraction system. The chemistry of AHA is affected by its degradation to acetic acid which is soluble in TBP and complicates the whole separation process.

Moreover, working on this project, we have developed our own computational model for calculation of distribution ratios of Pu(IV) from HNO_3 media by TBP. This includes a careful implementation of the Pu(IV) interaction with nitrate – and hydroxyl anions in aqueous phase and incorporation of the activity coefficients for the species considerably affecting the extraction of plutonium such as water, nitrate and Pu^{4+}.

Another success during the last years was a project on characterization the plutonium species present in the aqueous and organic phases of modified PUREX extraction system. Numerous Pu species might be present in the extraction system. Particularly, at the absence of AHA and a low nitric acid concentration (~0.1 M), the extraction of Pu by TBP is governed mainly by the disproportionation reaction of tetravalent plutonium. Because of the disproportionation reaction, the concentration of non-extractable Pu(III) increases in the aqueous solution, and prolonged extraction time yields in lowering the distribution ratios of Pu. Additions of nitrate and/or acid restrain the hydrolysis and disproportionation reaction of Pu(IV) significantly. Using the Vis-NIR spectroscopy, the OSU researchers identified the Pu(IV) species extracted by TBP from low nitric acid concentration, which significantly differ from the spectra of Pu(IV) extracted from higher HNO_3 concentrations. The spectrum of Pu(IV) complex in TBP extracted from 0.1M HNO_3 features much lower absorption at 490 nm comparing to the tetra-nitrate-Pu(IV) complex in TBP. These preliminary results suggest a presence of Pu(IV) hydrolyzed species in the organic phase of PUREX.

In order to resolve the spectra of tetravalent plutonium in the presence of AHA, the experimental data obtained by absorption spectroscopy were analyzed using the chemical equilibrium modeling software FITEQL 4.0, developed by Prof. John C. Westall of OSU. This involves an iterative application of a specified chemical equilibrium model to a set of equilibrium complexation data. Through the calculation of the sum of squares of residuals between the experimental complexation data and predictions made with initial estimates, values of extinction coefficients for the species of interest can be determined at specific wavelengths. Pu(IV) species in the organic phase (TBP) extracted from HNO_3/AHA system observed by Vis-NIR absorption spectroscopy were inferred as ternary complexes of $Pu(AHA)_x(NO_3)_{4-x}$ solvated with TBP. Co-extraction of Pu(IV)-mono- and di-acetohydroxamate species by TBP considerably increases the distribution ratios of Pu(IV), which has to be included for successful prediction of distribution ratios of Pu in the presence of AHA.

The reduction of Pu(IV) in the acidic solutions containing AHA has been known for many years; however, due to a very complex conditions present in the reaction system, the identification of processes responsible for oxidation-reduction reactions is quite complicated. We have conducted an extensive investigation, which led to a deconvolution of plutonium spectra containing various absorbing species, such as Pu(IV)-AHA complex, Pu(IV) and Pu(III). As a result of this investigation, several oxidation-reduction reactions have been proposed. Concentration profiles for major species were processed with model based on a set of differential equations that express the rate of each of the analyzed species. It was determined that the decomposition of Pu(IV)-mono-acetohydroxamate complex leads to the formation of Pu(III) and reaction can be described by second order. Reduced Pu(III) can be re-oxidized back to Pu(IV) by two additional reactions, which depends on concentration of AHA. Several catalysis/inhibition reactions are expected to control this complex redox system. Understanding of these important reactions is necessary for successful prediction of plutonium fate in the currently proposed reprocessing extraction schemes. There are still a lot of uncertainties in fundamental chemistry between actinides and weak complexes such as nitrates or hydroxides or other naturally occurring ligands. Therefore, identification and characterization of important actinide species in chemical matrices relevant to spent nuclear fuel reprocessing or to environmental contaminated sites is very important.

ACKNOWLEDGMENT

All the research work reported in this final project report was performed in TRUELAB, the Laboratory of Transuranic Elements at Radiation Center, Oregon State University (OSU).

INVESTIGATORS:

Dr. Alena Paulenova, Associate Research Professor and Director of Radiochemistry Program

Dr. Peter Tkac, Research Associate the OSU Radiation Center

M. Alex Brown, Research Graduate Assistant, PhD student at OSU

Brent S. Matteson, Research Graduate Assistant, PhD student at OSU

Jason E. Bruso, Research Graduate Assistant, MS student, NE program

Mathew A. Cleveland, Undergraduate Student, NE program

Publications

1. P. Tkac, A. Paulenova, G. F. Vandegrift, J. F. Krebs, Modeling of Pu(IV) Extraction from Acidic Nitrate Media by Tri-*n*-butyl Phosphate, J. Chem. Eng. Data, in press, ACS ASAP http://pubs.acs.org/doi/abs/10.1021/je800904t.
2. P. Tkac, A. Paulenova, G. F. Vandegrift, J. F. Krebs, Distribution and Identification of Plutonium(IV) Species in Tri-*n*-butyl phosphate/HNO_3 Extraction System Containing Acetohydroxamic Acid, J. Radioanal. Nucl. Chem., **2009**, *280(2)*, 339-342.
3. P. Tkac, A. Paulenova, Speciation of Molybdenum (VI) in Aqueous and Organic Phases of Selected Extraction Systems, Sep. Sci. Technol., **2008**, *43*, 2641-2657.
4. P. Tkac, A. Paulenova, The effect of Acetohydroxamic Acid on Extraction and Speciation of Plutonium, Sep. Sci. Technol., **2008**, *43*, 2670-2683.
5. P. Tkac, B. Matteson, J. Bruso, A. Paulenova, Complexation of Uranium (VI) with Acetohydroxamic Acid, J. Radioanal. Nucl. Chem., **2008**, *277(1)*, 31-36.
6. A. Paulenova, P. Tkac, G. F. Vandegrift, J. F. Krebs, Modeling of Distribution and Speciation of Plutonium in UREX Extraction System, Solvent Extraction: Fundamentals to Industrial Applications, ISEC **2008**, *1*, 599-604.
7. P. Tkac, A. Paulenova, K. Gable, Spectroscopic Study of the Uranyl-Acetohydroxamate Adduct with Tributyl Phosphate, Appl. Spectrosc., **2007**, *61*(*7*), 772-776.
8. A. Paulenova, P. Tkac, B. S. Matteson, Speciation of Plutonium and Other Metals Under UREX Process Conditions, Advanced Nuclear Fuel Cycles and Systems, GLOBAL **2007**, 723-727.
9. P. Tkac, A. Paulenova, Equilibrium of Molybdenum in Selected Extraction Systems, Advanced Nuclear Fuel Cycles and Systems, GLOBAL **2007**, 1513-1517.
10. M. Alyapyshev, A. Paulenova, M. A. Cleveland, J. E. Bruso, P. Tkac, Hydrolysis of Acetohydroxamic Acid Under UREX+ Conditions, Advanced Nuclear Fuel Cycles and Systems, GLOBAL **2007**, 1861-1864.

Submitted

11. M. A. Brown, P. Tkac, A. Paulenova, G. F. Vandegrift, Influence of Temperature on the Extraction of Pu(IV) by Tri-*n*-butyl Phosphate from Acidic Nitrate Solutions, submitted for publication
12. P. Tkac, A. Paulenova, Spectroscopic evidence of extraction of hydrolyzed Pu(IV) species by tri-*n*–butyl phosphate, submitted for publication

1. Extraction and solubility of acetohydroxamic acid (AHA) by tri-n-butyl phosphate

1.1. Introduction

For decades, irradiated spent nuclear fuel has been reprocessed by the PUREX process in order to recover uranium and plutonium. In this mature extraction separation process, hexavalent and tetravalent actinides are extracted from a nitric acid matrix as neutral solvate complexes of tri-n-butyl phosphate (TBP). Partitioning of Pu(IV) from U(VI) carried out through reduction of Pu(IV) to Pu(III) that is rejected back to aqueous phase. Several new salt-free reagents to separate plutonium and neptunium from hexavalent uranium have been proposed and tested, including hydroxylamine derivates. Acetohydroxamic acid (AHA) (Fig. 1.1) has been identified as a possible salt-free organic reagent to control concentrations of tetravalent plutonium and neptunium in UREX (modified PUREX) processes that use single cycle flowsheet and centrifugal extractors [Taylor et al., 1998a]. Hydroxamic acids are reducing chemical agents, but they react also as a di-oxygen chelating ligand. They have a high affinity to hard-acid cations [Barocas et al., 1966], and their reactions with iron and other metals are of interest in several scientific areas. However, most of the data in literature were obtained under neutral or lower acid conditions [Baroncelli & Grossi, 1965; May et al., 1998; Meloan et al., 1960; Koide et al., 1989]. Having the general formula R-CONHOH, they are structurally related to carboxylic acids R-CO-OH. However, their dissociation is much weaker (pK_A = 4.75 for acetic and 9.2 for acetohydroxamic acid), and their metal chelates are generally much stronger than related carboxylates (β_1= 2.8 for Fe(III)-acetate and β_1= 10.84 for Fe-AHA [Martel & Smith 2001]).

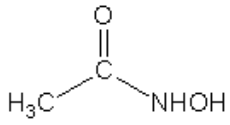

Figure 1.1 Structure of acetohydroxamic acid

The rich chemistry of hydroxamic acids and their wide implication have attracted a much recent attention [Munson 1982; Marmion & Nolan 2002; Marmion et al., 2000] Hydroxamic acids are *N*-hydroxy substituted derivatives of amides and involve, like amides, the simplest protein substructure (HNC=O). The hydrogen bonding abilities and association of amides have been examined extensively[2] due to the biological importance of amides. In hydroxamic acids, the OH group provides additional acceptor and donor sites for hydrogen bond formation.

Hydroxamate ions are powerful metal binding chelators and effective NO-donors [Marmion et al., 2000]. Due to their ability to form stable complexes with five-membered chelate rings with a variety of metal ions, including actinides, hydroxamic acids play important role in complexation chemistry of metals. Metal binding to hydroxamic acids (1:1) usually occurs in a bidentate fashion with the formation of singly or doubly deprotonated ligands [Abu-Dari et al., 1980; Gez et al., 2005].

The formation and structure of organic species containing AHA is of interest, both from the point of view of relative basicity and acidity of different AHA sites, as well as from the point of view of the interplay between the intermolecular hydrogen bond in an AHA-TBP complex and the intramolecular hydrogen bond that is present in the cis-keto tautomer of the AHA as well (Fig. 1.2)

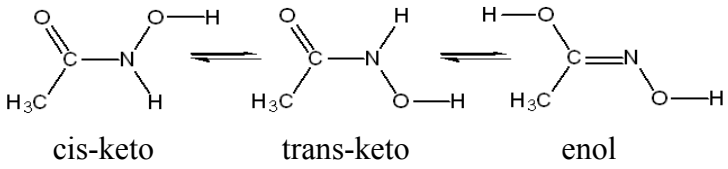

Figure 1.2 Isomers of acetohydroxamic acid

Although the association of amides with phosphoorganics has been extensively studied, as far as we know no data are available on the structure of tributyl phosphate-hydroxamic acid solvate complex. Possible structure of adduct formed in the organic phase is discussed.

1.2. Extraction and solubility of AHA in TBP

Solid acetohydroxamic acid was added in excess to n-dodecane, 100% TBP and 30% vol. % TBP in *n*-dodecane and mixed for 3 hours. The concentration of AHA dissolved in the organic phase was determined indirectly by UV-Vis spectroscopy. An aliquot of the organic phase was back-extracted by a tenfold excess (by volume) of distilled water. The concentration of the stripped AHA was determined colorimetrically using the calibration line for Fe(III)-AHA complex. The calibration line was made for several pH, using at least a twenty-fold excess of Fe(III) in order to ensure 1:1 complex formation and a permanent peak wavelength. To verify that all AHA from TBP-phase was back-extracted, a small volume of 0.1 M Fe^{3+} solution was added to the organic phase; nevertheless, no additional AHA was found in TBP.

The maximum soluble amount of AHA was found to be 9.4 g/l (0.125 M) and 43.5g/l (0.58M) for 30%TBP and 100% TBP, respectively. No detectable amount of AHA was found dissolved in 100 % *n*-dodecane. When TBP system was pre-equilibrated with water, significantly lower solubility of AHA was observed due to formation of TBP-water associates that indicates the hydrogen-bond mechanism of dissolution of AHA in TBP that is a more polar solvent than n-dodecane.

Interestingly, we have found that a small fraction of AHA can be extracted to TBP phase that can differ depending on initial aqueous concentrations of AHA, HNO_3 and $LiNO_3$ (Fig. 1.3). The amount of AHA found in TBP phase decreases with increasing concentrations of HNO_3 and $LiNO_3$ in aqueous phase. We have confirmed the presence of AHA in the organic extraction phase even after extraction from the aqueous phase containing six-molar nitric acid.

1.3. FT-IR spectroscopy of AHA adducts in TBP

Since the acetohydroxamic acid was found to be well-soluble in TBP, the spectroscopic analysis of the solutions of AHA in TBP was investigated in more detail. The infrared spectrum of TBP is very rich in absorption bands, so the spectrum of acetohydroxamic acid was largely obscured. However, characteristic peaks of hydroxyl and carbonyl group of AHA were clearly identified

and these two frequency regions, 3400-3100 cm^{-1} and 1700-1600 cm^{-1} respectively, were found to be diagnostic, see Fig. 1.4.

A relatively strong and broad absorption band at 3250 cm^{-1} corresponding to the stretching of the hydroxyl group [Saha et al., 2002] of acetohydroxamic acid was observed (Fig. 2A). If this band was an amide type NH stretch, it would be sharper [Higgins et al., 2006] with weak or medium intensity [Vien et al., 2001]. The intensity of this peak increases with an increase of AHA concentration, while the position remains unchanged. These assignments are supported by previous studies [Artemenko et al., 1976, 1980; Garcia et al., 2000], where it was found that in the sequence from a non polar solvent to polar the relative intensity of the absorption band of C=N group is lowered; therefore, the enol tautomers of AHA are not likely to be formed in polar solvents such as TBP. Furthermore, the formation of the C=N enol tautomer structure assumed for hydroxamic acids under alkaline conditions was recently refuted by FT-IR and FT-Raman spectral evidence in both solid and basic solution [Higgins et al., 2006]; therefore, the C=N enol forms were excluded from the evaluation and discussion in the present work.

In the carbonyl region, two peaks were identified for AHA dissolved in TBP: the carbonyl of the cis-keto isomer at 1690 cm^{-1} and trans-keto isomer (hydroxyl trans to the carbonyl) at 1675c m^{-1}. Because TBP has many H acceptor oxygen groups (P=O), the lower frequency for trans isomer can be explained by the fact that hydroxyl group of the cis isomer is in closer proximity to the carbonyl group and is slightly hindered (electronegative repulsion) from H-bond interaction with P=O groups. Whereas, the hydroxyl group of trans isomer would have no hindrance from the carbonyl and thus is more available for H-bonding with the P=O groups. The hydrogen bonding encourages a resonance which weakens the carbonyl bond and lowers the frequency. The carbonyl of the cis isomer (1690 cm^{-1}) has a much higher frequency in TBP than in the solid state [Higgins et al., 2006] of alkylhydroxamic acid due to lack of H-bonding for both the carbonyl and hydroxyl groups. Consequently, it was assumed that the keto form of acetohydroxamic acid will be present in the studied solvent and the double carbonyl band can be explained by formation of cis and trans isomers. The small changes in the shape of the phosphoryl peak of TBP in the presence of AHA suggest a weak hydrogen bonding P=O···H between TBP and AHA.

2. Hydrolysis AHA in the presence of mineral acid

2.1. Introduction

Under acidic conditions of hydrometallurgical processes, many organic molecules are destroyed in undergoing hydrolytic degradation reactions; therefore, the data on kinetics of hydrolysis, radiolysis and behavior of degradation products are necessary. In the present paper we will report the results on kinetics of the hydrolysis of AHA in nitric and perchloric acid media was investigated at several temperatures. The rate constants and thermodynamic data for the hydrolysis reaction were evaluated with respect to the concentrations of acetohydroxamic acid, nitrate and hydronium ions, and radiation dose. In this study, the kinetics of the hydrolysis of acetohydroxamic acid in nitric and perchloric acid media was investigated at several temperatures. The decrease of the concentration of AHA was determined via its ferric complex using UV-Vis spectroscopy. The data obtained were analyzed using the method of initial rates. The rate equation and thermodynamic data are discussed for the hydrolysis reaction with respect to the concentrations of acetohydroxamic acid, nitrate and hydronium ions, and radiation dose.

All kinetic experiments were carried out in small glass vials placed in a shallow water bath, maintaining
required temperature within ±0.05 °C. Desired concentrations of nitric or perchloric acid were prepared,
pipetted into vials, thermostated for at least 20 minutes, and a required volume of AHA stock solution (1M in distilled water) was added to achieve needed concentrations of mineral acid and AHA. The initial concentration of AHA in all kinetic experiments was 2.5×10^{-3} M. Degradation of AHA upon acidic hydrolysis was measured in aqueous solutions of nitric acid; additionally, a set of samples was irradiated with gamma Co-60 or agitated with organic phase to be used in the extractions (30 vol. % TBP in n-dodecane). The organic phase was pre-equilibrated with a double volume of the acid solution of the same concentration as to be used in the kinetic experiment. Agitation was repeated three times with fresh portion of aqueous phase. The concentration of AHA was monitored spectrophotometrically using Fe(III) that forms with AHA a bright-red complex which has a wide intensive peak in the 500 nm region of the UV-Vis

spectrum. Iron was added in 20-fold excess to confirm 1:1=Fe:AHA species ratio in measured absorbances of Fe(AHA) complex.

2.2. Hydrolysis of AHA: One phase system

The rate of reaction was monitored as a function of concentrations, time and temperature. The data obtained were analyzed using the method of initial rates. Reaction of hydrolysis of acetohydroxamic acid is catalyzed with hydronium ion first (and fast), then the protonized substrate is attacked with molecule of water that is the rate-limiting step [Connors 1990; Gosh 1997].

The hydrolysis of hydroxamic acid was examined first by Berndt, who reported results on the polar and steric effects on the acid-catalyzed hydrolysis of a series of aliphatic and benzohydroxamic acids [Berndt & Sharp, 1973; Berdnt & Ward, 1974]. Infrared spectroscopy of extraction samples revealed the presence of acetic acid, the product of hydrolysis, in the organic extraction phase (discussed later in 3.3).

$$CH_3CONHOH + H_3O^+ \rightarrow CH_3COOH + NH_3OH^+ \qquad (2.1)$$

The rate of this bimolecular reaction (Eq. 2.1) for both the acidic proton and AHA was determined to be pseudofirst order. Expressed in half-lives, data are listed in Table 2.1. As it is shown in Figs. 2.1 and 2.2, the rate of hydrolysis rises rapidly with the mineral acid concentration.

In the 1.5 molar acid solutions, the half-lifes of AHA are almost the same for both the nitric and perchloric acids. However, with increased concentration of acid, an evident difference between perchloric and nitric acid arises. For 2.5 molar mineral acid, the half-life of AHA in perchloric acid is about 1.3-fold longer than in nitric (Tab. 2.1). This observation is in a very good agreement with data presented by [Ghosh et al., 2003] who studied hydrolysis of di- and mono-hydroxamic acid in different mineral acids (HCl, H_2SO4, $HClO_4$), and also reported that hydroxamic acid degradation in perchloric acid media was the slowest.

Added neutral nitrate ($LiNO_3$) also speeds up the degradation of AHA as well (Tab. 1). It was reported

Earlier [Rudisill & Crooks, 2001] that at concentration of nitric acid above 2.5 M, nitric acid and hydroxylamine (HAN) react autocatalytically. The two net reactions are summarized by equations (2.2) and (2.3):

$$4\ NH_3OH^+ + 2\ HNO_3 \rightarrow 3\ N_2O + 3\ H_2O + 4H^+ \quad (2.2)$$

$$NH_3OH^+ + 2\ HNO_3 \rightarrow 3\ HNO_2 + H_2O + H^+ \quad (2.3)$$

$$3\ HNO_2 \rightarrow HNO_3 + 2\ NO + H_2O \quad (2.4)$$

The generation of HNO_2 in the reaction (2.3) is responsible for the autocatalytic nature of the reaction and generating large volumes of nitric acid in the reaction (2.4). Thus the additional amount of nitrate ions in the aqueous phase may work as HNO_3 provider.

Table 2.1 Hydrolysis of AHA (2.5×10^{-3} M) at 25°C in solutions of perchloric acid, nitric acid and addiational nitrate.

$[H^+]$, M	$T_{1/2}$, min	
	$HClO_4$	HNO_3
1.5 M H^+	466	457
2.0 M	432	383
2.5 M	379	289
1.5 M H^+ + 2.5 M $LiNO_3$	-	283
1.5 M H^+ + 4.5 M $LiNO_3$	-	271

2.2. Hydrolysis of AHA: Two phase system and thermodynamics

Degradation of AHA was studied also in the presence of the organic phase. The 30% TBP in n-dodecane was pre-saturated with nitric acid of the same concentration as used in the kinetic experiment. As it is shown in Table 2.2 for 25°C, the degradation of AHA is promoted by

the mineral acid concentration and temperature. At 25°C, the acetohydroxamic acid hydrolyzes faster in the two-phase system, while the opposite was observed at increased temperature (Fig. 2.3) that is probably caused by different extractability of nitric acid to tributylphosphate.

The linearized form of Arrhenius equation (Eq. 2.5) was used to determine A (frequency factor) and Ea
(activation energy) from the intercept and slope of a plot of ln(k) vs. 1/T (Figure 2.4)

$$\ln k = \ln A - E_a/RT \quad (2.5)$$

Using the Eyring formalism:

$$\Delta H^* = E_a - RT \quad (2.6)$$

$$\Delta S^* = R \ln A - R \ln (kT/h) - R \quad (2.7)$$

where k is Boltzmann constant, h is Planck constants, R is the gas constant, and T is the absolute temperature. The measured activation parameters for the reaction of acidic degradation of AHA were calculated. The calculated value of Ea was found to be 76.27 kJ/mol for hydrolysis in one-phase system, and is in a good agreement with the value 79.9 ± 2.9 kJ/mol reported by [Taylor et al., 1998b]. While Gibbs energy for all three compared system is about the same, the values of other three thermodynamic parameters differ significantly (Tab. 2.3).

The obtained data confirmed that hydrolytic and radiolytical degradation can have a significant effect on separation processes of actinides. The data observed for the reaction of acidic degradation of AHA follow the pseudo first order reaction model. Gamma-irradiation with the dose rate of 33kGy/s (gamma, Co-60) increases the rate of acidic degradation of AHA two-fold.

Table 2.2 Hydrolysis of AHA (2.5×10^{-3}M) solution in nitric acid in one- and two-phase system at 25°C

$[HNO_3]$, M	One-phase system			Two-phase system		
	$k'\times10^3$ min^{-1}	$T_{1/2}$ min^{-1}	$K\times10^3$	$k'\times10^3$ min^{-1}	$T_{1/2}$ min^{-1}	$K\times10^3$
1.5	1.52	457	1.01	2.36	294	1.57
2.0	1.81	383	0.90	2.60	266	1.30
2.5	2.4	289	0.96	3.78	183	1.51

Table 2.3 Thermodynamic parameters of hydrolysis of AHA

$[HNO_3]$ +$[LiNO_3]$ M	One-phase system		Two-phase system
	1.5-2.5 M	1.5 M $LiNO_3$ (0.5-4.5 M)	0.5-2.5 M TBP 30% in n dodecane
Ea [kJ/mol]	76.27	66.14	59.21
ΔH, average [kJ/mol]	73.68-	67.1	56.67
ΔS, average [J/mol/K]	79.24	-103.0	-135.88
ΔG, average [kJ/mol]	98.3	99.1	98.2

3. Uranium extraction by TBP: Effect of AHA

3.1. Introduction

Complexation of acetohydroxamate (AHA) with actinide cations in solutions leads to the formation of strong interactions; the binding strength increases with the effective charge[Choppn & Rao, 1984] of the cation Z_{eff}, that is, 4+ for tetravalent actinides, and only 3.3+ for the dioxocation of hexavalent uranium UO_2^{2+}. The stability constant values reported [Sinkov et al., 2006] for Pu(IV) and Np(IV) are β_1=14.2 and β_1=12.83, respectively. For U(VI) they are much

lower: β_1=7.99[10]and β_1=8.22[6]. Therefore, acetohydroxamic acid preferably will bind Pu(IV) and Np(IV) over the U(VI). Such selective binding of metals to chelators is the most common feature used to design a separation process. Depending on the hydrophilic properties of the complexing ligand, the extractability (defined as the partitioning between an organic phase and an initial aqueous solution) of metals bound in such complexes is usually drastically lowered, and differential extractability between two metals may be successfully used in the separation processes. Upon addition of acetohydroxamic acid, the extractability of plutonium and neptunium can be greatly diminished without significant changes of the extraction yields of uranium [Taylor et al., 1998b]. Besides chelation, the hydroxylamine group of AHA is a strong reductant, and reduction of the metal also leads to a significant decrease of their extractability [Taylor et al., 2000]. Complexation of uranyl cations with hydroxamic acids in solutions leads to the formation of 1:1 and 1:2 orange-red complexes. Under conditions of reduced acidity of solutions, the solubility of uranyl-hydroxamate complexes drops rapidly and the insoluble orange-brown uranyl(hydroxamate)$_2$ complex precipitates [Taylor et al., 2000]. In acidic solutions, the hydroxamic group is hydrolyzed to the parent carboxylic acid and hydroxylamine [Taylor et al., 2000; Karraker et al., 2001]. The effect of hydroxamic acid on uranium extraction with TBP and the chemistry of uranyl-hydroxamate complexes were not studied in details up to now. We report results on our investigation of the formation of complexes of hexavalent uranium with acetohydroxamic acid, and their distribution to organic phase of 30% TBP in n-dodecane as a function of different nitric acid, total nitrate, and acetohydroxamic acid concentrations. Both aqueous and organic phases were examined also by UV-Vis spectroscopy.

The 1.1 molar solution of tri-n-butylphosphate in *n*-dodecane (30 vol. %) was used for all extraction experiments. The organic phase was pre-equilibrated with the aqueous solution of the same composition (besides metal and AHA) to be used in the extraction. Distribution ratios were determined for two uranium concentrations (0.043 and 0.176 M) and several different combinations of HNO_3 (1-6 M) and $LiNO_3$ (2-5 M added to 1 M HNO_3) both with and without the presence of AHA in solution. The experiments were conducted in plastic liquid scintillation vials at a 1:1 volume ratio of organic: aqueous phase. Samples were agitated at ambient temperature for sufficient time, and centrifuged. The organic and aqueous phases were split, and

the concentration of uranium in the aqueous phase before and after extraction was determined using ICP-OES (Teledyne Leeman Prodigy).

3.2. Extraction of U(VI)

The extraction of uranium was examined for two different concentrations of uranium (series A and B in Figure 3.1) and several different combinations of HNO_3 and $LiNO_3$ concentrations. It was observed that added lithium nitrate leads to increased extraction of metals to the TBP organic phase that is caused by the salting-out effect of $LiNO_3$. The addition of non-extractable nitrate salt to the HNO_3 aqueous phase generally increases the amount of extractable species (nitric acid, extractable metals) into the organic phase by TBP [Chaiko & Vandegrift, 1998]. In accordance with previously published results [Schulz et al., 2000; Stas et al., 2005], the distribution ratio of uranium reaches a maximum at 5-6 M nitrate (Fig. 3.1).

While our results on extraction of plutonium and zirconium with TBP in the presence of AHA show a significant decrease in the yields, the difference in the distribution ratios of uranyl in the absence and presence of AHA (0.4 M) is minimal, and within the range of experimental uncertainty for three parallel extractions. Similar results for uranium were reported also by [Schroeder et al., 2001].

Table 3.1 summarizes the percentage of uranium extracted from the different nitric acid and nitrate solutions and then back-extracted with acetohydroxamic and nitric acid stripping solutions. Generally, the high concentrations of nitric acid and nitrate in initial aqueous phase resulted in larger yields of uranium in extraction and low yields in back-extraction experiments. Although the effect of AHA on stripping of uranium from TBP-organic phase was minimal, a little tendency of increased complexation with uranium with decreased initial concentration of HNO_3 is observed.

In the presence of AHA, an evident change in color of aqueous solutions of uranium was observed. Formation of uranyl-AHA complex was confirmed by the hyperchromic shift in uranium spectrum including the region beyond 500 nm. Although increasing concentration of nitric acid suppresses the chelation of uranyl with AHA, the presence of their complex was observed even for 1M HNO_3 (Figure 3.2). These observations suggest a strong complexation ability of acetohydroxamic acid with uranium. The stability constant $\log\beta_1$ equal to 8.22 for

uranyl-AHA complex was reported by [Koide et al., 1989]. No reduced uranium (IV) was observed in aqueous or organic phase.

However, when uranyl nitrate was dissolved in TBP, without presence of AHA and HNO_3, change in color from yellow to green was observed over time (Figure 3.3). This was assigned to photo-reduction reaction.

In the presence of AHA and low nitric acid concentration, formation of uranium precipitates was observed in the solution. This precipitates are believed to be a mixture of uranyl nitrates and uranyl-acetohydroxamates (Figure 3.4).

Table 3.1 Percentage of the extracted and back-extracted uranium in the presence and absence of acetohydroxamic acid in aqueous phase.

Aqueous extraction phase			Extraction	U back-extraction yield (%)	
U = 0.046 M, no AHA			(TBP)	Stripping phase	
$[H^+]$ (M)	$[LiNO_3]$ (M)	$[(H+Li)NO_3]$ (M)	(U, %)	0.3 M HNO_3	0.4 M AHA + 0.3 M HNO_3
1	0	1	87.7	26.4	26.9
2	0	2	94.1	19.1	20.0
3	0	3	96.2	16.2	16.3
4	0	4	97.3	12.5	12.8
5	0	5	97.7	10.8	10.9
6	0	6	97.6	10.3	10.6
0.2	0.8	1	91.2	33.1	35.0
0.4	0.6	1	89.4	31.3	33.1
0.6	0.4	1	88.5	29.2	33.6
0.8	0.2	1	87.0	26.9	28.6
1	1	2	96.6	21.2	22.8
1	2	3	98.7	17.8	18.7
1	3	4	99.3	15.2	16.4
1	4	5	99.6	13.3	13.9
1	5	6	99.7	12.9	13.7

3.3. U(VI)-AHA complex in TBP

When we studied the impact of AHA added to the aqueous phase of uranyl nitrate prior to extraction with tributyl phosphate (TBP), we observed the presence of a new compound in the organic phase that suggests more complex chemistry during the extraction than expected; hence, more detailed spectroscopic characterization of the species present in both aqueous and organic phases was required.

In order to investigate U-AHA complexation in TBP several samples with different concentration of AHA and uranium were combined. The solid uranyl nitrate hexahydrate was dissolved in tributyl phosphate organic solvent to make 0.1 M stock solution. The small layer of crystallization water from UNH rejected from the organic phase was removed after a short centrifugation. To prepare samples with different ratios of UN and AHA, the 0.3 M stock solution of AHA in TBP, prepared from solid AHA and diluted to desired concentrations, was combined with the uranyl nitrate/TBP solution. Two set of samples, without and with uranyl nitrate (0.045 M constant) were prepared. The concentrations of AHA in both sets were: 0.023, 0.03, 0.045, 0.068, 0.09 and 0.135 M.

When the TBP-solutions of AHA and uranyl nitrate (UN) were combined, the characteristic yellow color of uranyl turned orange. The lines A and B in Figure 3.5 illustrate the changes in spectra for the same concentration of uranium in TBP and AHA-TBP solutions. The shift in uranium spectrum (B) confirms that a new complex has been formed in the organic phase. In addition, a similar spectrum (C) was observed for the extraction organic phase that was agitated with aqueous phase containing both uranyl nitrate and AHA for several days.

The nature of uranium-AHA species in TBP phase was investigated by Job's method of continuous variations. The concentrations of uranium and AHA were in the range of 0.01-0.04 M. Figure 3.6 displays the plot of absorbances at 485 nm for the system of UN, AHA and TBP for different molar fractions (x) of AHA and UN in TBP. The maximal absorbance was observed at x(AHA) = 0.5 that suggests formation of a quaternary complex $UO_2(NO_3)$(AHA).2TBP.

In order to confirm the stoichiometry of the complexes of uranium (VI) and other actinides with AHA in tri-n-butylphosphate, investigation of these systems via infrared spectroscopy was also performed.

Distribution of uranyl ion between the tributyl phosphate (1.1M in n-dodecane) and nitric acid as aqueous phase was extensively studied, including UV-Vis and infrared spectroscopy [Tkac et al., 2008; Chiarizia et al., 2003]. Upon the extraction of uranium from nitric acid solutions of $UO_2(NO_3)_2$, the initially colorless organic phase develops the characteristic uranyl-yellow color. Chemical analyses, spectroscopic and EXAFS data confirmed [Chiarizia et al., 2003] that uranium is extracted as the $UO_2(NO_3)_2$. 2TBP adduct. When AHA is added to an aqueous uranyl nitrate solution, the liquid turns red due to formation of a red ternary complex of $UO_2(AHA)(NO_3)$. Formation of the higher complex [Meloan et al., 1960] $UO_2(AHA)_2$ is more favorable only in basic media when hydroxamic acid is more deprotonated (pK_A = 9.02). Although increasing concentration of nitric acid suppresses the chelation of uranyl with AHA, the presence of the red $UO_2(NO_3)AHA$ complex was observed even in 1M HNO_3 [Tkac et al., 2008]. We have found that the high extraction yields of uranium with TBP are not decreased upon addition of AHA; however, after a prolonged contact with tributyl phosphate, typically uranyl-yellow organic phase turns orange. The significant increase of the UV-Vis absorbance observed for the organic phase (Figure 3.5) can be explained only by the forming of a red uranyl-hydroxamate complex in the organic phase with the contact time. Such a finding suggests that after a rapid extraction of uranyl nitrate, a slow distribution and solvation of the mixed uranyl-hydroxamate-nitrate complex occurs. The stoichiometry of the uranyl-hydroxamate species in the organic phase was measured by the UV-Vis spectroscopy utilizing the "slope method" and Job's method of continuous variations published elsewhere [Meloan et al., 1960]. For varying concentrations of uranyl and AHA, both methods indicated a 1:1 ratio of UO_2:AHA. In order to study the structure of solvates of tributyl phosphate with uranyl nitrate in the presence of acetohydroxamic acid, UV-Vis and FT-IR spectroscopy was employed. Characteristic peaks in IR spectra and their assignments for bonds and species involved in $UO_2(NO_3)_2$-AHA/TBP-dodecane systems are listed in Table 3.2.

Figure 3.7 displays infrared transmittance spectra of two samples with the same concentrations of AHA in TBP without (Spectrum 1) and with 0.045M uranyl nitrate (Spectrum 2). Broad and

weak absorptions at 3400-3600 cm^{-1} region (Fig 3.7A), attributed to the hydrogen bonded hydroxyl group of water molecules absorbed by TBP [Tomaselli et al., 1980], enlarged when the concentration of water increased by addition of the hexahydrate of the uranyl nitrate to the system. The significant differences of the spectra are observed in the 3400-3100 cm^{-1} and 1700-1600 cm^{-1} frequency regions that are diagnostic for acetohydroxamic acid, and it confirms that the main changes in complexation bonds occur between uranyl and AHA. The intensities of the hydroxyl stretching band of AHA at 3250 cm^{-1} are significantly decreased and slightly shifted (~10 cm^{-1}) to the lower frequencies in the presence of uranium that indicates that chelation of uranyl with AHA occurs through replacing of hydrogen in the OH group of acetohydroxamic acid (Fig. 3.7A, Spectrum 2). Also the region of carbonyl stretching vibration of the hydroxamate group differs: the intensity of the C=O stretching band at 1690 cm^{-1} is much lower when uranyl-nitrate is present (Fig. 3.7B, Spectrum 2). Additionally, formation of a broad peak at ~1635 cm^{-1} confirms the association of the uranyl with the carbonyl site of acetohydroxamic acid that causes stretching of the C=O bond and shift in ~60 cm^{-1} to the lower frequency. In the absence of AHA in TBP, all frequencies in the infrared spectra collected for the sample of uranyl nitrate in tributyl phosphate were consistent with those presented in the literature [Borkowski et al., 2002; Burger 1984; Tomaselli et al., 1980; Nukada et al., 1960; Ferraro et al., 2001] earlier: the band at 941 cm^{-1} assigned to the uranyl nitrate, the phosphoryl peak shifted by ~90 cm^{-1} from 1285 cm^{-1} to 1192 cm^{-1} due to strong coordination of UO_2^{2+} cation to the oxygen atom of P=O group and the symmetric stretch [Burger, 1984; Ferraro et al., 2001] at 1526 cm^{-1} of bidentate nitrate group coordinated with uranyl (Table 3.2, Figure 3.8). The C-O-P vibration of TBP at 1028 cm^{-1} was affected neither by presence of uranium, HNO_3 nor acetohydroxamic acid.

Figure 3.8 compares the spectra of the adduct of $UO_2(NO_3)_2$.2TBP [Burger 1984; Ferraro et al., 2001] prepared by dissolution of UNH in 30% TBP (Spectrum 3.8C) and the extraction organic phase (Spectrum 3.8D) that was obtained after equilibration of 30% TBP with the aqueous phase of $UO_2(NO_3)_2$ and AHA in 0.1M nitric acid. The concentration of HNO_3 extracted to TBP from 0.1M HNO_3 is very low; hence, no major peak of TBP-HNO_3 adducts appeared in the spectrum. Appearance of two new peaks at 1751 cm^{-1} and 1725 cm^{-1} in extraction sample can be assigned to non-H-bonded and H-bonded form of acetic acid, respectively. The presence of acetic acid which was formed due to acidic hydrolysis of acetohydroxamic acid under extraction condition

(Eq. 3.1) confirms a good extractability of acetic acid by TBP. Hydroxamic group relatively easily undergoes acidic hydrolysis [Taylor et al., 1998b; Karraker 2001; Ghosh et al., 2004], and the degradation leads to accumulation of the parent carboxylic acid and hydroxylamine:

$$CH_3CONHOH + H_3O^+ \rightarrow CH_3COOH + NH_3OH^+ \quad (3.1)$$

Similarly to acetohydroxamic acid, the infrared spectrum of the acetic acid extracted to TBP does not exhibit any strong changes in the phosphoryl region. The distribution ratio (D=0.22) and the extraction constant (K_{ex}=0.4) for acetic acid with TBP/n-alkane were determined earlier [Yang et al., 1996]. The values, measured at 20^{o}C, decrease with elevated temperature.

The spectra of the $UO_2(NO_3)_2$.2TBP sample (Spectrum 3.8C); and the sample of the extraction organic phase (Spectrum 3.8D); differ significantly also in the phosphoryl region: appearance of the P=O stretch at 1192 cm^{-1} confirms the strong complexation between TBP and uranyl; however, the definite changes in the shape of this peak indicate that the coordination of uranyl and TBP is perturbed due to strong bonding between uranyl cation and AHA. A different shape of spectrum in Fig. 3.8D in the phosphoryl region can be also explained by the presence of an additional broad underlying absorbance at 1220cm^{-1} and 1175cm^{-1} (possibly C-O and C-C-O stretch of acetic acid) that is causing the 1192cm^{-1} band to appear weaker than it really is. The peak at ~1635 cm^{-1} of the carbonyl band of hydroxamate is shifted due to coordination with uranyl. No significant absorbances at 1690 cm^{-1} or 1675 cm^{-1} indicate that all AHA present in the organic phase is complexed with uranium. Additionally, the absence of the stretching band at 3250 cm^{-1} characteristic for the hydroxyl group of AHA (region not displayed in the Figure 3.8) in the extraction sample spectrum also confirms that all AHA found in organic phase is associated with uranium. Extensive research on distribution of uranium(VI) between nitric acid and diluted tributyl phosphate confirmed that U(VI) is extracted as the neutral adduct complex [Nukada et al., 1960; Borkowski et al., 2002; Chiarizia et al., 2003] $UO_2(NO_3)_2$.2TBP where the uranyl forms bidentate chelates with nitrate anions with the chelate bonds in the equatorial plane perpendicular to the O=U=O rod. Comparison of the infrared spectra for both UN (Spectrum 3.8C) and extraction organic (Spectrum 3.8D) samples indicates that the analogical adducts of tributyl phosphate with the neutral complex are formed when larger concentrations of acetohydroxamic acid in uranium aqueous solution are present. The analysis of the data acquired

by infrared spectroscopy confirms that uranyl cation is complexed with AHA by co-ordination with two oxygen atoms of the -CONHO- group forming a five-membered chelate ring in the equatorial plane; hence, the structure of the ternary uranyl-nitrate-acetohydroxamate complex solvated with two molecules of tributyl phosphate $UO_2(AHA)(NO_3).2TBP$ can be presented as it is shown in the Fig. 3.9.

Table 3.2. Characteristic vibrational frequencies of TBP, AHA and $UO_2(NO_3)_2$

Stretch assignment	FT-IR frequency (cm^{-1})		Diagnostic for
	Literature [ref.]	This work	
UO_2^{2+}	940 [16, 28]	941	Uranyl nitrate
C-O-P	1028 [17]	1028	TBP
P=O	1282 [17]	1285	TBP
P=O	1191-1192 [17]	1192	TBP-coordinated with uranium
ONO	1526-1528 [16]	1526	Nitrate coordinated with uranium
C=O	1625 [21]	1690	AHA (cis-keto)
C=O	1663-1668 [21]	1675	AHA (trans-keto)
C=O		1630-1640	AHA (C=O-UO_2)
C=O	1780-1760 [18]	1751	Acetic acid*
C=O	~1730 [18]	1725	H-bonded Acetic acid*
OH	3173 [19]	3250	AHA (NOH)
OH	3400-3600 [20]	3490, 3552	OH (hydrogen bonded H_2O)

* acetic acid due to hydrolytic degradation of acetohydroxamic acid

Once one nitrate at uranyl is replaced with acetohydroxamate and the ternary complex of $UO_2(AHA)(NO_3)$ in aqueous phase is formed, then upon a prolonged agitation with TBP it can be extracted as a neutral adduct complex of $UO_2(AHA)(NO_3).2TBP$ with the distribution ratio (D) of uranium, as follows:

$$D = \frac{\Sigma[UO_2^{2+}]_{org}}{\Sigma[UO_2^{2+}]_{aq}} = \frac{[UO_2(NO_3)_2.2TBP] + [UO_2(AHA)(NO_3).2TBP]}{\Sigma[UO_2(AHA)_n(NO_3)_{2-n}]} \quad (3.2)$$

The amount of the ternary complex of uranium with acetohydroxamate and nitrate $UO_2(AHA)(NO_3)$ in aqueous phase increases with pH, but under stronger acidic conditions in both aqueous and organic phase the uranium species without AHA are predominant. The extraction of acetohydroxamate complex is kinetically slow (several days); hence, no significant effect on the distribution of uranium in real extraction processes is expected. Results acquired by infrared spectroscopy confirmed that uranyl cation forms with the -CONHO- group of AHA the five-membered-two oxygen chelate ring. The presence of acetic acid as a hydrolysis product of AHA was also identified in the TBP organic phase. The shift of the carbonyl band from 1690 cm^{-1} to 1675 cm^{-1} in the IR spectra of AHA indicates that the carbonyl site is involved in the intermolecular hydrogen bonding between two AHA molecules.

4. Plutonium extraction by TBP

4.1. Introduction

Over the past the two decades, various reprocessing schemes have been proposed for extraction of actinides from fission products and other elements present in spent nuclear fuel. Most current reprocessing schemes operate using a tri-*n*-butyl phosphate (TBP) based extraction process—the PUREX process (Plutonium and Uranium Recovery by EXtraction). Knowledge of stoichiometric and distribution relationships for tetravalent plutonium in solvent extraction systems related to the PUREX process, together with knowledge of Pu speciation over a wide range of experimental conditions are important for the separation process design. Measured values of distribution ratios serve as a database for the development of computing codes for modeling and simulation of extraction processes.

In the modified PUREX process, UREX, uranium and technetium are extracted from the bulk of the dissolved fuel to tri-*n*-butyl phosphate (TBP), and one of the possible solutions for separation of both plutonium and neptunium from uranium in the UREX process is the introduction of a hydrophilic ligand to the extraction system that will selectively complex Pu and

Np in the aqueous phase and greatly diminish their extractability. Effective hold-back ligands should meet required criteria such as strong complexation of tetravalent actinides in nitric acid media, low extractability, formation of no precipitates, gaseous or volatile products, chemical and radiolytical stability, low material corrosion activity, and commercial availability. Several new salt-free reagents to separate Pu(IV) and Np(VI) from U(VI) have been proposed and tested, including carboxylic derivates of hydroxylamine such as acetohydroxamic acid (AHA) or formohydroxamic acid (FHA) [Taylor et al., 1998b].

All extraction experiments were performed with tri-*n*-butyl phosphate (TBP) diluted with *n*-dodecane to 1.1M (30 volume %). Prior to extraction, the organic phase was pre-equilibrated with the same aqueous phase as used in the extraction experiments except for the addition of the tracer Pu(IV). Distribution ratios of Pu(IV) were measured in batch experiments at 1/1 aqueous/organic volume phase ratio for 4 minutes at ambient temperature conditions 22±2 °C. After agitation, phases were separated after a short centrifugation, and aliquots from both the organic and aqueous phases were taken for determination of activity of Pu using a liquid scintillation counter.

After dissolution of Pu-239 in nitric acid, a mixture of hexavalent and tetravalent oxidation states of Pu was obtained. Therefore, Pu was reduced by addition of acidified hydrogen peroxide, and then, Pu(III) was re-oxidized to Pu(IV) by a cautious addition of crystals of solid $NaNO_2$. Impurities of Am-241 (for Pu-239) were removed by anion exchange chromatography using a small column filled with the resin Dowex 1x-4, conditioned with 7M HNO_3. Plutonium, dissolved in concentrated HNO_3, was placed on the top of the resin bed, and Am washed out with several column volumes of 7M HNO_3. Finally, Pu(IV) was eluted with 0.36 M HCl. Purity of the tetravalent oxidation states of Pu was confirmed by absorption spectroscopy and using the extraction scheme with thenoyl trifluoroacetone (TTA) in xylene from 1M nitric acid and it was found to be >99.5%.

4.2. Distribution ratios of Pu(IV) between $HNO_3/LiNO_3$ and TBP

The extraction experiments of tetravalent plutonium were examined for several concentration combinations of HNO_3, $LiNO_3$, and acetohydroxamic acid. Our experimental values of Pu(IV) distribution ratio are average values of at least two extraction experiments, and

they were measured by both direct and back extraction and are collected in Table 4.1. For the extraction of Pu(IV) from HNO_3 by TBP, the distribution ratios increase with the increasing nitric acid concentration through the maximum at 6-8M HNO_3 (Figure 4.1). Due to competition between the nitric acid and $Pu(NO_3)_4$ for the TBP available for complexation, further increase of the nitric acid concentration is accompanied with decrease of the distribution ratio of Pu(IV). Also the increase of total nitrate concentration leads to formation of higher Pu-nitrate complexes in aqueous phase that can be: $Pu(NO_3)^{3+}$, $Pu(NO_3)_2^{2+}$, $Pu(NO_3)_4$ and $Pu(NO_3)_6^{2-}$ [Veirs et al., 1998]. Due to the formation of anionic Pu species, extraction of Pu(IV) under high HNO_3 conditions decreases.

In general, upon addition of a non-extractable nitrate salt ($LiNO_3$), a strong salting-out effect is observed, and increased extraction yields of extractable species such as nitric acid and neutral metal-nitrate complexes (e.g., with tetra- and hexavalent actinides) into organic phase by TBP are measured. Much higher D(Pu) values were observed when some portion of HNO_3 was replaced by addition of $LiNO_3$ in the aqueous phase (Figure 4.2). This effect is evident for say 2M HNO_3/3.9M $LiNO_3$ with $\Sigma NO_3^- = 5.9M$, where D(Pu)=187 compared to D(Pu)= 45 at 6M HNO_3. The main reason of this increase is lowering the HNO_3 extraction and competition with Pu(IV) for available TBP [McKay, 1956]. However, the extraction of nitric acid and Pu(IV) is significantly higher in the presence of additional non-extractable nitrate due to strong salting-out effect which increases the extraction of extractable species such as HNO_3 and $Pu(NO_3)_4$.

Distribution ratios for Pu at low nitric acid (<1 M) are strongly dependent on processes that take place in the aqueous phase, such as hydrolysis and disproportionation reactions. Data of distribution ratios for Pu(IV) in HNO_3<1M obtained after 4 minutes extraction time differ significantly from those reported by [Petrich and Kolarik, 1981]. Significantly lower distribution ratios for Pu(IV) were obtained after 10 minutes contact time (Table 4.1). The main reason for inconsistency of distribution ratios for low nitric acid concentration is disproportionation of Pu(IV) and formation of non-extractable Pu(III) and partially extractable Pu(VI). The processes affecting extraction and speciation of Pu at low nitric acid concentration will be discussed later in 6.2.

Table 4.1 Distribution ratios of Pu(IV) (Pu-239, ~1×10^{-7} M) from various HNO_3, $LiNO_3$ and AHA concentrations after 4 minutes mixing (*10 minutes mixing), experimental vs. calculated values.

$[HNO_3]$ (M)	$[LiNO_3]$ (M)	$[NO_3]$ total	[AHA] (M)	D(Pu(IV)) exp
0.10	-	0.10	-	2.13E-01
0.20	-	0.20	-	5.35E-01
0.40	-	0.40	-	1.34E+00
0.60	-	0.60	-	2.16E+00
0.80	-	0.80	-	3.48E+00
1.00	-	1.00	-	4.24E+00
1.00	-	1.00	-	5.29E+00
1.00	-	1.00	-	4.24E+00
1.01	-	1.01	-	3.87E+00
1.00	-	1.00	-	3.83E+00
1.00	-	1.00	-	3.83E+00
1.00	-	1.00	-	4.24E+00
1.00	-	1.00	-	4.68E+00
0.10	-	0.10	-	*3.00E-02
0.20	-	0.20	-	*8.00E-02
0.40	-	0.40	-	*4.00E-01
0.60	-	0.60	-	*1.15E+00
0.80	-	0.80	-	*1.67E+00
1.00	-	1.00	-	*2.12E+00
1.00	-	1.00	-	*2.52E+00
2.00	-	2.00	-	8.86E+00
2.00	-	2.00	-	8.76E+00
2.99	-	2.99	-	1.61E+01
3.00	-	3.00	-	1.59E+01
4.00	-	4.00	-	2.42E+01
4.03	-	4.03	-	2.40E+01
5.00	-	5.00	-	3.76E+01
5.02	-	5.02	-	3.69E+01
6.00	-	6.00	-	4.43E+01
6.01	-	6.01	-	4.50E+01
7.03	-	7.03	-	4.68E+01
8.06	-	8.06	-	4.63E+01
8.99	-	8.99	-	3.14E+01
10.02	-	10.02	-	3.10E+01
10.96	-	10.96	-	1.57E+01
11.98	-	11.98	-	1.21E+01
0.50	0.48	0.98	-	4.69E+00
0.50	0.48	0.98	-	3.27E+00
0.50	1.45	1.95	-	1.01E+01
0.50	1.45	1.95	-	6.34E+00

[HNO_3] (M)	[$LiNO_3$] (M)	[NO_3] total	[AHA] (M)	D(Pu(IV)) exp
0.50	2.43	2.93	-	1.99E+01
0.50	2.43	2.93	-	1.45E+01
0.50	3.41	3.91	-	9.47E+01
0.50	3.41	3.91	-	8.08E+01
0.50	4.39	4.89	-	4.56E+02
0.50	4.39	4.89	-	3.46E+02
0.50	5.36	5.86	-	3.03E+02
1.00	0.98	1.98	-	1.25E+01
1.00	0.98	1.98	-	1.25E+01
1.00	1.95	2.95	-	2.57E+01
1.00	1.95	2.95	-	2.55E+01
1.00	2.92	3.92	-	9.14E+01
1.00	2.92	3.92	-	8.86E+01
1.00	3.89	4.89	-	2.66E+02
1.00	3.89	4.89	-	2.43E+02
1.00	4.87	5.87	-	1.08E+02
1.00	4.87	5.87	-	1.05E+02
2.00	0.96	2.96	-	1.85E+01
2.00	1.93	3.93	-	4.45E+01
2.00	2.91	4.91	-	1.04E+02
2.00	3.89	5.89	-	1.87E+02
2.00	4.86	6.86	-	2.18E+02
2.00	5.84	7.84	-	3.41E+02
0.10	-	0.10	4.0E-01	3.64E-04
0.20	-	0.20	4.0E-01	1.75E-03
0.40	-	0.40	4.0E-01	8.37E-03
0.60	-	0.60	4.0E-01	1.97E-02
0.80	-	0.80	4.0E-01	3.42E-02
1.00	-	1.00	4.0E-01	6.49E-02
1.00	-	1.00	4.0E-01	5.03E-02
1.01	-	1.01	4.0E-01	6.03E-02
2.00	-	2.00	4.0E-01	1.13E-01
2.00	-	2.00	4.0E-01	1.21E-01
2.99	-	2.99	4.0E-01	2.00E-01
3.00	-	3.00	4.0E-01	2.16E-01
4.00	-	4.00	4.0E-01	3.89E-01
4.03	-	4.03	4.0E-01	3.53E-01
5.00	-	5.00	4.0E-01	1.65E+00
5.02	-	5.02	4.0E-01	1.56E+00
6.00	-	6.00	4.0E-01	4.90E+00
6.01	-	6.01	4.0E-01	4.47E+00
0.50	0.48	0.98	4.0E-01	5.62E-02
0.50	1.45	1.95	4.0E-01	3.65E-01

[HNO_3] (M)	[$LiNO_3$] (M)	[NO_3] total	[AHA] (M)	D(Pu(IV)) exp
0.50	2.43	2.93	4.0E-01	1.03E+00
0.50	3.41	3.91	4.0E-01	2.97E+00
0.50	4.39	4.89	4.0E-01	6.05E+00
1.00	0.98	1.98	4.0E-01	2.40E-01
1.00	1.95	2.95	4.0E-01	6.75E-01
1.00	2.92	3.92	4.0E-01	1.67E+00
1.00	2.92	3.92	4.0E-01	1.66E+00
1.00	3.89	4.89	4.0E-01	4.03E+00
1.00	3.89	4.89	4.0E-01	4.01E+00
1.00	4.87	5.87	4.0E-01	8.35E+00
1.00	4.87	5.87	4.0E-01	8.22E+00
2.00	0.98	2.98	4.0E-01	3.90E-01
2.00	1.93	3.93	4.0E-01	9.43E-01
2.00	2.91	4.91	4.0E-01	2.32E+00
2.00	3.89	5.89	4.0E-01	5.97E+00
2.00	4.87	6.87	4.0E-01	1.73E+01
1.00	-	1.00	1.7E-03	3.75E+00
1.00	-	1.00	8.9E-03	2.88E-01
1.00	-	1.00	2.7E-02	1.64E-01
1.00	-	1.00	5.3E-02	1.25E-01
1.00	-	1.00	8.0E-02	1.03E-01
1.00	-	1.00	1.1E-01	9.35E-02
1.00	-	1.00	2.4E-01	4.98E-02
1.00	-	1.00	4.0E-01	6.49E-02
1.00	-	1.00	8.3E-01	3.37E-02
0.10	1.00	1.10	-	1.90E+00
0.10	1.00	1.10	-	1.40E+00
0.20	1.00	1.20	-	3.36E+00
0.20	1.00	1.20	-	2.66E+00
0.40	1.00	1.40	-	5.89E+00
0.40	1.00	1.40	-	4.98E+00
0.60	1.00	1.60	-	7.47E+00
0.60	1.00	1.60	-	6.81E+00
0.80	1.00	1.80	-	1.01E+01
0.80	1.00	1.80	-	8.27E+00
1.00	1.00	2.00	-	1.28E+01
1.00	1.00	2.00	-	1.06E+01
2.00	1.00	3.00	-	2.44E+01
3.01	1.00	4.01	-	3.50E+01
4.00	1.00	5.00	-	4.43E+01
5.01	1.00	6.01	-	6.06E+01
6.00	1.00	7.00	-	6.36E+01
7.01	1.00	8.01	-	5.88E+01

[HNO_3] (M)	[$LiNO_3$] (M)	[NO_3] total	[AHA] (M)	D(Pu(IV)) exp
8.00	1.00	9.00	-	4.30E+01
8.99	1.00	9.99	-	2.94E+01
10.00	1.00	11.00	-	1.93E+01
10.99	1.00	11.99	-	1.38E+01
12.00	1.00	13.00	-	1.05E+01
1.00	-	1.00	1.1E-04	7.86E+00
1.00	-	1.00	3.3E-04	7.55E+00
1.00	-	1.00	7.8E-04	5.83E+00
1.00	-	1.00	8.0E-04	2.17E+00
1.00	-	1.00	1.0E-03	1.94E+00
1.00	-	1.00	1.7E-03	3.75E+00
1.00	-	1.00	3.0E-03	9.25E-01
1.00	-	1.00	6.0E-03	5.93E-01
1.00	-	1.00	8.5E-03	4.66E-01
1.00	-	1.00	8.9E-03	2.88E-01
1.00	-	1.00	2.7E-02	1.64E-01
1.00	-	1.00	5.3E-02	1.25E-01
1.00	-	1.00	8.0E-02	1.03E-01
1.00	-	1.00	1.0E-01	8.70E-02
1.00	-	1.00	1.1E-01	9.35E-02
1.00	-	1.00	1.5E-01	7.78E-02
1.00	-	1.00	2.0E-01	6.79E-02
1.00	-	1.00	2.4E-01	4.98E-02
1.00	-	1.00	3.0E-01	6.38E-02
1.00	-	1.00	4.0E-01	5.60E-02
1.00	-	1.00	4.0E-01	5.03E-02
1.00	-	1.00	4.0E-01	6.49E-02
1.00	-	1.00	5.0E-01	5.24E-02
1.00	-	1.00	6.0E-01	4.51E-02
1.00	-	1.00	7.0E-01	4.13E-02
1.00	-	1.00	8.3E-01	3.37E-02

4.3. Distribution ratios of Pu(IV) between nitrate, AHA and TBP

Addition of AHA causes a significant decrease of distribution ratios of plutonium due to hydrophilic Pu-acetohydroxamate complexes formed in the aqueous phase (Table 4.1; Figures 4.2-4.4). Obviously, despite the presence of AHA, the most important factor affecting the extraction of Pu(IV) is the concentration of HNO_3 and total nitrate. At concentrations of 0.1M HNO_3 and 0.4M HAHA, distribution ratio of Pu(IV) drops down to ~$3.6x10^{-4}$, while at 1M HNO_3 is almost 200x higher. On the other hand, increasing of HNO_3 concentration leads to

higher Pu extraction due to protonation and hydrolysis of HAHA. Even relatively low concentrations of HAHA (10^{-2}M in 1M HNO_3) lower the extraction of Pu(IV) by a factor of more than 10. Addition of $LiNO_3$ to the aqueous solution containing Pu, HNO_3, and HAHA increases the distribution ratio (Figure 4.2) the same way as it does in the absence of HAHA. On the other hand, the distribution data for Pu(IV) from 0.5M HNO_3, 0.3M HAHA, and various concentration of $NaNO_3$ reported by [Karraker, 2002], decrease with increasing total nitrate concentration, and are in strong discrepancies with our experimental data (Figure 4.2). As the author in his paper commented, such a behavior was not expected and it was explained by possible changes in the activity of HAHA after addition of $NaNO_3$. However, our experimental data for constant (0.5; 1 and 2M) concentrations of HNO_3, 0.4M HAHA and various concentration of $LiNO_3$ show a simultaneous increase of Pu(IV) extraction yield with increased concentration of $LiNO_3$ and dominant salting out effect of nitrate on extraction of Pu(IV).

A steep reduction of extraction yields of tetravalent plutonium from 1M HNO_3 by 30% TBP in *n*-dodecane upon addition of acetohydroxamic acid is displayed in Figure 4.4. Already a very small concentration of acetohydroxamic acid reduces the extraction yield of Pu dramatically due to the formation of a strong Pu-acetohydroxamate complex in aqueous solution. Another reason for decrease of distribution ratios for plutonium in the presence of HAHA is reduction of Pu(IV) and formation of Pu(III) in the aqueous phase. Our preliminary results on reduction of Pu(IV) in the presence of acetohydroxamic acid shows that reduction is significantly faster than it was expected. At low HAHA/Pu(IV) ratio, the amount of Pu(III) produced within 5-10 minutes after addition of HAHA can be as much as 15-20%. These data were obtained from stationary experiments, however it is expected that vigorous mixing will accelerate the reduction of Pu(IV) even more.

4.4. Distribution ratios of Pu(IV) between nitrate and TBP. Effect of temperature

In order to facilitate large-scale industrial applications of liquid-liquid separation processes, knowledge of the thermodynamic constants associated with the distribution of metal ions between immiscible media is necessary. The enthalpy and entropy constants derived for the

distribution reaction of metal neutral complexes give important information about hydration and organic phase salvation [Rydberg et al., 2004]; however, very few investigations have been dedicated to this problem. To date, the data reported [Moiseenko & Rozen, 1960; Ramanujan et al., 1978; Kolarik, 1984] concerning the effect of temperature on extraction of plutonium under PUREX conditions has been contradictory. Table 4.2 compares selected distribution data. Moiseenko & Rozen [1960] found that increasing temperature decreases the distribution of Pu(IV) while Kolarik [1984] and Ramanujan *et al.*[1978] argue the opposite trend at acid concentrations below 6*M*. Danesi *et al.* [1965] studied the effect of temperature on the extraction of plutonium nitrates into long chain amines and found the distribution to decrease with temperature. Also, the extraction of Pu(VI) from nitric acid into TBP was found to decrease with according to Sajun *et al*. [1981].

Table 4.2 Comparison of selected literature on the distribution of Pu(IV) into TBP from ~1M HNO_3 at various temperatures.

[Rydberg, 2004]		[Moiseenko, 1960]		[Kolarik, 1984]		[Ramanujan, 1978]	
T/K	$D_{Pu(IV)}$	T/K	$D_{Pu(IV)}$	T/K	$D_{Pu(IV)}$	T/K	$D_{Pu(IV)}$
293	1.4	293	2.8	283	2.3	294	1.4
303	1.3	303	3.0	298	2.8	303	0.6
323	1.2	313	3.2	333	3.7	313	0.3

The mechanism by which Pu(IV) is extracted into TBP was assumed to be similar to that of hexavalent uranium [Rydberg *et al.*, 2004] The plutonium in aqueous solutions is complexed with neutral aqua ligands. The nitrate ions then fill the four valence shells as bidentate ligands and two TBP molecules form the adduct complex $Pu(NO_3)_4 \cdot TBP_2$. The rate determining step is the transfer of the plutonium complex from the aqueous phase into the organic phase.

$$Pu(NO_3)_4 \cdot TBP_{2,aq} \rightarrow Pu(NO_3)_4 \cdot TBP_{2,or} \tag{4.1}$$

The equilibrium constant at specific temperatures, $K_{ex(T)}$, for the complexation of Pu(IV) by TBP is:

$$K_{ex}(T) = \frac{[Pu(NO_3)_4 \cdot TBP_2][H_2O]^n}{[Pu^{4+}(H_2O)_n][NO_3^-]^4[TBP_f]^2} \frac{\gamma_{Pu(NO_3)_4 \cdot TBP_2} \gamma_{H_2O}^n}{\gamma_{Pu^{4+}(H_2O)_n} \gamma_{NO_3^-}^4 \gamma_{TBP_f}^2} \tag{4.2}$$

The distribution coefficient of Pu(IV) is defined as the concentration ratio of plutonium in the organic and aqueous phases, or

$$D_{Pu(IV)} = \frac{[Pu(IV)]_{or}}{[Pu(IV)]_{aq}}. \tag{4.3}$$

The equilibrium constant $K_{ex}(T)$ from equation (4.2), can be defined also as:

$$K_{ex}(T) = \frac{D_{Pu(IV)}[H_2O]^n}{[NO_3^-]^4[TBP_f]^2}(1 + \beta_1\{NO_3^-\} + \beta_2\{NO_3^-\}^2) \frac{\gamma_{Pu(NO_3)_4 \cdot TBP_2} \gamma_{H_2O}^n}{\gamma_{Pu^{4+}(H_2O)_n} \gamma_{NO_3^-}^4 \gamma_{TBP_f}^2} \tag{4.4}$$

where γ represents the activity coefficients of each species and T is the absolute temperature (K) of the extraction reaction. The activity coefficients of plutonium in the organic phase and TBP_f are assumed to be one. The activity coefficients of Pu^{4+} were estimated using specific ion interaction theory (SIT) and the approach of chemical analogs and similar behavior of tetravalent thorium and plutonium. The SIT interaction parameter, Δε, was chosen to be 0.31 as reported by Neck *et al*. [2006] for thorium solutions. The influence of temperature on the stability constants β_1 and β_2 should be considered. Numerous studies [Grenthe & Noren, 1960; Laximinarayanan et al., 1964; Danesi et al., 1966; Shilin & Nazarov, 1966; Moskvin, 1969, 1971; Lahr & Knock, 1970; Baqawde et al., 1976] have been conducted on the plutonium-nitrate system but to our knowledge, none have investigated the effects of temperature on the nitrate complexation with Pu(IV). This work assumes β_1 and β_2 to be dependent on ionic strength but independent of temperature as well as the concentration of water and the dehydration energy of Pu(IV). Eq. (4.4) can then be written as:

$$K_{ex}(T) = \frac{D_{Pu(IV)}}{[NO_3^-]^4[TBP_f]^2}\left(1 + \beta_1\{NO_3^-\} + \beta_2\{NO_3^-\}^2\right) \frac{1}{\gamma_{Pu^{4+}} \gamma_{NO_3^-}^4} \tag{4.5}$$

To calculate thermodynamic characteristics, equilibrium constants were determined at different temperatures. Using the equation for Gibbs energy

$$\Delta G^o = -RT \ln K_{ex}(T) \tag{4.6}$$

and:

$$\Delta G^o = \Delta H^o - T\Delta S^o \tag{4.7}$$

a Van't Hoff plot of the natural logarithm of K_{ex}(T) versus the inverse temperature will yield a slope proportional to the enthalpy and an intercept proportional to the entropy.

Experimental data show that the distribution of Pu(IV) is a complex process. Figure 4.5 plots the distribution as a function of agitation time at various nitric acid concentrations. The distribution decreases with time because of the production of an inextractable species of plutonium at concentrations of 1M and below. It was assumed that 4 min. extraction time was sufficient to achieve equilibrium at acid concentrations $\geq 2M$. Values of $D_{Pu(IV)}$ as a function of nitric acid concentration are shown in Figure 4.6. As the concentration of nitric acid increases, the distribution of Pu(IV) increases until a maximum of approximately 7M HNO_3. Beyond 7M, the distribution of Pu(IV) begins to decrease as the majority of the TBP is complexed with nitric acid. Table 4.3 specifically lists the forward and back extraction values at nitrate concentrations between 2M – 5M for each temperature.

Table 4.3 The distribution of Pu(IV) for nitrate concentrations between 2*M* – 5*M*. (D_{Pu}^{I}) forward extractions; (D_{Pu}^{II}) back extractions.

HNO_3, M	$LiNO_3$, M	Total NO_3^-, M	T/K=294			T/K=303			T/K=313		
			$D_{Pu\ I}$	$D_{Pu\ II}$	D_{Pu} average	$D_{Pu\ I}$	$D_{Pu\ II}$	D Pu average	$D_{Pu\ I}$	$D_{Pu\ II}$	D Pu average
2.0	-	2.0	6.1	5.7	5.9±0.3	3.7	3.7	3.7±0.0	2.4	2.2	2.3±0.2
2.4	-	2.4	11.3	9.6	10.5±1.2	8.5	7.3	7.9±0.8	6.6	4.3	5.4±1.7
2.9	-	2.9	12.1	12.5	12.3±0.3	11.2	11.5	11.4±0.2	8.3	8.8	8.5±0.4
3.4	-	3.4	16.2	16.0	16.1±0.1	15.9	15.5	15.7±0.3	14.7	16.5	15.6±1.3
3.9	-	3.9	19.1	18.6	18.9±0.3	18.9	21.3	20.1±1.7	18.7	21.3	20.0±1.8
4.9	-	4.9	26.3	30.5	28.4±3.0	26.1	29.5	27.8±2.4	25.1	31.3	28.2±4.4
2.0	0.5	2.5	12.3	9.4	10.9±2.0	8.0	6.1	7.1±1.4	5.3	2.6	4.0±1.9
2.0	1.0	3.0	18.4	16.0	17.2±1.7	15.1	13.1	14.1±1.4	9.6	8.1	8.9±1.0
2.0	1.5	3.5	27.8	26.2	27.0±1.1	22.8	19.1	20.9±2.7	17.9	15.9	16.9±1.5
2.0	2.0	4.0	38.2	39.0	38.6±0.6	34.5	32.0	33.3±1.7	28.8	32.1	30.4±2.4
2.0	3.0	5.0	68.5	89.8	79.2±15.1	59.5	84.1	71.8±17.4	57.0	88.9	72.9±22.5

From the distribution data, the equilibrium constants at each temperature can be calculated using Eq. (4.5). Bromley's method [Bromley, 1973] was used to calculate the activities of nitrates in solution; SIT found the variations in activities with temperature. The concentration of TBP_f, β_1 and β_2 as a function of nitrate concentration were reported in the recent work [Tkac et al., 2009] and were employed in calculation of the equilibrium constant at a given temperature.

Table 4.4 lists the activities of Pu^{4+}, nitrate, TBP_f concentrations and the calculated equilibrium constants at different temperatures. It can be seen that the extraction equilibrium constants change with nitrate concentration. This behavior was also reported by Moiseenko & Rozen [1960]. The gradient is likely associated with some error in the activity coefficient assumptions, such as assuming the organic solution activities of TBP_f and $Pu(NO_3)_4 \cdot TBP_2$ to be set equal to one. As it was mentioned before, no sufficient literature exists on the values of plutonium-nitrate stability constants at different temperatures; therefore, all β were assumed independent of temperature. The behavior of $\ln K_{ex}(T)$ with nitrate concentration, however, is linear and can be extrapolated to $[NO_3^-] = 0M$ where the activity coefficient is equal to one. Using computer software, linear trends can be fit to give the extrapolated equilibrium constants for each temperature. The extrapolated $\ln K_{ex}^0(T)$ values are listed in Table 4.4.

Table 4.4 Parameters used to calculated equilibrium constants and Gibbs free energies for various nitric acid concentrations.

HNO_3, M	TBP, M	$\gamma\ Pu^{4+}$	$\{NO_3^-\}$	ln $K_{ex}(T)$			T/K	T/K	T/K
				T/K 294	T/K 303	T/K 313	294	303	313
2.0	0.45	0.0010	1.75	12.0	11.4	11.0			
2.3	0.35	0.0012	2.06	12.7	12.4	12.0	ln $K_{ex}^0(T)$		
2.9	0.24	0.0016	2.86	12.8	12.7	12.4	10.1	9.4	8.7
3.4	0.18	0.0020	3.59	13.2	13.2	13.2			
3.9	0.13	0.0024	4.54	13.7	13.7	13.7	$\Delta G(T)$/kJ·mol^{-1}		
4.9	0.07	0.0033	6.68	14.9	13.6	14.9	-24.8	-23.8	-22.6

Plotting the natural logarithm of $K_{ex}^0(T)$ versus inverse temperature, as in Figure 4.7, reveals a line ($R^2 = 0.99$) with a slope and intercept of 6.99 and -13.6, respectively. These parameters

yield ΔH = -58.1 kJ·mol^{-1} and ΔS = -113 J·mol^{-1}·K^{-1} which suggest an exothermic reaction that should be, according to Eq. (4.7), less spontaneous with increasing temperature. This trend is in agreement with the decreasing distribution values at higher temperatures. The values calculated for $\Delta G(T)$ are listed in Table 4.4. Moiseenko & Rozen [1960] reported an enthalpy of -25.1 kJ·mol^{-1} without an entropy value for a similar system containing 20 vol. % TBP in kerosene.

Salting-out agents can vastly increase the distribution of Pu(IV). The addition of an inextractable nitrate salt, in this case lithium nitrate, lowers the concentration of nitric acid while keeping the total nitrate concentration high. Systems containing 2M HNO_3 and 1M – 3M $LiNO_3$ were used to analyze the distribution of Pu(IV). Table 4.3 lists values of $D_{Pu(IV)}$ for systems containing lithium nitrate. The equilibrium constants at each nitrate concentration and temperature were calculated using Eq. (4.5) and are listed in Table 4.5.

Table 4.5 Parameters used to calculated equilibrium constants and Gibbs free energies for various nitric acid concentrations.

NO_3^-	TBP	γ Pu^{4+}			$\{NO_3^-\}$			T/K	T/K	T/K
M	M	T/K 294	T/K 303	T/K 313	T/K 294	T/K 303	T/K 313	294	303	313
2.0	0.45	0.0009	0.0008	0.0006	1.62	1.62	1.63			
2.5	0.36	0.0011	0.0010	0.0007	2.32	2.30	2.27	$\ln K_{ex}^0(T)$		
3.0	0.29	0.0013	0.0012	0.0009	3.18	3.15	3.11	10.4	9.5	8.7
3.5	0.24	0.0017	0.0015	0.0011	4.17	4.14	4.10			
4.0	0.19	0.0020	0.0018	0.0014	5.25	5.21	5.16	$\Delta G(T)$/kJ·mol^{-1}		
5.0	0.13	0.0031	0.0027	0.0022	7.74	7.69	7.63	-25.2	-24.0	-22.7

Plotting the natural logarithm of the equilibrium constants as a function of nitrate concentration, as in Figure 4.8, produces three isothermal trends that can be extrapolated to $[NO_3^-]$ = 0M (R^2 = 0.99 for all temperatures). The Van't Hoff plot for this system is shown in Figure 4.7 (R^2 = 0.99). The enthalpy and entropy were calculated to be -62.8 kJ·mol^{-1} and -128 J·mol^{-1}·K^{-1}, respectively. It should be reinstated that the distribution ratios at a constant nitrate concentration are much higher for systems with added nitrate than those with nitric acid only on account of the increased nitrate and TBP_f concentrations. The thermodynamic characteristics,

however, should be similar. Therefore, an average enthalpy and entropy can be calculated from the two systems: ΔH = -60.4 ± 3.34 kJ·mol^{-1} and ΔS = -120 ± 10.6 J·mol^{-1}·K^{-1}.

5. Modeling of distribution ratios of plutonium(IV)by TBP

5.1. Introduction

Modeling of distribution ratios for Pu(IV) from nitric acid by TBP is very important for prediction of extraction behavior under various initial conditions without requiring additional experiments. In order to calculate the distribution ratio of Pu(IV), all metal species present in the aqueous and organic phases must be taken into account. To determine the speciation distribution of Pu(IV) in aqueous solutions containing nitric acid from low to moderate concentrations, at least the first two stability constants of hydroxo complexes and nitrate complexes of Pu(IV) must be applied. Determination of the stability constants for ternary hydroxonitrate complexes of Pu(IV) is complicated due to very complex chemistry of plutonium. Also the previously reported values of stability constants for the $Pu(OH)^{3+}$, $Pu(OH)_2^{2+}$, $Pu(NO_3)^{3+}$ and $Pu(NO_3)_2^{2+}$ complexes must be applied with care.

Several modeling approaches of extraction processes developed in the US were recently reported in the literature; for example, AMUSE (Argonne Model for Universal Solvent Extraction), SX Solver [Lumetta, 2002] and SXLSQI [Kang et al., 2005]. The models differ mainly by the way that species activities in the aqueous and organic phase are evaluated, including the activities of water and the organic solvent. AMUSE is a process modeling tool, whereas SX Solver and SXLSQI are equilibrium modeling programs. The latter two applications differ in the way the aqueous activities are calculated. SX Solver and AMUSE use the same methodology for calculation of aqueous-phase activities.

Here, we report our attempt to develop a computational model of distribution ratios of Pu(IV) evaluating the speciation of Pu(IV) in the HNO_3/TBP extraction system and applying the mean aqueous activity coefficients of species and critically evaluated stability constants. Comparison of the calculated values with the experimental results and previously-reported data [Petrich & Kolarik, 1998; Karraker, 2001] for the distribution ratios of Pu(IV) for a set of various concentrations of HNO_3 and $LiNO_3$ are discussed.

5.2. Speciation of Pu(IV) in the aqueous phase

The highly-charged cation Pu^{4+} hydrolyzes more readily than any other of the plutonium species and undergoes hydrolysis in aqueous solution even under relatively high acidic conditions. The hydrolysis constant for the tetravalent actinides increases in the order of decreased ionic radius and increasing Lewis acidity from Th(IV) to Pu(IV) [Walther et al., 2007]: Th(IV) < U(IV) < Np(IV) < Pu(IV). The hydrolysis reaction of Pu(IV) can be written as:

$$Pu^{4+} + xH_2O \Leftrightarrow Pu(OH)_x^{4-x} + xH^+ \tag{5.1}$$

The apparent constant of hydrolysis K_H is given by:

$$K_{H,x} = \frac{[Pu(OH)_x^{4-x}]\cdot[H^+]^x}{[Pu^{4+}]} \tag{5.2}$$

with the corresponding formation constants β of plutonium(IV) hydroxo-complex:

$$\beta_x = \frac{[Pu(OH)_x^{4-x}]}{[Pu^{4+}]\cdot[OH^-]^x} \tag{5.3}$$

Reliable thermodynamic data for Pu(IV) are difficult to obtain because of the complicated redox chemistry of plutonium, i.e., Pu(III), Pu(IV), Pu(V), and Pu(VI) are known to co-exist in aqueous solutions. The determination of thermodynamic data of Pu(IV) is further complicated by hydrolysis even at low pH (pH ~ 1) and the formation of polymeric/colloidal species. A number of studies on the hydrolysis constants for mononuclear species, $Pu(OH)_x^{4-x}$ (x = 1 to 4), have been performed over recent decades and are well summarized by [Lemire et al., 2001] and later updated by [Guillaumont et al., 2003]. The methods frequently used for determination of the hydrolysis constant are Vis-NIR spectroscopy, solvent extraction and potentiometry. Since the

solubility of Pu(IV) hydroxide is low, the ability to investigate its aqueous speciation by spectroscopic techniques is rather poor [Neck and Kim, 2001]. As the Pu^{4+} ion undergoes hydrolysis reactions even at low pH, the solubility product evaluated from experimental solubility data depends directly on the hydrolysis constants applied to calculate the Pu^{4+} concentration [Knopp et al., 1999].

The Pu(IV) hydrolysis in weakly acidic solutions leads to polynucleation, which grows further to colloidal aggregation [Johnson & Toth, 1998]. As demonstrated by [Kim & Kanellakopulos, 1989], colloidal Pu(IV) can be produced even at pH 0 to 1 at the Pu concentrations below 10^{-3} $mol \cdot L^{-1}$. Colloids may be considered as long-lived metastable amorphous particles. They remain stable in solution, devoid of precipitation from oversaturated solutions, and lead to apparent Pu(IV) concentrations significantly exceeding the thermodynamic solubility. Investigation of plutonium chemistry by conventional absorption spectroscopy requires a concentration of (10^{-4} to 10^{-3}) $mol \cdot L^{-1}$, which considerably exceeds the solubility limit of the Pu(IV) hydrous oxides at pH = 1 to 2 [Walther et al., 2007]. When the concentration exceeds the solubility limit, the formation of Pu(IV) colloids, which remain in solution without precipitation, is the predominant reaction [Neck and Kim, 2001]. The formation of colloids at higher Pu concentrations and higher pH can lead to inaccurate interpretation of experimental results. Therefore, more satisfactory data on hydrolysis constants can be obtained by solvent extraction using trace concentrations of Pu. Metivier and Guillaumont, 1972 applied solvent extraction with Pu-238 to measure all four constants of plutonium hydrolysis: K_{H1}=0.355; K_{H2}=0.178; $K_{H3}=5.01\times10^{-4}$ and $K_{H4}=5.01\times10^{-7}$. As can be seen from Table 5.1, where several earlier literature data are summarized, their constants differ by an order of magnitude from the others reported; however, the solubility of amorphous $Pu(OH)_4$ in the range of pH=0 to 12 determined by [Knopp et al., 1999] agrees very well with the pH-dependence predicted by the hydrolysis constants determined by [Metivier & Guillaumont, 1972].

In order to obtain a complete set of formation constants for mononuclear species $An(OH)_n^{4-n}$, Neck and Kim, 2001 estimated the unknown constants by applying two different methods based on: (i) an empirical inter-correlation between hydrolysis constants of actinide ions at different oxidation states, and (ii) a semi-empirical approach, in which the decrease of stepwise complexation constants for a given metal-ligand system is related to the increasing electrostatic

repulsion between the ligands. For Pu(IV), the estimated values [Neck and Kim, 2001] were close to experimental values determined by [Metivier and Guillaumont, 1972], which are considered to be the most reliable data on hydrolysis of tetravalent plutonium by these and other authors now [Walther et al., 2007; Guillaumont et al., 2003; Knopp et al., 1999]. Therefore; the speciation and extraction model of Pu(IV) in the mixed electrolyte $HNO_3/LiNO_3$ presented in this paper employs the first two hydrolysis constants determined by [Metivier and Guillaumont, 1972].

Table 5.1 Review of Pu(IV) hydrolysis constants

Ionic strength mol·L^{-1}	Medium	log K_{H1}	log K_{H2}	Ref.
1	$HClO_4/LiClO_4$	-0.45	-1.2	[Metivier & Guillaumont, 1972]
2	$HClO_4/LiClO_4$	-1.26	-	[Rabideau, 1957]
2	$HClO_4/NaClO_4$	-1.73	-1.94	[Rabideau & Kline, 1960]
0.5	HCl/NaCl	-1.65	-	[Kraus & Nelson, 1950]
0.5	$HClO_4/NaClO_4$	-1.60	-	[Kraus & Nelson, 1950]
1	$HClO_4/NaClO_4$	-1.51	-	[Rabideau & Lemons, 1951]
0.5	$HClO_4/NaClO_4$	-1.57	-	[Yusov et al., 2004]
0.1	$HClO_4/NaClO_4$	-1.2	-	[Yusov et al., 2004]
0.19	$HClO_4$	-1.96	-	[Cleveland, 1968]
0.06	$HClO_4$	-1.48	-	[Cleveland, 1968]

Increasing the nitric acid concentration and/or addition of non-extractable nitrate salts to the aqueous phase suppresses hydrolysis of Pu(IV) and favors formation of nitrate complexes. Determination of formation constants for weak complexes, such as Pu nitrate complexes, is limited, because it is difficult to maintain constant ionic strength (IS) due to the necessity to use high concentrations of the ligand [Spahiu & Puigdomenech, 1998]. It is also important to note that at I>0.1 mol·L^{-1}, activity coefficients depend not only on the ionic strength but also on the composition of the electrolyte medium [Spahiu & Puigdomenech, 1998], so the earlier assumption that the equilibrium constant at the same ionic strength but in different background electrolytes is the same is not valid.

A number of speciation studies reporting application of various modern methods (Vis-NIR, NMR, EXAFS and computer modeling) to investigate the complexation between tetravalent plutonium and nitrate in aqueous solutions were recently published [Spahiu & Puigdomenech, 1998, Veirs et al., 1994; Allen et al., 1996; Berg et al., 1998, 2000]. Only four major species of tetravalent plutonium, the mono-, di-, tetra- and hexanitrate complexes ($Pu(NO_3)^{3+}$, $Pu(NO_3)_2^{2+}$, $Pu(NO_3)_4$, $Pu(NO_3)_6^{2-}$) were identified as the major species present over a wide range of concentration of nitric acid [Veirs et al., 1994]. However, only the presence of $Pu(NO_3)_6^{2-}$ at nitric acid concentrations above 10 $mol \cdot L^{-1}$ may be considered as well established. Numerous studies provided evidence for the existence of Pu(IV)-nitrate complexes with coordination numbers lower than six, particularly plutonium mono- and dinitrate species. The stability constants for the first two Pu(IV)-nitrate complexes determined by simultaneous analysis of spectra at multiple wavelengths in the ionic strength range of IS=(0.3 to 19) $mol.kg^{-1}$ are discussed in the paper of [Berg et al., 1998]. In that work each formation constant was corrected for the incomplete dissociation of nitric acid using the specific ion interaction theory (SIT) [Grenthe & Puigdomenech, 1997]. According to literature data, no good values for the higher Pu-nitrate complexes exist, and it is assumed that in the considered concentration range of (0.1 to 4) $mol \cdot L^{-1}$ NO_3^- only mono and di-nitrate species of Pu(IV) are present in aqueous solution:

$$Pu^{4+} + NO_3^- \Leftrightarrow Pu(NO_3)^{3+} \tag{5.4}$$

$$Pu^{4+} + 2NO_3^- \Leftrightarrow Pu(NO_3)_2^{2+} \tag{5.5}$$

As a result of all the issues identified for interpretation of the hydrolysis constants of Pu(IV) and the formation constants of Pu(IV) nitrates, we attempted to estimate the speciation of Pu(IV) in aqueous solutions by selecting the critically evaluated and best available values of the constants employed in the calculations. The stability constants $\log \beta^0_1$=2.12 and $\log \beta^0_2$=3.66 for the $Pu(NO_3)^{3+}$ and $Pu(NO_3)_2^{2+}$ complexes reported by [Berg et al, 1998], together with thermodynamic hydrolysis constants $\log K^0_{H1}$=0.6, $\log K^0_{H2}$=0.63 obtained by [Metivier and Guillaumont, 1972] were selected for our modeling work. Both hydrolysis and complexation constants were adjusted for changing ionic strength by the SIT approach.

5.3. Extraction of nitric acid by TBP

A very important factor in the modeling of the extraction of metals is the calculation of the free extractant concentration available for the metal complexation. Tri-*n*-butyl phosphate extracts a significant amount of HNO_3; hence, speciation of HNO_3 in the organic phase was studied extensively and several models were proposed by various authors [Chaiko & Vandegrift, 1988; Naganawa & Tachimori, 1993]. Equilibrium of HNO_3 between aqueous and organic TBP-*n*-dodecane phases was successfully modeled by [Chaiko & Vandegrift, 1988]. Extraction of nitric acid by TBP can be expressed by the following reaction equilibria (eqs 5.6-5.8):

$$H^+ + NO_3^- + \overline{TBP} \overset{KT_1}{\Leftrightarrow} \overline{TBP \cdot HNO_3} \tag{5.6}$$

$$H^+ + NO_3^- + 2\overline{TBP} \overset{KT_2}{\Leftrightarrow} \overline{TBP_2 \cdot HNO_3} \tag{5.7}$$

$$H^+ + NO_3^- + \overline{TBP \cdot HNO_3} \overset{KT_3}{\Leftrightarrow} \overline{TBP \cdot 2HNO_3} \tag{5.8}$$

where the over-bars represent species in the organic phase. Depending on the total nitrate and hydrogen ion concentrations, three complexes between TBP and HNO_3 can be formed (eqs 6-8) with extraction equilibrium constants determined [Chaiko & Vandegrift, 1988]: (KT_1=0.185; KT_2=0.444 L·mol^{-1} and KT_3= 1×10^{-4}), respectively. At various concentrations of HNO_3 and NO_3^- in the aqueous phase, different species in the organic phase are formed. Formation of the TBP·2HNO_3 complex in a considerable amount is relevant only to a nitric acid concentration above 6 mol·L^{-1}. TBP_f, the fraction of TBP non-complexed with HNO_3 and available for metal extraction will be much lower in the system with a high nitrate concentration. The mass balance of tri-*n*-butyl phosphate can be defined as follows:

$$\begin{aligned}[\overline{TBP}]_f &= [\overline{TBP}]_T - [\overline{TBP \cdot HNO_3}] - 2[\overline{TBP_2 \cdot HNO_3}] - [\overline{TBP \cdot 2HNO_3}] = \\ &= [\overline{TBP}]_T - KT_1 \cdot [\overline{TBP}]_T \cdot \{HNO_3\} - KT_2 \cdot [\overline{TBP}]_T^2 \cdot \{HNO_3\} - KT_3 \cdot [TBP]_T \cdot \{HNO_3\}^2\end{aligned} \tag{5.9}$$

where $\overline{[TBP]}_T$ denotes the total concentration of TBP in the organic phase, $\overline{[TBP]}_f$ is the equilibrium concentration of TBP non-complexed with HNO_3, and $\{HNO_3\}$ is the aqueous activity of nitric acid.

5.4. Calculation of the distribution ratios of Pu(IV).

Speciation diagrams for Pu(IV) species in nitric acid solutions generated using the HySS [Alderighi et al., 1999] modeling program are displayed in Figure 5.1. Calculated results suggest that at 0.1 mol·L^{-1} HNO_3 more than 90 % of Pu (Fig. 5.1a), and in the presence of 1 mol L^{-1} lithium nitrate, about 55 % of Pu (Fig. 5.1b) is present as hydrolyzed plutonium. Even at 0.6 mol·L^{-1} HNO_3, more than 10 % of total Pu(IV) is still hydrolyzed. However, the increase of nitrate and acid concentration lead to formation of Pu(IV) mono- and dinitrate species that predominate at ≥ 0.4 mol·L^{-1} HNO_3. According to this speciation model based on the literature data, in order to determine the distribution by TBP of all Pu(IV) species present in aqueous solutions over a wide range of nitric acid and lithium nitrate concentrations, five Pu(IV) species must be considered to be present: Pu^{4+}, $Pu(OH)^{3+}$, $Pu(OH)_2^{2+}$, $Pu(NO_3)^{3+}$ and $Pu(NO_3)_2^{2+}$. The formation constants for ternary Pu-hydroxonitrate complexes and higher Pu-nitrate species ($Pu(NO_3)_4$ and $Pu(NO_3)_6^{2-}$) remain yet unknown; hence, only the first two nitrate complexes were included in this model and the calculated values were compared with the values of the distribution ratios measured for the range of (0.1 to 4) mol·L^{-1} HNO_3 and total nitrate ≤ 4 mol· L^{-1}. We performed the calculation of the distribution ratio of Pu(IV) assuming the extraction of the $Pu(NO_3)_4$ species coordinated with two molecules of TBP [Schulz et al., 1984] as an anhydrous solvate adduct:

$$Pu^{4+}(H_2O)_n + 4NO_3^- + \overline{2TBP} \overset{K_1}{\Leftrightarrow} \overline{[Pu(NO_3)_4 \cdot TBP_2]} + nH_2O \qquad (5.10)$$

where *n* represents the hydration number of the cation, which refers to the number of waters of hydration lost during complexation with TBP. For simplicity, we assumed that a single hydration

number is satisfactory to sufficiently describe the extraction behavior of tetravalent plutonium over the whole range of conditions. According to [Allen et al., 1996], the hydration number for $Pu(NO_3)_2^{2+}$ (predominant species in the range of (0.2 to 4) mol·L^{-1} HNO_3, see Fig. 5.1) determined by EXAFS was 7.

Predicting distribution ratios of Pu(IV) by TBP from the proton/metal-nitrate electrolyte medium is strongly dependent on the calculation of activities of all species present in the extraction system together with providing reasonable values for their complexation constants. The extraction constant for the Pu-tetranitrate species can be expressed as follows:

$$K_1 = \frac{\overline{[Pu(NO_3)_4 \cdot TBP_2]} \cdot [H_2O]^n}{[Pu^{4+}(H_2O)_n] \cdot [NO_3^-]^4 \cdot \overline{[TBP]}^2} \frac{\overline{\gamma_{Pu(NO_3)_4 \cdot TBP_2}} \cdot (\gamma_{H_2O})^n}{\gamma_{Pu^{4+}} \cdot (\gamma_{NO_3^-})^4 \cdot \overline{(\gamma_{TBP})}^2} \tag{5.11}$$

where $\gamma(H_2O)$, $\gamma(Pu^{4+})$, $\gamma(NO_3^-)$ are the activity coefficients of the aqueous species, $\gamma(Pu(NO_3)_4 \cdot TBP_2)$ and $\gamma(TBP)$ are the activity coefficient of the species in the organic phase, and it was assumed that the activity coefficients of neutral species in the organic phase are equal to one. Due to a low solubility of TBP in aqueous solution, the activities of aqueous species are not affected. Since the concentration of Pu(IV) (~1×10^{-7} mol·L^{-1}) is negligible compared to concentration of TBP (1.1 mol·L^{-1}), the calculation of free TBP was based on the distribution ratio of nitric acid [Chaiko & Vandegrift, 1988] using eq 5.9. The mean activity coefficients of H^+, NO_3^- and H_2O were calculated by the method of Bromley [Bromley, 1973].

There are large discrepancies between values of the activity coefficients reported for plutonium and other actinide metals. Berg et al., 1998 reported the values of interaction parameters for $Pu(NO_3)^{3+}$ and $Pu(NO_3)_2^{2+}$ complexes, but not for Pu^{4+}. Finally, Neck et al., 2006 determined the interaction parameter $\Delta\varepsilon(Pu^{4+}, NO_3^-) = 0.31$ by using the approach of chemical analogs and the similar behavior of tetravalent Th and Pu. The reported value [Neck et al., 2006] $\Delta\varepsilon(Th^{4+}, NO_3^-) = 0.31 \pm 0.12$ gives a better linear correlation between $\varepsilon(M^{Z+}, NO_3^-)$ and $\varepsilon(M^{Z+}, ClO_4^-)$ or $\varepsilon(M^{Z+}, Cl^-)$ and $\varepsilon(M^{Z+}, ClO_4^-)$ than other values [Chaiko & Vandegrift, 1988] reported earlier. Therefore, in this work, the activity coefficients of Pu^{4+} in the nitrate system were calculated by the SIT approach using the interaction parameter $\Delta\varepsilon(Pu^{4+}, NO_3^-) = 0.31$, adopting the value recently determined for Th^{4+} in nitrate media by Neck et al., 2006.

By simply assuming that one hydroxo group replaces one molecule of water and each nitrate group replace two molecules of water in the hydration shell associated with the plutonium cation, the concentration of total aqueous $[Pu(IV)]_T$ can be described as:

$$[Pu(IV)]_T = [Pu^{4+}(H_2O)_n]\cdot\left(1 + K_{H1}\frac{1}{\{H^+\}\cdot\{H_2O\}} + K_{H2}\frac{1}{(\{H^+\}\cdot\{H_2O\})^2} + \right.$$
$$\left. + \beta_1\frac{\{NO_3^-\}}{\{H_2O\}^2} + \beta_2\frac{\{NO_3^-\}^2}{\{H_2O\}^4}\right) \qquad (5.12)$$

where K_{H1}, K_{H2}, β_1, and β_2 are the first two constants of hydrolysis and nitrate complexation, respectively, and terms in {} are activities of the species. Therefore, when the only extractable species is plutonium tetranitrate coordinated with two molecules of TBP, the distribution ratio for Pu(IV) can be expressed by combination of eqs 11 and 12 as follows:

$$D_{Pu(IV)} = \frac{\overline{[Pu(IV)]_T}}{[Pu(IV)]_T} =$$
$$= \frac{\gamma_{Pu^{4+}}\cdot\{TBP\}_f^2\cdot K_1\cdot\{NO_3^-\}^4}{\left(1 + K_{H1}\frac{1}{\{H^+\}\cdot\{H_2O\}} + K_{H2}\frac{1}{(\{H^+\}\cdot\{H_2O\})^2} + \beta_1\frac{\{NO_3^-\}}{\{H_2O\}^2} + \beta_2\frac{\{NO_3^-\}^2}{\{H_2O\}^4}\right)\cdot\{H_2O\}^n} \qquad (5.13)$$

Comparison of the values of the distribution ratio of Pu(IV) calculated by eq 13 ($K_1=1.77\times10^5$) with the experimental data and literature data [Petrich & Kolarik, 1998; Karraker 2001] as displayed in Figure 5.2, does not provide a satisfactory fit ($R^2=0.884$) for concentrations higher than 1 mol·L^{-1} HNO_3, and suggests a need for reevaluation of the species and constants included in the model. An alternative view is that Pu-nitrate can be solvated not only by two molecules of free TBP, but also the $TBP_2\cdot HNO_3$ adduct is capable of plutonium extraction. To the best of our knowledge, the formation of the $Pu(NO_3)_4\cdot TBP_2\cdot HNO_3$ species has not been confirmed experimentally; however, the hypothesis that either $TBP_2\cdot HNO_3$ alone or two species TBP and $TBP\cdot HNO_3$ together are capable of coordinating plutonium tetranitrate is widely accepted. A similar mechanism was proposed also for other neutral extractants, for example, for extraction of uranium from nitric acid by amides [Musikas et al., 1991]. Accepting this approach, the

formation of two organic plutonium species containing four and five nitrate molecules solvated with TBP is considered in the present model (eqs 5.10 and 5.14):

$$Pu^{4+}(H_2O)_n + 4NO_3^- + \overline{TBP} + \overline{TBP \cdot HNO_3} \overset{K_2}{\Leftrightarrow} \overline{Pu(NO_3)_4 \cdot TBP_2 \cdot HNO_3} + nH_2O \qquad (5.14)$$

Adding the equilibrium constant K_2 representing the extraction of Pu-tetranitrate associated with $TBP_2 \cdot HNO_3$, distribution ratios can be calculated by eq 5.15 where the index *n* over the activity of water represents the number of hydration molecules released after complexation of Pu with TBP. The best fit was obtained for *n*=7 and this is in excellent agreement with the hydration number reported by Allen et al., 1996:

$$D_{Pu(IV)} = N \cdot \gamma_{Pu^{4+}} \cdot \left(K_1 \cdot \{NO_3^-\}^4 + K_2 \cdot \{NO_3^-\}^5 \cdot \{H^+\} \right) \qquad (5.15)$$

$$\text{where } N = \frac{\{TBP\}_{free}^2}{\left(1 + K_{H1} \cdot \frac{1}{\{H^+\} \cdot \{H_2O\}} + K_{H2} \cdot \frac{1}{(\{H^+\} \cdot \{H_2O\})^2} + \beta_1 \cdot \frac{\{NO_3^-\}}{\{H_2O\}^2} + \beta_2 \cdot \frac{\{NO_3^-\}^2}{\{H_2O\}^4}\right) \cdot \{H_2O\}^n} \qquad (5.16)$$

A correlation plot of experimental data and values of $D_{Pu(IV)}$ calculated using eq 15 and is displayed in Figure 5.3. Since the extraction constants $K_1=1.06\times10^5$ and $K_2=2.12\times10^4$ are expressed in activities, they are dimensionless thermodynamic equilibrium constants.

Examining the calculated values of extraction constants, two different sets of hydrolysis constants, from reference 11 and 13, which differ by one order of magnitude, were applied; however, both sets of data provided very similar results, which differed by less than 5 %. Including the K_2 extraction constant for the $Pu(NO_3)_4 \cdot TBP_2 \cdot HNO_3$ species and optimization of the K_1 and K_2 values using MS Excel™ Solver plug-in provided a reasonable fit between calculated and experimental data (R^2= 0.971). The Solver was set to find optimal values of extraction constants with minimum differences between the calculated and experimentally observed distribution ratios. Introducing the second extraction constant K_2 produced very good results even for data with low nitric acid concentrations (acquired after 10 minutes contact time)

and in the presence of additional $LiNO_3$. Better fit for the data at low acid concentration is due to lower value of K_1 extraction constant.

Based on the calculated data, it can be estimated that the formation of the $Pu(NO_3)_4 \cdot TBP_2 \cdot HNO_3$ adduct is predominant at $HNO_3 \geq 2$ mol·L^{-1}. Accepting two TBP adducts (TBP_2 and $TBP_2 \cdot HNO_3$) capable of coordinating $Pu(NO_3)_4$ produced a very good fit and eq 15 can be used for calculating the distribution ratios of Pu(IV) over a wide range of nitric acid and additional nitrate concentrations.

Despite an extensive research in the extraction of tetravalent plutonium from nitric acid by TBP, there are only a few papers reporting the plutonium extraction constants. The significant differences in the previous data are caused mainly by the calculation method of the complexation constants and the activity coefficients of all relevant species. For example, [Moiseenko & Rozen, 1960] determined the extraction constant of 2.6×10^4 at 20º C. They applied a simplified approach to calculation of the apparent distribution constant assuming that the $Pu(NO_3)_4 \cdot 2TBP$ adduct is the only extractable species in a wide range of (0.1 to 10) mol·L^{-1} HNO_3. On the contrary, [Rubisov & Solovkin, 1982] concluded that three hydrolyzed species are present in the aqueous solutions and are extractable as neutral adducts with nitrates and two molecules of TBP. Surprisingly, the largest extraction constant (4.17×10^4) they reported was for the mono-hydroxo species of Pu(IV), while the constant calculated for $Pu(NO_3)_4 \cdot 2TBP$ was only 1.9×10^2. The other two constants were 1.19×10^3 for the TBP adduct with di-hydroxo, and 9.4 for the adduct with tri-hydroxo species. Moreover, it seems like that [Rubisov and Solovkin, 1982] did not evaluated the nitrate speciation of Pu(IV) in aqueous solutions. Also, in neither of these papers, the activity of water or the association of Pu(IV) with $TBP_2 \cdot HNO_3$ adduct were considered.

Summarizing, it can be concluded that the calculation of the extraction constants strongly depends on the concept how all the assumptions regarding to Pu disproportionation, hydrolysis and complexation with nitrate were made. Since the activity coefficients for Pu^{4+} implied in this work are very small ($\sim 10^{-3}$) even small changes in the interaction parameter $\Delta\varepsilon(Pu^{4+}, NO_3^-)$ can considerably affect the values of K_1 and K_2 extraction constants. Just for example, assuming the activity coefficients for Pu^{4+} in the whole range of experimental conditions equal to one, the best fit between the experimental and calculated data (R^2=0.89) was obtained for extraction constants K_1=51.1 mol·L^{-1} and K_2=45.2 mol·L^{-1}.

This model should not be used indiscriminately. Due to processes involving disproportionation and extraction at the same time and difficulties in obtaining consistent data for extraction of Pu(IV) from low nitric acid concentration, the determination of the extraction constant for Pu-hydrolyzed species is more complicated and cannot be solved without additional data on disproportionation of Pu(IV) in two phase system.

6. Spectroscopic investigation of Pu species at low HNO_3

6.1. Introduction

The complex chemistry of plutonium under low nitric acid concentration can significantly affect the extraction of tetravalent plutonium by tri-*n*-butyl phosphate (TBP) in *n*-dodecane. At low HNO_3 concentrations, the main Pu(IV) species present in the aqueous solution are $Pu(OH)^{3+}$ and $Pu(OH)_2^{2+}$. Moreover, due to the disproportionation reaction of Pu(IV), a mixture of Pu(III), Pu(IV), Pu(V) and Pu(VI) must be considered. Also the colloidal Pu(IV) can be present under certain conditions. Within many extraction studies related to the extraction of Pu(IV) by TBP from nitric acid, the extraction of only neutral tetra-nitrate Pu species is generally well accepted. However, possibility of the presence of ternary metal(IV)-hydroxo-nitrates in TBP was envisioned in earlier papers [Smirnov-Averin et al., 1963; Woodhead 1964; Woodhead & McKay, 1965; Solovkin 1971; Rubisov & Solovkin, 1982]. The presence of hydrolyzed species of U(IV) in a TBP-containing organic phase was observed by [Smirnov-Averin et al., 1963] in 1963 and later by Woodhead [Woodhead 1964; Woodhead & McKay, 1965] by Vis-NIR spectroscopy. In their work, the U(IV) hydrolyzed species $U(OH)(NO_3)_3$ in TBP was prepared by mixing $Cs_2U(NO_3)_6$ with hydrated TBP and compared with extraction of U(IV) from dilute nitric acid solutions. However, the presence of plutonium(IV)-hydroxo-nitrates in TBP was only briefly discussed, and no spectral evidence has been presented [Woodhead 1964]. Solovkin and Rubisov [Solovkin 1971; Rubisov & Solovkin, 1982] included hydrolyzed Pu(IV) species extracted by TBP from low nitric acid concentration into their calculation models. As Pu^{4+} cation is more liable to be hydrolyzed than is U^{4+}, the possibility for the formation of TBP adducts with mixed hydroxo-nitrate plutonium species from lower HNO_3 concentration are highly expected. In this work we will present and discuss experimental data that confirms the extraction of ternary hydroxo-nitrate Pu(IV) species by TBP from low nitric acid concentrations.

Spectroscopic investigation of Pu speciation in aqueous and organic solutions was performed with Pu-242. Spectra were collected by OLIS RSM 1000 spectrometer in 1 cm glass micro cuvette against the blank solution that was always identical with the analyzed solution except the component of interest.

6.2. Processes affecting speciation of Pu in aqueous phase

The highly-charged cation Pu^{4+} tends to hydrolyze more easily than any other of the plutonium species, even under highly acidic conditions. Hydrolyzed Pu(IV) can further react to form multinuclear metal oligomers and colloids [Johnson, 1978; Soderholm et al., 2008]. The formation of colloids at higher Pu concentrations and higher pH can lead to inaccurate interpretation of experimental results. Another important reaction occurring under low acidity and further affecting Pu behavior is the disproportionation of Pu(IV) and the formation of Pu(III), Pu(V) and Pu(VI):

$$2Pu^{4+} + 2H_2O \Leftrightarrow Pu^{3+} + PuO_2^+ + 4H^+ \quad (6.1)$$

$$Pu^{4+} + PuO_2^+ \Leftrightarrow Pu^{3+} + PuO_2^{2+} \quad 6.2)$$

Since the conversion of PuO_2^+ to PuO_2^{2+} is fast reaction, practically only Pu(III), Pu(IV) and Pu(VI) can be identified in the solution. This can be represented by simplified total reaction:

$$3Pu^{4+} + 2H_2O \Leftrightarrow 2Pu^{3+} + PuO_2^{2+} + 4H^+ \quad (6.3)$$

Very complex chemistry of plutonium at low acid concentration involving the presence of hydrolysis products and various Pu oxidation states can significantly affect the extractability of plutonium by tri-*n*-butyl phosphate (TBP); therefore, quantifying the speciation in both aqueous and organic phase is very important. In this report, the stability constants log β^0_1=2.12 and log β^0_2= 3.66 for the $Pu(NO_3)^{3+}$ and $Pu(NO_3)_2^{2+}$ complexes reported by [Berg et al., 1998], and hydrolysis constants log K^0_{H1}=0.6 and log K^0_{H2}=0.6 obtained by [Metivier & Guillaumont, 1972] were used to recalculate the stability constants at 1 M HNO_3 by SIT approach. The reasons for selection of the values of hydrolysis and complexation constants of Pu(IV) with nitrate are

discussed elsewhere [Tkac et al., 2009]. Recently, Walther et al., 2007 observed that identification of hydrolyzed Pu(IV) species by Vis-NIR spectroscopy from $HClO_4$ solutions is not possible because the first and the second hydroxide complex of Pu(IV) do not differ from the hydrated Pu^{4+} ion. All changes in the absorption spectra originate from the formation of Pu-polymeric species and colloids. However, the molar extinction coefficient for Pu-polymeric species is hard to determine, since it is more unlikely, that only one well defined size of polymeric species, but rather broad size distribution and particles of different size having different absorptivity are present in the solution [Walther et al., 2007]. Spectrum of colloidal Pu(IV) species differ significantly from the spectrum of monomeric Pu(IV) and polymer has a characteristic strong absorption at 400-500 nm, well known absorption peak at 620 nm and weak band at 740 nm [Weigel et al., 1986; Walther et al., 2007; Soderholm et al., 2008]. Nevertheless, spectrum of Pu(IV) in perchloric acid differ significantly from the spectra of Pu(IV) in nitric acid. Increasing the nitric acid concentration or addition of nitrate salts to the aqueous phase, suppresses the hydrolysis of Pu(IV) and favors formation of Pu(IV) nitrate complexes, which changes the spectrum of Pu(IV) progressively due to formation of various nitrate complexes with different extinction coefficients. According to Berg et al. [1998], mono- and di- nitrate species have a maximum at ~ 475 nm, whereas the spectrum of hydrated Pu^{4+} ion has a maximum at ~ 469 nm. Also, the extinction coefficient of Pu^{4+} ion at 469 nm is significantly lower than those of Pu(IV)-nitrate species at 475 nm. Seeing that, one can expect that increase of Pu(IV) -mono and –di-nitrate species in the aqueous solution at constant Pu(IV) concentration, will give a higher absorbance at 475 nm. At very high aqueous concentrations of HNO_3 (> 8 M), formation of anionic $Pu(NO_3)_6^{2-}$ with characteristic peaks at ~490, ~610, ~744 nm change the spectrum of Pu(IV) dramatically [Ryan, 1960]. On the other hand, it is generally accepted that for extraction of Pu(IV) by TBP from a wide range of nitric acid, only neutral Pu(IV)-tetranitrate species are present in the organic phase.

At low nitric acid concentrations, the distribution ratios of Pu(IV) ($D_{Pu(IV)}$) by TBP is strongly affected (Table 4.1) by the processes occurring in the aqueous phase such as hydrolysis, disproportionation and at higher Pu concentrations, also formation of colloidal Pu. Due to these complex reactions, depending on the experimental conditions used, the distribution ratios of Pu by TBP obtained by various authors can differ significantly, which has been illustrated

previously [Petrich & Kolarik, 1981; Tkac et al., 2009]. Especially, at low nitric acid concentrations distribution of Pu species is primarily driven by disproportionation reaction of Pu(IV). Therefore, distribution ratios obtained by a simple counting of activity in the organic and aqueous phase cannot be presented as $D_{Pu(IV)}$ due to occurrence of various oxidation states of Pu. Moreover, prolonged mixing time at low HNO_3 concentration leads to the accumulation of Pu(III) and Pu(VI), which are poorly extracted. In our earlier work [20], strong inconsistency in forward and back-extraction of plutonium (performed with trace concentration of Pu-239, $\sim 1\times10^{-7}$ M) at low concentration of HNO_3 was observed. Higher acid concentration prevents the disproportionation reaction, and good agreement between forward and back-extraction suggest an equilibrium process. The main reason for the inconsistency of distribution ratios of Pu (initially Pu(IV)) at low HNO_3 concentration is the undergoing disproportionation and possibility of formation of colloidal Pu(IV). To investigate how the disproportionation of Pu(IV) can affect the extraction of Pu by TBP, we performed several experiments with low nitric acid concentration. The initial concentration of Pu in the aqueous phase was $1\text{-}3\times10^{-3}$ M. Figure 6.1 shows the time dependence spectra of disproportionation of Pu(IV) in 0.1 M HNO_3 with the formation of Pu(III) and Pu(VI).

The concentrations of Pu(III), Pu(IV) and Pu(VI) species were determined by deconvolution of the absorption spectra in the region of 400-700 nm.

Experimental data were fitted by the following kinetic equation derived from equation 6.3:

$$-\frac{1}{3}\frac{d[Pu(IV)]}{dt}=\frac{1}{2}\frac{d[Pu(III)]}{dt}=\frac{d[Pu(VI)]}{dt}=k'[Pu(IV)]^3 \qquad (6.4)$$

As suggested by Rabideau [1953], the disproportionation reaction of Pu(IV) undergoes following reaction scheme:

$$Pu(OH)^{3+}+Pu(OH)_2^{2+}\Leftrightarrow Pu^{3+}+PuO_2^{+}+H_2O+H^{+} \qquad (6.5)$$

$$Pu^{4+}+PuO_2^{+}\Leftrightarrow Pu^{3+}+PuO_2^{2+} \qquad (6.6)$$

The proposed reaction shows that Pu(IV)-mono and –di-hydroxo species must be present in the aqueous solution. Therefore, as the concentration of nitrate increases, the disproportionation reaction of Pu(IV) is suppressed by the formation of Pu(IV)-nitrate species. This is in good agreement with our experimental results, where the disproportionation of Pu(IV) significantly

developed only in 0.1 and 0.2 M HNO_3 (Fig. 6.2), whereas in 0.4 M HNO_3 only about 10 % of the Pu(IV) disproportionated after 15 hours. The apparent kinetic constant k' (Eq 6.4) determined for 0.1 M and 0.2 M HNO_3 were 529 and 85 $mol^{-2} \cdot L^2 \cdot min^{-1}$, respectively. It has to be noted that kinetic constants determined should only be used to illustrate the effect of HNO_3 concentration on the disproportionation of Pu(IV) and its effect on distribution ratio of Pu. Fig. 6.2 also illustrates how significantly the disproportionation of Pu(IV) slowed down after increase of the acidity from 0.1 to 0.2 M. From these data it is evident that prolonged contact time between aqueous and organic phase would lead to lower distribution ratios of Pu due to lowering the total concentration of Pu(IV) and increasing the concentration of non-extractable Pu(III) and partially extractable Pu(VI) in the extraction system. The experimental data on Fig. 6.2 are consistent with the stoichiometry described by eq. 6.3, hence the concentration of Pu(III) is twice the concentration of Pu(VI).

To better understand the behavior of Pu in the organic and aqueous phase during the extraction from low nitric acid concentration, we were monitoring the Pu species in the extraction system at different time periods by an absorption spectroscopy. During the extraction, Pu(III) and Pu(VI) were produced and accumulated in the aqueous phase, while no detectable amount of Pu(III) and Pu(VI) (by Vis-NIR spectroscopy) was observed in the TBP after extraction, verifying the low extractability of these oxidation states of plutonium. The concentration of Pu(IV) in the organic phase was progressively decreasing due to undergoing disproportionation of Pu(IV) in the aqueous phase (Fig. 6.3). Since the Pu(III) is non-extractable by TBP, the concentrations of Pu(III) in the aqueous phase of the TBP/0.1 M HNO_3 system can provide an information about the undergoing disproportionation of Pu(IV). The comparison of the concentrations of Pu(III) in aqueous phase of one and two phase system at constant total Pu concentration reveal that under the two phase mixing conditions (HNO_3/TBP), the disproportionation of Pu(IV) is faster comparing to non mixing one phase aqueous experiment. No disproportionation of Pu(IV) in the organic phase was observed within several weeks. This is most likely due to coordination of Pu(IV) with TBP and absence of ion-ion interaction necessary for the disproportionation of Pu(IV).

Under certain conditions, when the total initial concentration of HNO_3 in the aqueous phase was 0.1 M HNO_3, also extraction of colloidal Pu species by TBP was detected. This was

observed visually as an organic phase was foggy and colloidal particles were clearly evident. The distribution of Pu into organic phase was also confirmed by LSC. The Vis-NIR spectra of these samples are displayed on Fig. 6.4 and differ significantly from the spectra of polymeric Pu in the aqueous solution observed by other authors. This might be due to a light scattering that overlap the spectrum of Pu colloids in the organic phase and due to different content of water surrounding Pu colloid. In the contrast to the samples of Pu(IV) in TBP extracted from 0.1 M HNO_3 without any visual or spectroscopic evidence of colloidal particles (presence of colloids cannot be fully excluded even in these samples, as they can be dissolved), the samples of Pu in TBP with the colloidal Pu were not spectroscopically stable. Fig. 6.4 shows that colloidal Pu present in the aqueous phase and extracted by TBP can differ. This is most likely due to different size of colloidal particles. The samples of Pu in the organic phase after the separation from the aqueous phase were also examined after a one week period. The sample of Pu colloid in TBP with lower absorbance (#1, Fig. 6.4) probably aggregated more over a time, while the changes in the spectrum of sample #2 shows the decrease in the absorbance over a period of a one week, which is most likely due to a partial depolymerization of Pu. Moreover, after the contact of the polymeric Pu species in TBP with 1 M $LiNO_3$, colloidal Pu was not back-extracted and remained in the organic phase. After a centrifugation (17500 rpm/10 minutes) of TBP containing Pu-colloid, a reddish solid phase (Fig. 6.5) was observed at the bottom of extraction vial. However, the spectrum of TBP after centrifugation revealed that some portion of Pu colloid remains dissolved (Fig. 6.6).

These data clearly indicate that the distribution ratios for Pu (initially Pu(IV)) from low nitric acid can be significantly affected by the processes undergoing in the aqueous phase such as disproportionation and polymerization of Pu(IV) at higher concentrations. Moreover, we have to keep in mind that even the colloidal particles of Pu were not visually or spectroscopically detected in all the samples obtained after the extraction from low HNO_3 concentrations, the presence of small amount of dissolved Pu colloids cannot be excluded.

In order to distinguish any differences in the Pu(IV) species extracted by TBP, Vis-NIR spectra of the organic phase were taken after the extraction of Pu from a wide range of initial HNO_3 concentration. The concentrations of Pu in TBP were determined from LSC data and were used to calculate the molar absorptivities of Pu species in the organic phase. It has to be noted

that the summation of the total CPM (counts per minute) from the aqueous and organic phase after the extraction were consistent with the deviation of less than a one percent. The spectra of Pu species in 30 % TBP extracted from the range of 0.1-6 M HNO_3 are shown on Fig. 6.7. It shows systematic changes in the absorption region of 400-520 nm with a characteristic peak of Pu(IV) located at ~ 490 nm, and the changes in the range of 500-750 nm. With increasing aqueous nitric acid concentration, different Pu(IV) species are being extracted, which is indicated by the increase in the ~ 490 nm absorption peak. Also position of the peak maxima change with changing initial aqueous HNO_3 concentration, where the spectra of Pu(IV) in the TBP extracted from 0.1-0.8 M HNO_3 have a peak maxima at 488.5 nm with a shoulder at 485 nm. This can be explained by the presence of a mixture of Pu species with a different absorptivity. The species with a shoulder at lower wavelength could be assigned to partially hydrated Pu(IV) species, similarly as the aqueous spectra of Pu(IV)-hydroxo species have the maxima at ~ 469 nm and lower absorptivity comparing to Pu(IV)-nitrate species. Therefore, the lower extinction coefficient of Pu(IV) species in TBP at ~ 490 nm suggest lower content of nitrate associated with Pu. Also, the region of 500-750 nm shows systematic changes in the spectra of Pu(IV) in TBP depending on aqueous HNO_3 concentration. At lower HNO_3 concentrations, formation of a double peak was observed with maxima at ~ 725 and ~ 741 nm, while at higher acidity this feature disappears and the formation of a new peak at ~ 705 nm emerge. We assigned the formation of this double peak at 720-750 nm to bonding of two different ligands with plutonium: hydroxo and nitrate. As the proportion of hydroxo to nitrate decreases with nitric acid concentration, the absorption at ~ 490 nm increases and the double peak at 720-750 disappears. Spectra of Pu(IV) in TBP extracted from 0.4-0.8 M HNO_3 had very similar absorption features, as well as the spectra of Pu(IV) extracted from 6-10 M HNO_3. Spectra of Pu(IV) extracted from 0.4; 0.6 and 0.8 M HNO_3 (Fig 6.8) were assigned as Pu(IV) hydroxo-nitrate species. Figure 6.9 compares the spectra of ternary hydroxo-nitrate Pu(IV) species extracted from the range of 0.4-0.8 M HNO_3, with the spectra of Pu(IV) extracted from 6-10 M HNO_3, assigned to tetra-nitrate Pu(IV) species.

The differences in the spectra of Pu extracted from 0.1; 0.2 and 0.4 M HNO_3 (Fig. 6.8) are mainly in the region of < 500 nm; however, also changes at 700-750 nm are noticeable. This might be explained by slightly lower content of nitrate associated with Pu(IV), as well as by a

partial presence of dissolved Pu-colloid species extracted from 0.1 and 0.2 M HNO_3 as indicated also by higher absorption of Pu < 480 nm.

Although the presence of Pu(IV) hydrolyzed species in aqueous solutions of HNO_3 > 1 M is minimal (Fig. 5.1), the spectra of Pu(IV) indicate the presence of ternary hydroxo-nitrate species in TBP even at higher initial aqueous concentrations of HNO_3. This can be assigned to significant amount of water extracted by TBP, which according to Chiarizia and Briand [2007] in 20 % v/v TBP in *n*-octane, is higher than the content of nitric acid up to ~ 1.5 M initial aqueous concentration of HNO_3. The water content in the organic phase decreases when more HNO_3 is extracted by TBP, indicating a competition of water and HNO_3 for the P=O donor group of TBP. It is believed that the content of the water extracted by TBP plays an important role during the extraction of Pu(IV). The Vis-NIR spectra of Pu(IV) species extracted from the range of 0.8-4 M HNO_3 have a several isosbestic points at ~ 463; 480; 510; 537; 585 and 657 nm. This confirms that in this range of nitric acid, distribution of two different Pu(IV) species is responsible for changes of Pu(IV) spectra in the TBP. As we have already discussed, the species with a similar proportion of OH^- and NO_3^- are extracted from the range of 0.4 – 0.8 M HNO_3 and slightly higher presence of hydroxo group associated with Pu(IV) after extraction from 0.1 and 0.2 M HNO_3 is expected.

Therefore, it can be concluded that the major differences in spectra of Pu(IV) in TBP extracted from various concentrations of HNO_3 are due to different content of nitrate and hydroxo groups associated with Pu(IV) by formation of ternary hydroxo-nitrate complex. This is supported mainly by major differences in absorption at ~ 490 nm and in the region of 500 – 750 nm, which is most likely due to a different absorptivity of hydroxo- and nitrate- coordinated Pu(IV) similarly as observed for Pu(IV) in the aqueous phase elsewhere.

7. Spectroscopic investigation of Pu species in the presence of AHA

7.1. Introduction

Within past one-two decade, various reprocessing schemes have been proposed for extraction of actinides from fission products and other elements present in spent nuclear fuel. Most of current reprocessing schemes operate using tri-*n*-butyl phosphate (TBP) based extraction

process. One of these is UREX+ process, which consists of four solvent extraction steps: UREX, CCD-PEG, TRUEX and TALSPEAK. The UREX process introduces acetohydroxamic acid (AHA), which prevents extraction of plutonium and neptunium to tri-*n*-butyl phosphate by reduction of Pu(VI) and Np(VI) to pentavalent oxidation state and formation of non-extractable acetohydroxamate species of tetravalent metals. Uranium (VI) is not affected by AHA and together with technetium is extracted to TBP.

The speciation of Pu(IV) (Pu-242, 2.26×10^{-3}M) in 1M nitric acid and various concentration of acetohydroxamic acid (2.5×10^{-4} M - 0.8 M AHA) were investigated by Vis-NIR spectroscopy. To study the speciation of Pu with acetohydroxamic acid under acidic conditions (HNO_3) also hydrolytic degradation of AHA and reduction of Pu(IV) to Pu(III) by AHA should be considered. As it has been found from our preliminary data, reduction of Pu(IV) to Pu(III) by AHA is very slow (several hours are needed for complete reduction). Therefore, in a short time period (2-3minutes), instability of Pu(IV)-acetohydroxamate complexes and hydrolysis of AHA in acidic conditions affects complexation between Pu(IV) and AHA just slightly. However, all Vis-NIR spectra of Pu in the presence of AHA and HNO_3 were taken under the shortest operation time to minimize changes of conditions due to hydrolytic and redox reactions.

Addition of acetohydroxamic acid to the aqueous solution containing Pu(IV) in nitric acid causes significant changes in speciation of plutonium. Due to strong complexation affinity of acetohydroxamic acid toward metals, addition of AHA suppresses the hydrolysis reaction of Pu(IV) possible at low concentration of nitric acid:

$$Pu(OH)^{3+} + HAHA \Leftrightarrow Pu(AHA)^{3+} + H_2O \qquad (7.1)$$

where AHA refers to the dissociated and HAHA the protonated (undissociated) form of acetohydroxamic acid.

Depending on concentration of AHA, formation of three Pu-acetohydroxamate complexes in aqueous phase should be considered:

$$Pu^{4+} + HAHA \Leftrightarrow Pu(AHA)^{3+} + H^+ \qquad (7.2)$$

$$Pu^{4+} + 2HAHA \Leftrightarrow Pu(AHA)_2^{2+} + 2H^+ \qquad (7.3)$$

$$Pu^{4+} + 3HAHA \Leftrightarrow Pu(AHA)_3^{+} + 3H^+ \qquad (7.4)$$

Stability constants for Pu(IV)-acetohydroxamate species $\log\beta_1$=14.2; $\log\beta_2$=24.1; $\log\beta_3$=32.2 and dissociation constant pK_a(HAHA)=9.018 for ionic strength 2 mol·L^{-1} ($NaClO_4$) were previously determined by Carrott et al., [2007]. Due to protonation of HAHA and relatively fast reaction of acidic hydrolysis of HAHA, formation of Pu-AHA complexes in the presence of high concentration of nitric acid is suppressed.

7.2 Speciation of Pu(IV) in the presence of AHA

A steep reduction of extraction yields of tetravalent plutonium (Pu-239) from 1M HNO_3 by 30% TBP in *n*-dodecane upon addition of acetohydroxamic acid is displayed in Figure 7.1.
Already a very small concentration of acetohydroxamic acid reduces the extraction yield of Pu dramatically due to the formation of a strong Pu-acetohydroxamate complex in aqueous solution. At concentration of AHA >0.1M, extraction yield of Pu decreases only slightly and even at very high concentration of AHA (0.1-0.8 M), still reasonable amount of Pu is extracted to the organic phase. These species of Pu extracted to organic phase are expected to be ternary complexes of $Pu(AHA)_x(NO_3)_{4-x}$ solvated with TBP. Extraction of metal-acetohydroxamate solvates to organic phase have been observed also for U(VI) and Mo(VI) [Tkac & Paulenova, 2008] by 30% TBP in the presence of AHA. The presence of Pu(IV)-acetohydroxamate complex in TBP is supported also by coloring of the organic phase after extraction in the presence of AHA (Figure 7.2)

Addition of acetohydroxamic acid to aqueous solution of Pu(IV) in nitric acid lead to significant change of absorption spectra in Vis-NIR region (Figure 7.3). These changes are due to formation of Pu-acetohydroxamate complexes. In general, complexation of Pu(IV) in HNO_3 by acetohydroxamic acid can be written as:

$$Pu(IV) + xHL + nH^+ + yNO_3^- = [Pu(L)_x(NO_3^-)_y]^{(4-x-y)+} + (n+x)H^+ \qquad (7.5)$$

where HL denotes protonated (non-dissociated) acetohydroxamic acid. For a conditions where Pu(IV) and HNO_3 concentration are constant, we can assume that the absorbance variations are attributed to the variation in the Pu(IV) distribution among $[Pu(IV)]_{free}$ (non-compexed with AHA), Pu(IV)-mono-, di- and tri-acetohydroxamate species. The mass balance for total Pu concentration $[Pu(IV)]_{tot}$ in aqueous solution is written:

$$[Pu(IV)]_{tot} = [Pu(IV)]_{free} + [Pu(IV)L_1] + [Pu(IV)L_2] + [Pu(IV)L_3] \qquad (7.6)$$

Because all Pu(IV) species on the right side of equation (7.6) contribute to absorption spectra, the absorbance of plutonium solution at a given wavelength, when concentrations of HNO_3 and Pu(IV) are constant and concentration of AHA are changed, can be expressed as:

$$A_{(ij)} = \varepsilon_{Pu(free)(i)} \cdot [Pu]_{free(j)} + \varepsilon_{Pu(L1)(i)} \cdot [PuL_1]_{(j)} + \varepsilon_{Pu(L2)(i)} \cdot [PuL_2]_{(j)} + \varepsilon_{Pu(L3)(i)} \cdot [PuL_3]_{(j)} \quad (7.7)$$

where $A_{(ij)}$ is absorbance of system at the wavelength i and concentration of ligand j, ε is extinction coefficient for particular absorbing species in solution.

Plutonium(IV)-acetohydroxamate species were resolved from the experimental data obtained by absorption spectroscopy using the chemical equilibrium modeling software FITEQL 4.0 [Herbelin & Westall, 1999]. FITEQL 4.0 involves the iterative application of a specified chemical equilibrium model to a set of equilibrium complexation data. Since FITEQL is a nonlinear optimization program, initial estimates for the values of the adjustable parameters are needed. Through calculation of the sum of squares of residuals between the experimental complexation data and predictions made with initial estimates, values of extinction coefficients (ε) for Pu-AHA, Pu-AHA_2 and Pu-AHA_3 complexes at λ=423 nm were determined for the complexation reactions specified (eq 7.5). The experimental values of Pu concentration (2.26×10^{-3}M), hydrogen ion concentration (1M HNO_3), various concentrations of acetohydroxamic acid (2.5×10^{-4}-8×10^{-1}M) and stability constants determined for Pu-AHA complexes [Carrott et al., 2007] were taken as inputs for distribution of plutonium species. Using the chemical equilibrium modeling it was found that formation of three Pu-acetohydroxamate species formed is possible in 1M HNO_3 and studied range of AHA concentration (Figure 7.4). Under conditions of lower AHA concentrations, mainly the non-acetohydroxamate and mono-acetohydroxamate species of Pu are formed. At 0.1M concentration of AHA and higher, which is more relevant to UREX process conditions, the di-acetohydroxamate species of plutonium becomes predominant and also concentration of Pu-tri-acetohydroxamate species grows up. Values of log ε for Pu-AHA, Pu-AHA_2 and Pu-AHA_3 calculated by FITEQL 4.0 at 423 nm are 2.29, 2.72 and 2.80 $dm^3 \cdot mol^{-1} \cdot cm^{-1}$, respectively. Figure 7.5 compares experimental absorbance of Pu(IV) at λ=423 nm with absorbance calculated from equation (7.7) as a function of [AHA, free]. In this case, [AHA, free] denotes the concentration of non-complexed protonated ligand, which was calculated from pKa and given concentrations of AHA, Pu and HNO_3 using FITEQL.

Extinction coefficients for Pu-AHA, Pu-AHA_2 and Pu-AHA_3 species determined by FITEQL produced a very good agreement between the experimental data and calculated values of absorbance. Effect of nitric acid concentration on speciation of plutonium in 0.4M AHA was fitted by HYSS (Hyperquad Simulation and Speciation program) [Alderighi et al., 1999]. From the data obtained from speciation diagram generated for 1-6 M concentration range of nitric acid, we observed that mono and di-acetohydroxamate species of plutonium are predominant in selected range of HNO_3, although the fraction of Pu non-complexed with AHA grows up with the nitric acid concentration. As we reported earlier, at these very high concentrations of nitric acid, a hydrolytical degradation of AHA is rapid and it will significantly affect the complexation of Pu with acetohydroxamate. The presence of Pu-acetohydroxamate species was confirmed even in a very high concentration of nitric acid by Vis-NIR spectroscopy (Figure 7.6). Changes of Pu spectra due to formation of Pu-acetohydroxamate species with maximum at 423 nm can be explained by interaction of metal and bidentate bonded ligand as it was previously observed for complexation of Pu(IV) with nitrate [Veirs et al., 1994]. Formation of plutonium-acetohydroxamate species at very high concentration of acid confirm the very strong complexation power of AHA toward Pu(IV).

7.3 Speciation of Pu(IV) in TBP in the presence of AHA

All experimental data obtained from: (i) distribution experiments of plutonium in TBP/HNO_3/AHA system; (ii) absorption spectroscopy suggest that some portion of Pu-acetohydroxamate species present in aqueous solution can be extracted to TBP as solvated ternary plutonium-acetohydroxamate-nitrate complexes. It was also confirmed visually after an extraction experiment with higher Pu concentration (Pu-242), when after addition of AHA to aqueous phase containing Pu(IV) in HNO_3, color of solution turned red-brown due to formation of Pu-acetohydroxamate complexes. The same color, but with smaller intensity was also observed in the organic phase after extraction (Fig. 7.2).

To determine the Pu species present in the organic phase, Vis-NIR spectroscopy was employed. Figure 7.7 shows the absorption spectra of Pu(IV) in TBP after extraction from aqueous solution containing 2; 4 and 6 M HNO_3 with absence and presence of 0.4 M AHA.

Because addition of acetohydroxamic acid decreases distribution ratio of plutonium, low absorbance of Pu in TBP could be expected for experiments with AHA. However, the spectra of Pu(IV) in the organic phase after extraction with AHA in 2M (Figure 7.7A) and 4M (Figure 7.7B) nitric acid have higher absorbance in the range of 400-600 nm than samples without AHA. This can be explained only by the extraction of Pu-AHA species with higher extinction coefficient. Although Pu-acetohydroxamate species can be formed even in aqueous phase of 6M nitric acid (Figure 7.6), its extraction is significantly reduced and spectra of Pu in TBP for system with and without acetohydroxamic acid differs just slightly (Figure 7.7C).

Influence of concentration of AHA on extraction of Pu-acetohydroxamate species to TBP from 1M HNO_3 was also investigated. For better illustration, spectra are divided into two graphs for concentration range of 5×10^{-3}–5×10^{-2}M AHA (Figure 7.8A) and 1×10^{-1}–8×10^{-1}M AHA (Figure 7.8B). As can be seen from the speciation diagram of Pu (Figure 7.4) mono- and di-acetohydroxamate species of Pu are predominant in selected range of AHA and 1M HNO_3. Analogous to previous experiments, we have observed an increase of Pu absorbance in TBP for the range of 400-480nm and 500-600nm with an increase of AHA concentration (Figure 7.8A). Plutonium is extracted with TBP in the form of neutral solvate adducts; therefore, when the ternary complexes $Pu(AHA)_x(NO_3)_{4-x}$ are predominant they also can be solvated and transferred into organic phase. At the lowest concentration of AHA in aqueous phase the mono-acetohydroxamate complexes of Pu are more likely to be extracted. At higher AHA concentrations, Pu-di-acetohydroxamate species with higher extinction coefficient become predominant and their extraction increases absorbance of Pu in the organic phase, even though concentration of Pu in TBP decreases with AHA.

From the graph plotted for larger concentrations of AHA (Figure 7.8B) it is clear that further increase of AHA concentration in the aqueous phase up to 0.8M actually decreases the absorbance of Pu in organic phase; however, the shape of spectra is still characteristic for Pu-acetohydroxamate complex species. This behavior can be explained by following: (1) Pu-tri-acetohydroxamate species are probably not extracted or they are extracted just slightly; (2) decrease of Pu concentration in TBP phase has higher effect on absorbance of Pu than extraction of Pu-tri-acetohydroxamate species with higher extinction coefficient. Concerning the fact that concentration of $Pu\text{-}AHA_3$ species in the aqueous solution is very low comparing to $Pu\text{-}AHA_2$

and Pu-AHA, their extraction and contribution to spectra of Pu in TBP is probably minimal, and main species extracted at higher AHA concentration are most likely Pu-di-acetohydroxamate species.

Figures

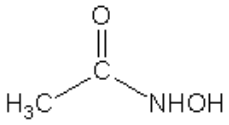

Figure 1.1 Structure of acetohydroxamic acid

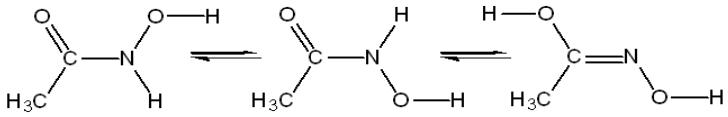

Figure 1.2 Isomers of acetohydroxamic acid

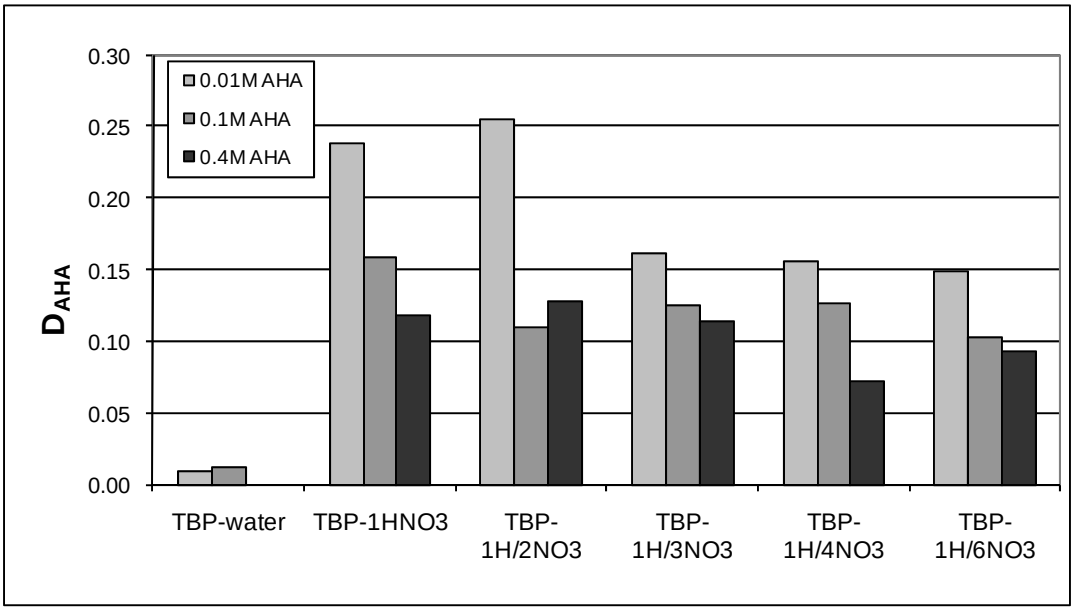

Figure 1.3 Distribution ratios of acetohydroxamic acid by 30 % TBP in n-dodecane

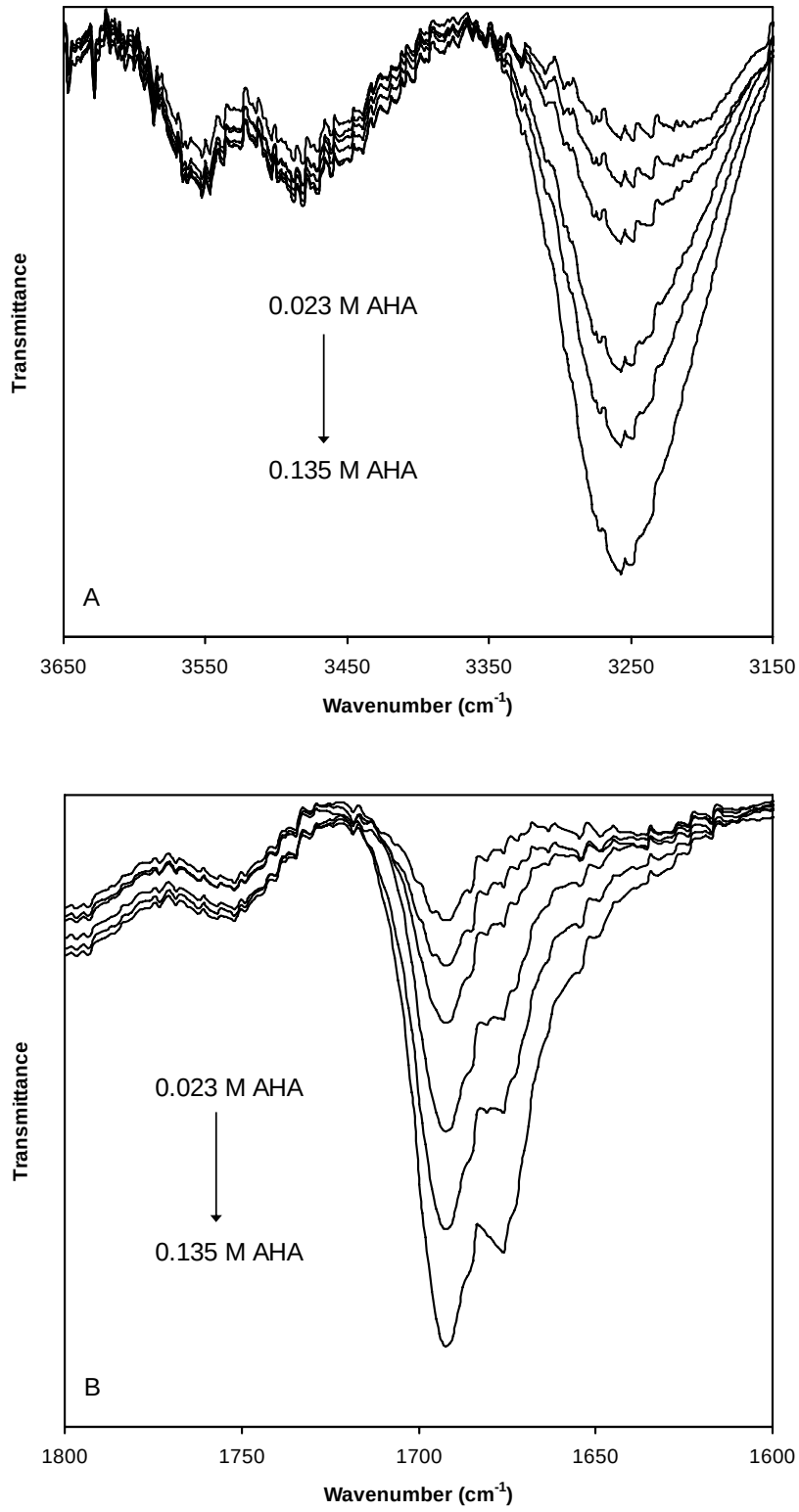

Figure 1.4 FT-IR spectra for the hydroxyl band (A), and the carbonyl band (B) for 0.023, 0.030, 0.045, 0.068, 0.090 and 0.135 M AHA in 100% TBP

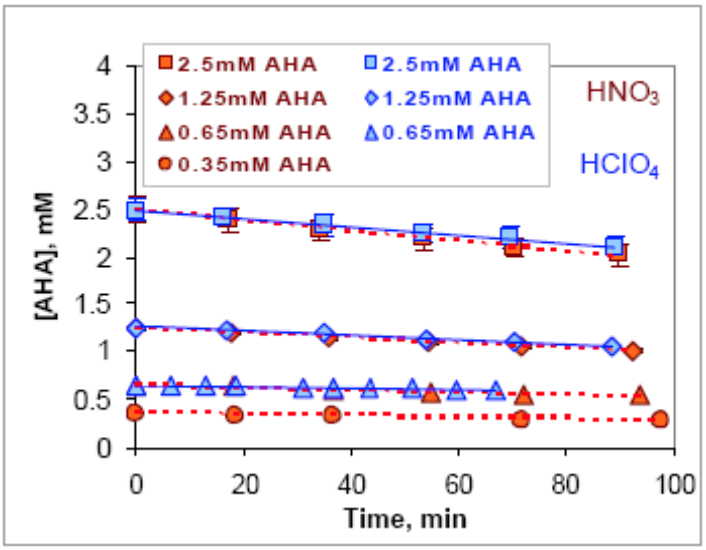

Figure 2.1 Degradation of AHA in 2.5 M HNO_3 or $HClO_4$ as a function of the initial AHA concentration and time: $[AHA]_{initial}$ = 0.35-2.5 mM

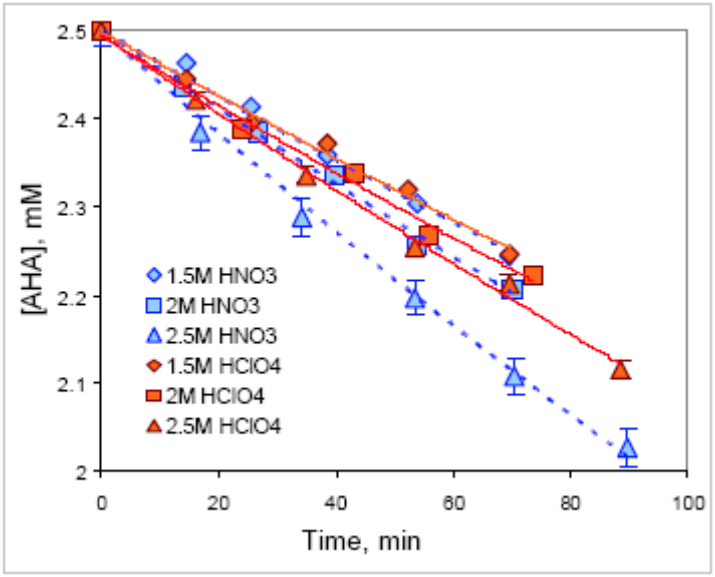

Figure 2.2 Degradation of AHA as a function of the mineral acid concentration and time: $[AHA]_{initial} = 2.5\times10^{-3}$M

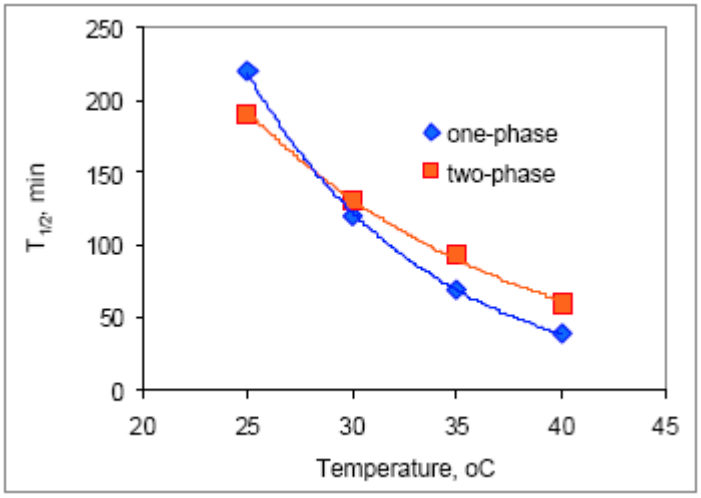

Figure 2.3 A half-life of AHA (T½, min) measured as temperature dependence for 2.5×10^{-3}M AHA

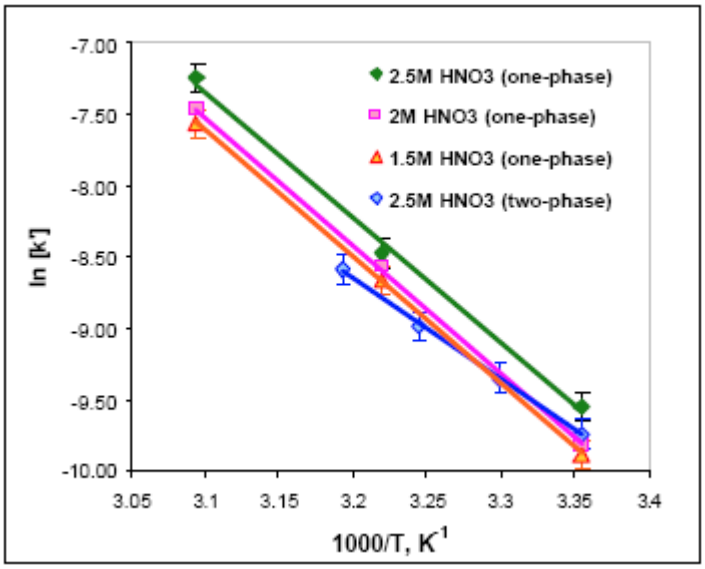

Figure 2.4 The Arrenius plot of the rate constant measured for AHA in three nitric acid concentrations (1.5; 2 and 2.5M) at three temperatures.

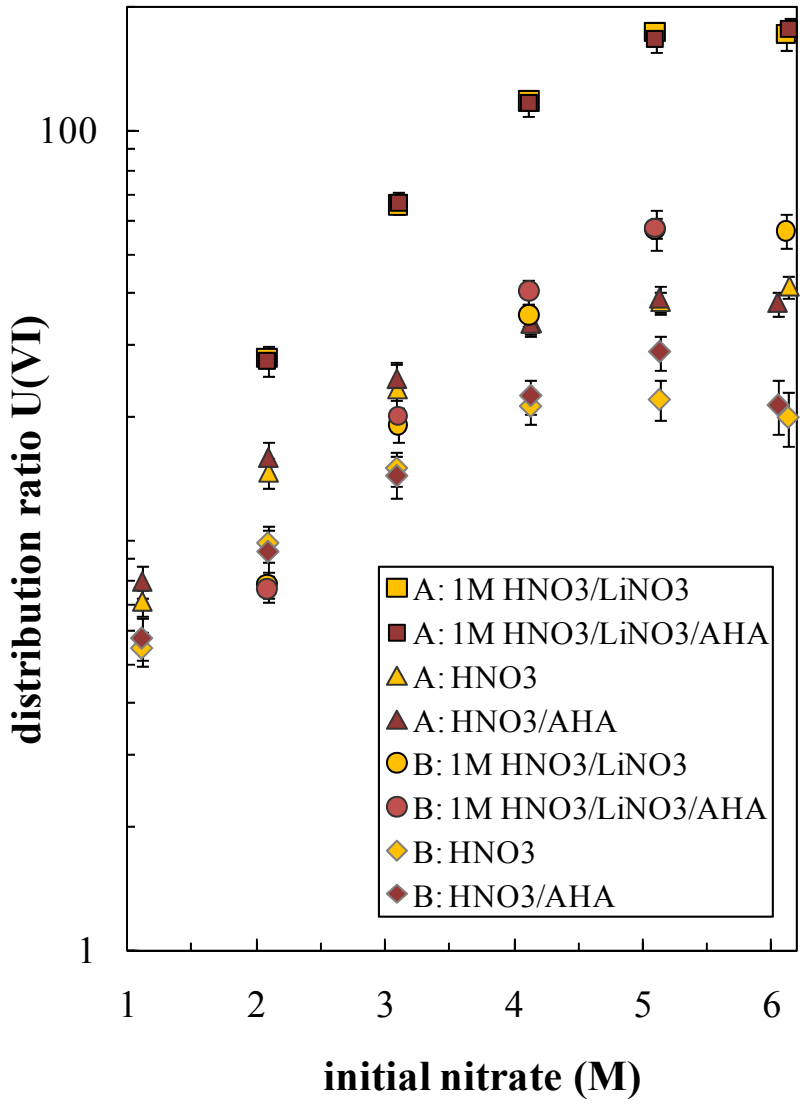

Figure 3.1 Extraction of uranium from nitric acid with and without presence of AHA and $LiNO_3$. Concentration of U(VI): A= 0.043 M, B = 0.176 M

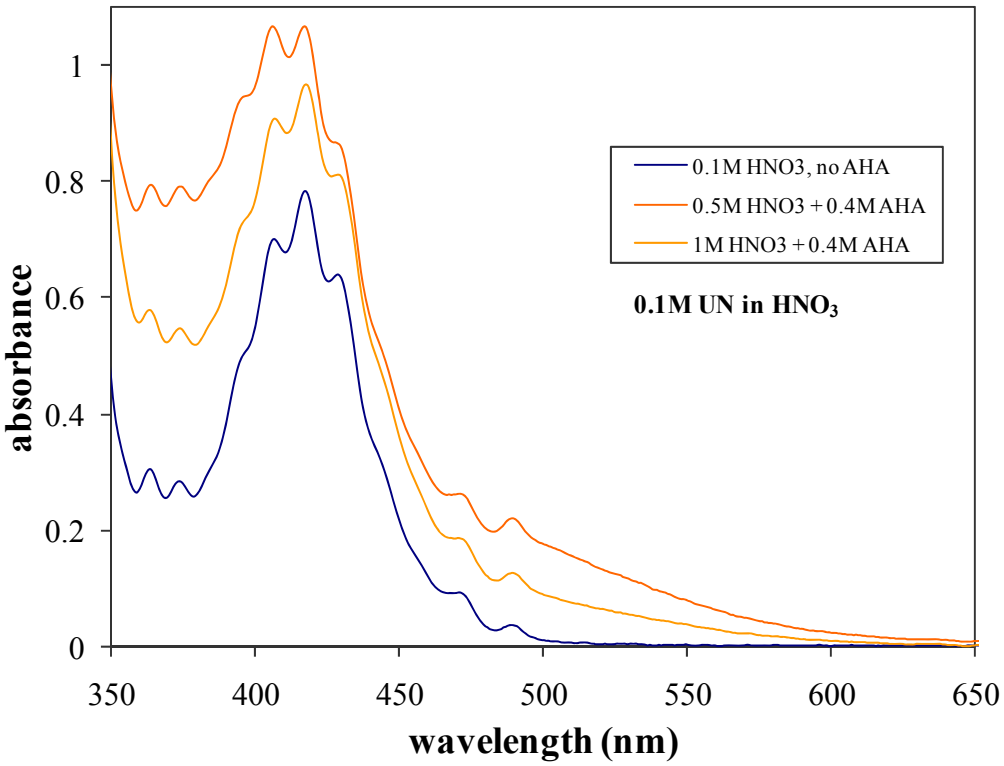

Figure 3.2 UV-VIS spectra of uranium(VI)-AHA complexes in aqueous solutions of nitric acid.

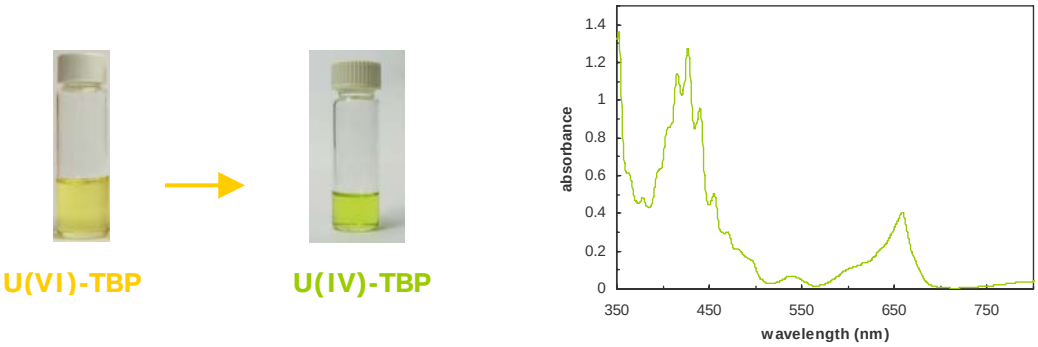

Figure 3.3 Oscilation oxidation-reduction reaction of U(VI) and U(IV) in TBP

Figure 3.4 Uranium solids containing acetohydroxamic acid produced at low nitric acid concentration

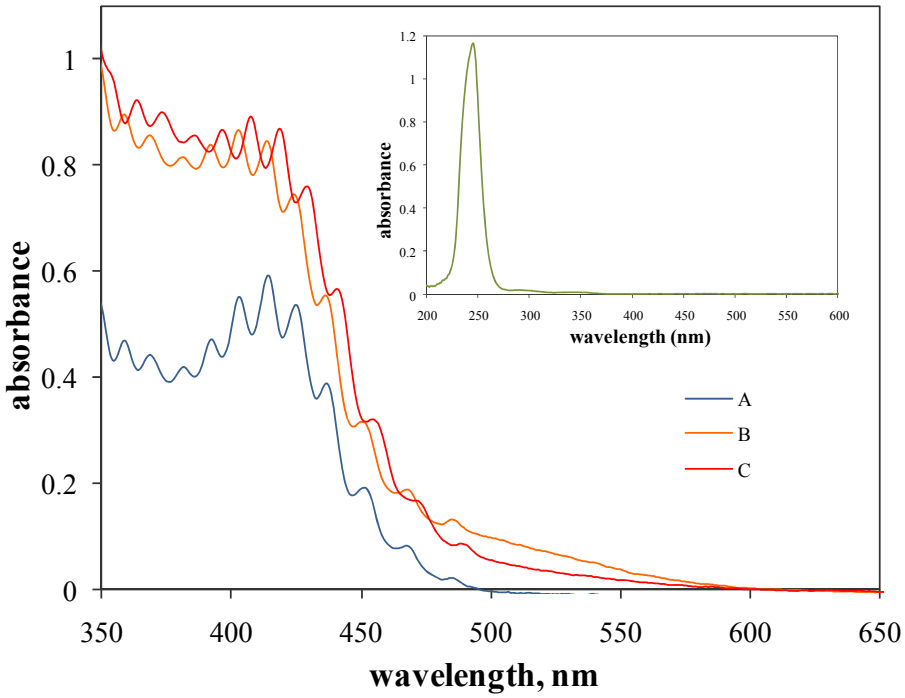

Figure 3.5 Spectra of uranium in organic phases: A: UN in TBP, B: UN-AHA -TBP complex prepared by combination of UN and AHA in TBP, C: Extraction organic phase agitated for several days. Initial concentrations in aqueous phase: 0.2 M UN; 0.1 M HNO_3 and 0.7 M AHA. Inset: Spectrum of AHA in 30% TBP/n-dodecane.

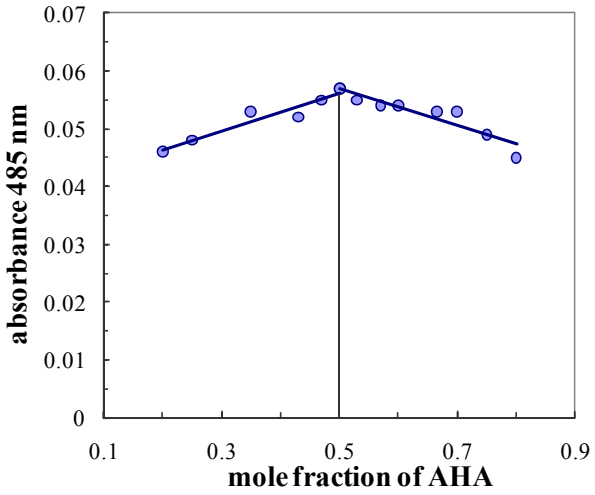

Figure 3.6 Absorbance of uranium-AHA complex in TBP at 485 nm as a function of molar fraction of acetohydroxamic acid.

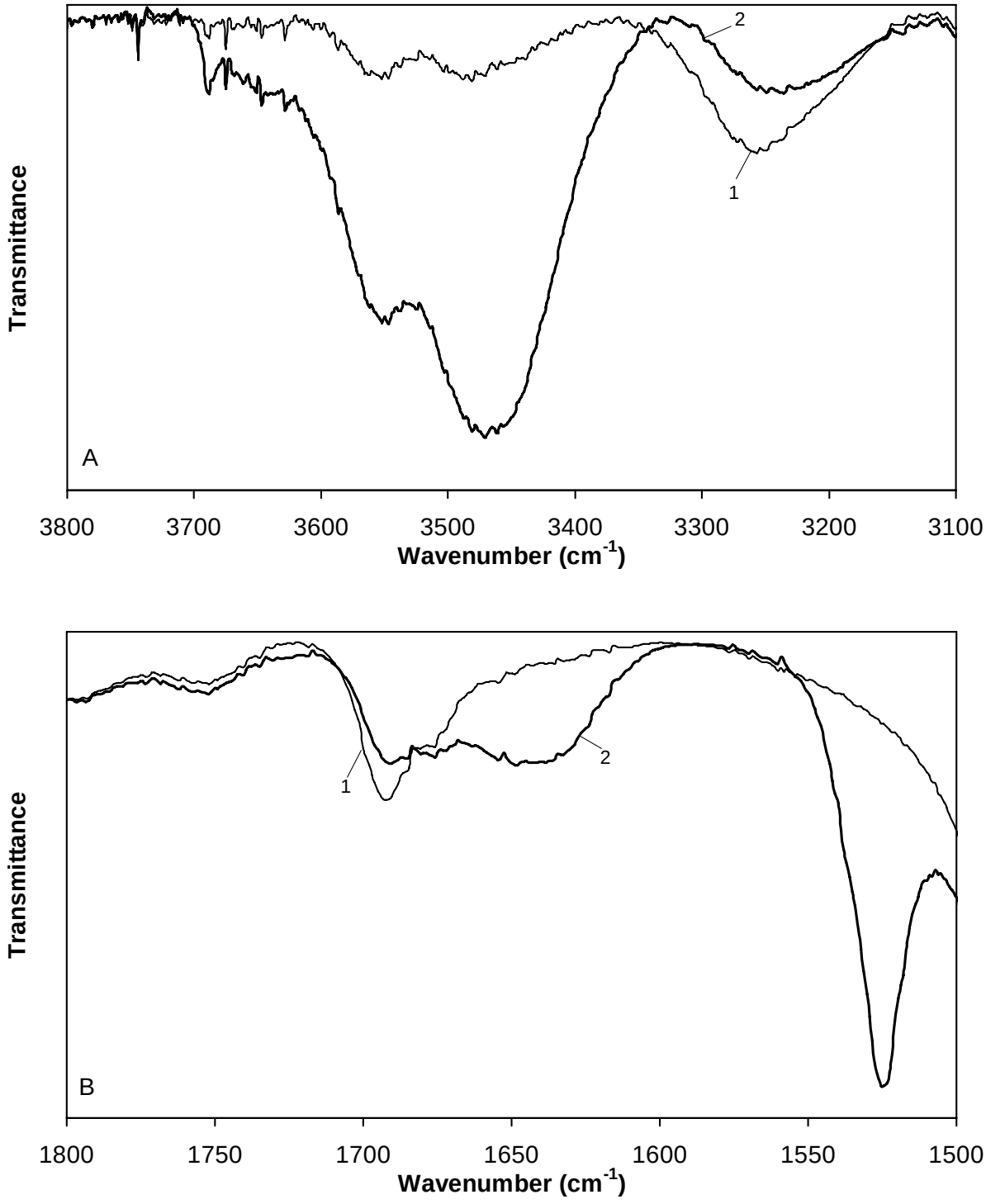

Figure 3.7 The FT-IR spectra of the 0.0675M AHA solution in TBP (spectrum 1) and the 0.0675M AHA and 0.045M $UO_2(NO_3)_2$ in TBP (spectrum 2): region of hydroxyl band of AHA (A); region of carbonyl band of AHA (B).

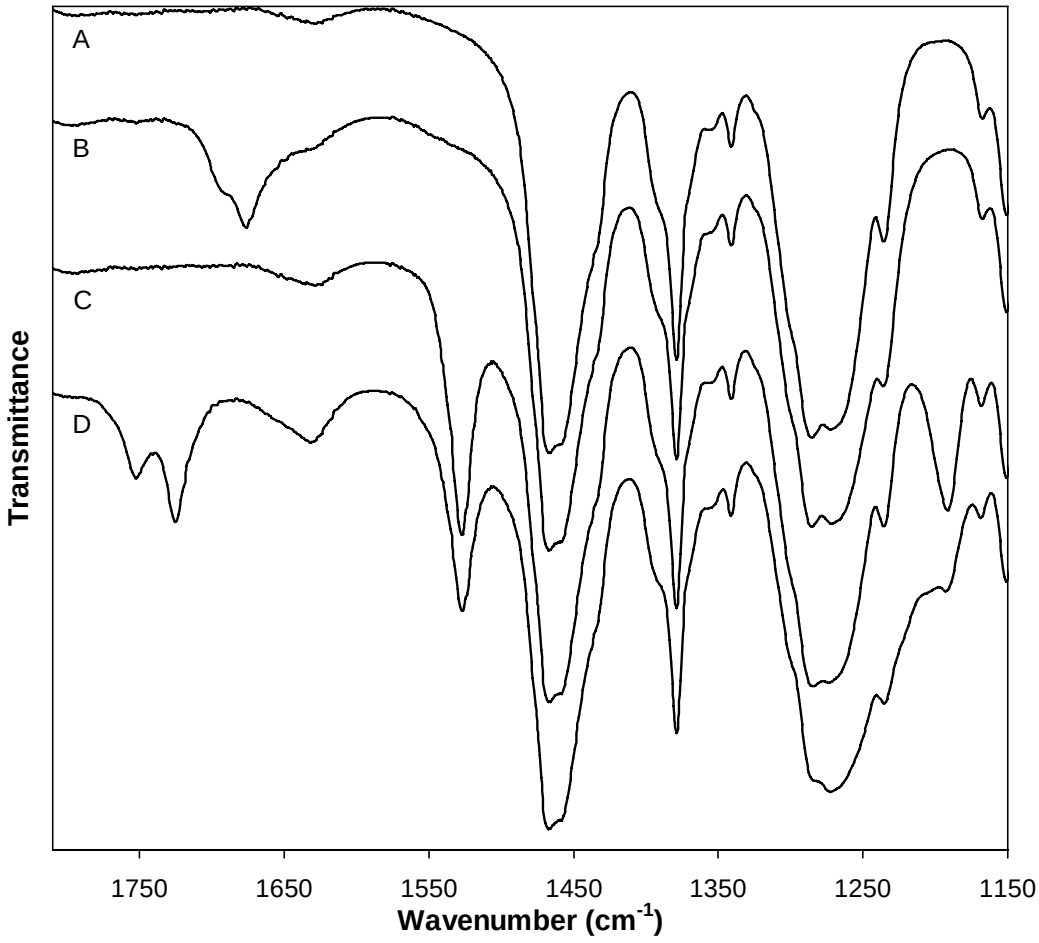

Figure 3.8 The FT-IR spectra of the organic extraction phase (D) of 30% TBP equilibrated with the $UO_2(NO_3)_2$/AHA/HNO_3 aqueous phase, compared with the spectra of 30% TBP (A); 0.1M AHA in 30%TBP (B); 0.045M $UO_2(NO_3)_2$ in 30% TBP (C).

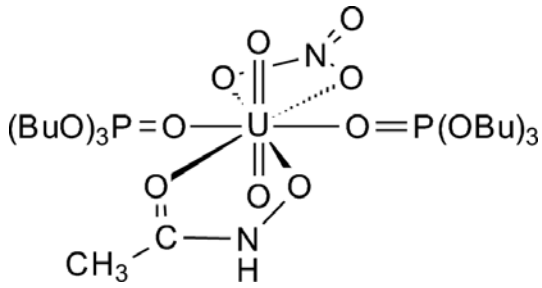

Figure 3.9 The proposed structure of the solvated complex of $UO_2(AHA)(NO_3).2TBP$

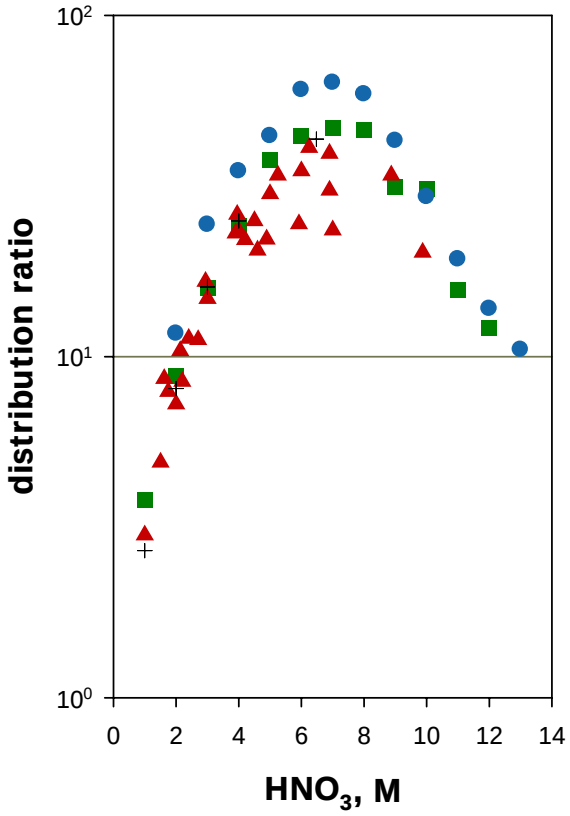

Figure 4.1 Distribution ratio of Pu(IV) from various range of nitric acid and $LiNO_3$: (■) 0.1-12M HNO_3; (●) 1M $LiNO_3$ and 0.1-12M HNO_3; (▲) data from ref. [Petrich & Kolarik, 1998]; (+) data from ref [Karraker 2002].

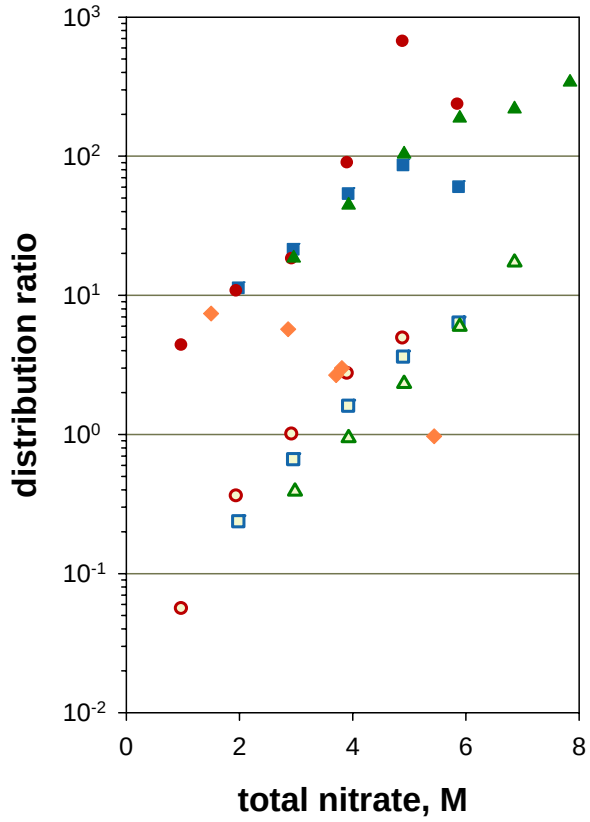

Figure 4.2 Distribution ratio of Pu(IV) from HNO_3 and various addition of nitrate in the absence (open symbols) and presence (full symbols) of acetohydroxamic acid (0.4M) and addition of $LiNO_3$. HNO_3 concentration: (●○) 0.5M; (■□) 1M; (▲△) 2M; (◆) data from ref. [Karraker 2002], 0.5M HNO_3, addition of $NaNO_3$ and 0.3M HAHA

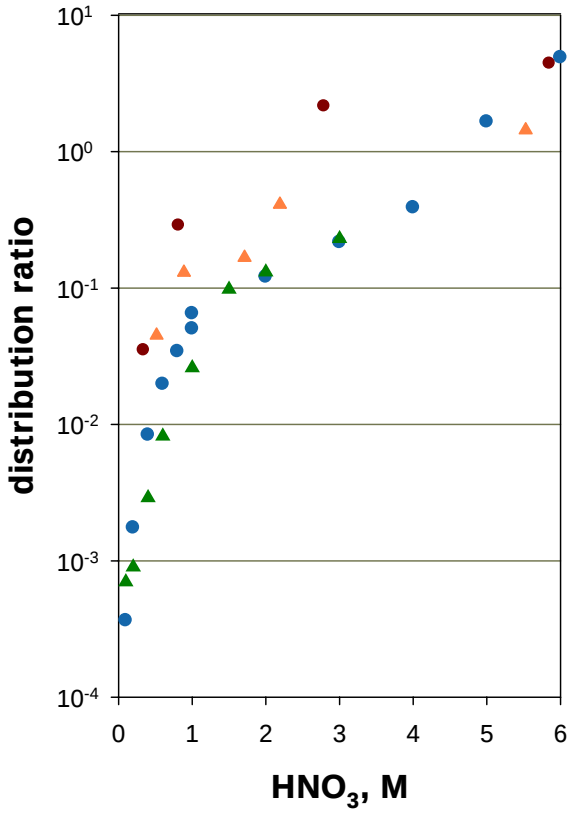

Figure 4.3 Distribution ratio of Pu(IV) from various range of nitric acid in the presence of HAHA (●) 0.1-6M HNO_3 + 0.4M HAHA; (▲) data from ref. [Carrott et al., 2007], 0.5M HAHA; (●) data from ref. [Karraker 2002] 0.1M HAHA; (▲) data from ref. [Karraker 2002], 0.3M HAHA.

.

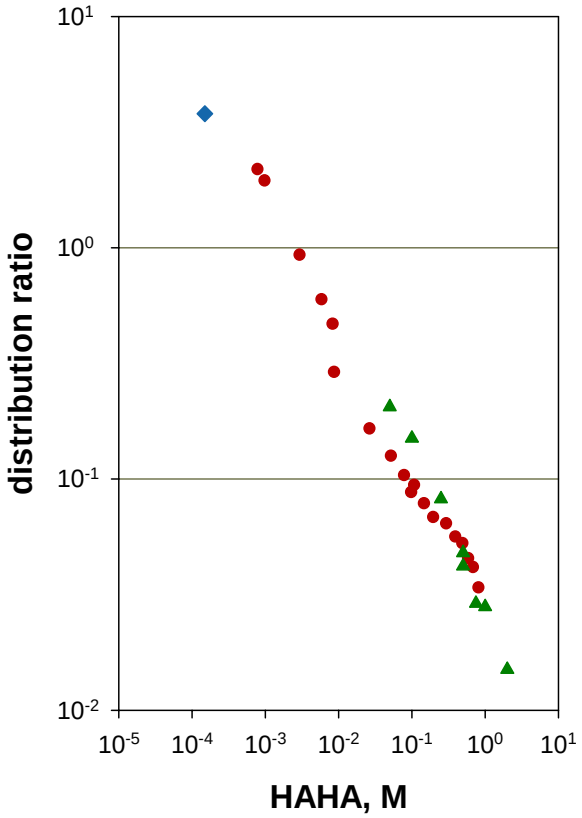

Figure 4.4 Distribution ratio of Pu(IV) from 1M HNO_3 and various concentration of acetohydroxamic acid: (●) $8x10^{-4}$ - $8.8x10^{-1}$ M HAHA; (▲) data from ref. [Carrott et al., 2007], 0.05-2M HAHA;(◆) no AHA.

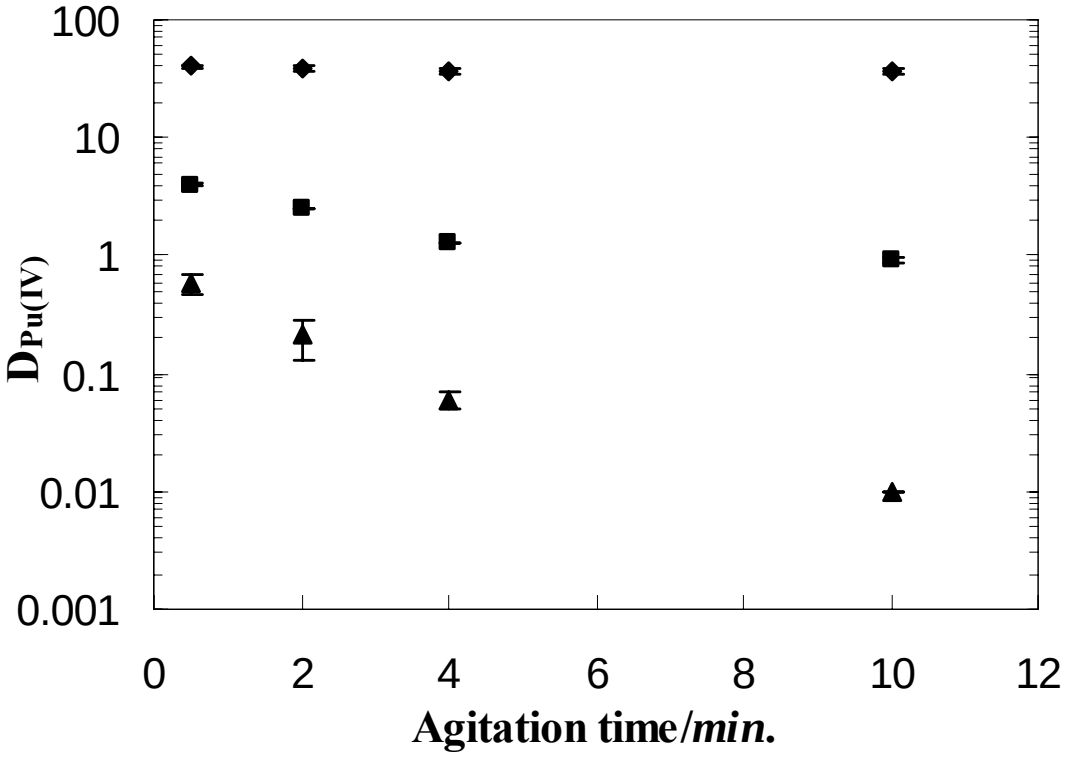

Figure 4.5 The effect of agitation on the distribution of plutonium at 294 K: (♦) 7*M* HNO_3; (■) 1*M* HNO_3; (▲) 0.1*M* HNO_3.

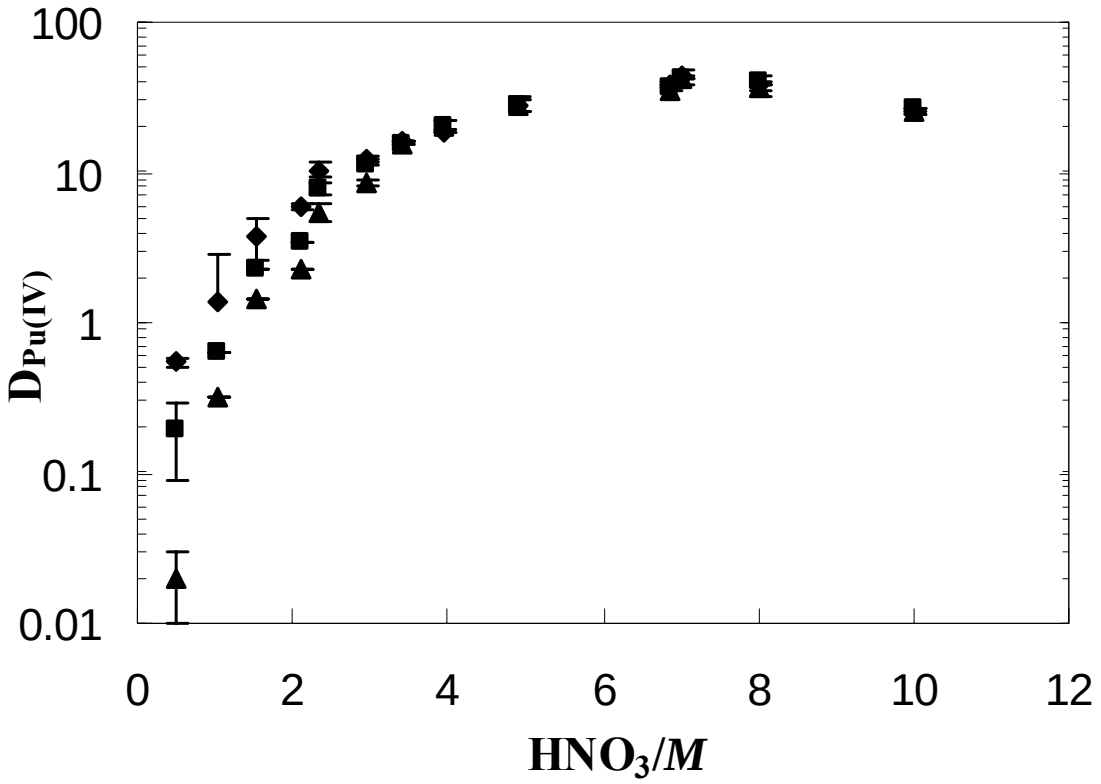

Figure 4.6 The distribution of plutonium at various temperatures for a system containing nitric acid: T = (♦) 294 K; (■) 303 K; (▲) 313 K.

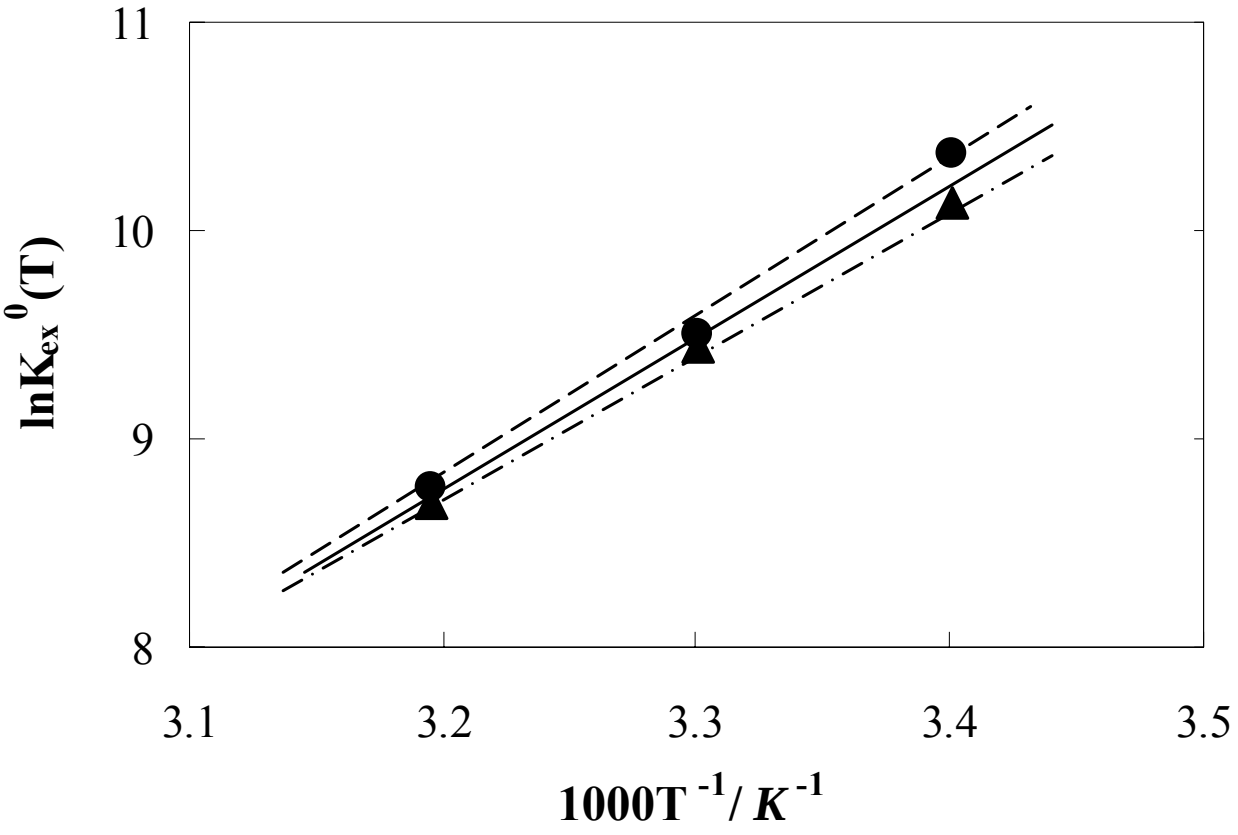

Figure 4.7 Van't Hoff plots for systems containing (▲) nitric acid: slope = 6.99, y-intercept = -13.6; (●) 2*M* HNO3 + LiNO3: slope = 7.56, y-intercept = -15.4; (line) average linear regression.

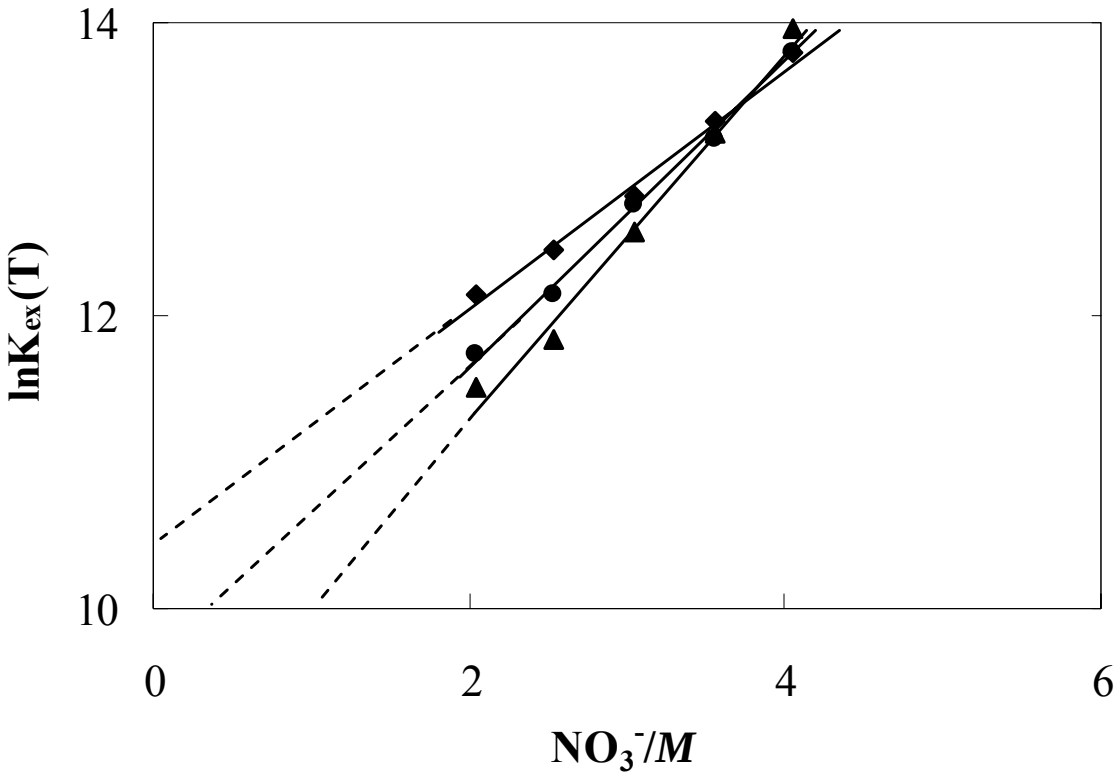

Figure 4.8 The equilibrium constants at various temperatures calculated by Eq. (11) for a system containing 2*M* HNO_3 and $LiNO_3$. Values for $\ln K_{ex}^{0}(T)$ were found at the extrapolated point $[NO_3^-] = 0M$. T = (♦) 294 K; (●) 303 K; (▲) 313 K.

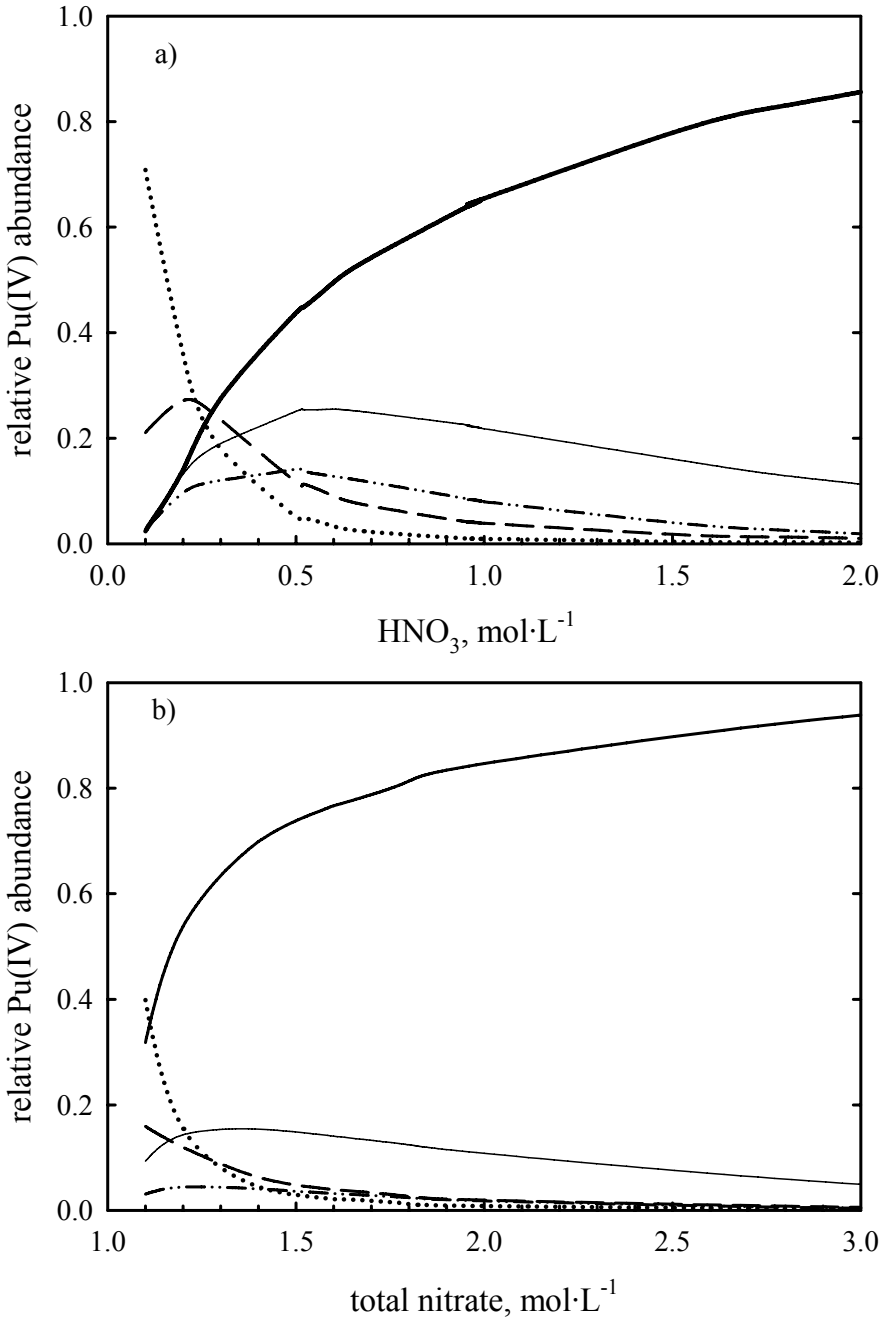

Figure 5.1 The speciation distribution diagram of Pu(IV) in aqueous solution containing: a) (0.1 to 2) mol·L^{-1} HNO_3, b) 1 mol·L^{-1} $LiNO_3$ and various HNO_3 concentration. – ·· – Pu^{4+}; – – – $Pu(OH)^{3+}$; ····· $Pu(OH)_2^{2+}$; —— $Pu(NO_3)^{3+}$; ═══ $Pu(NO_3)_2^{2+}$.

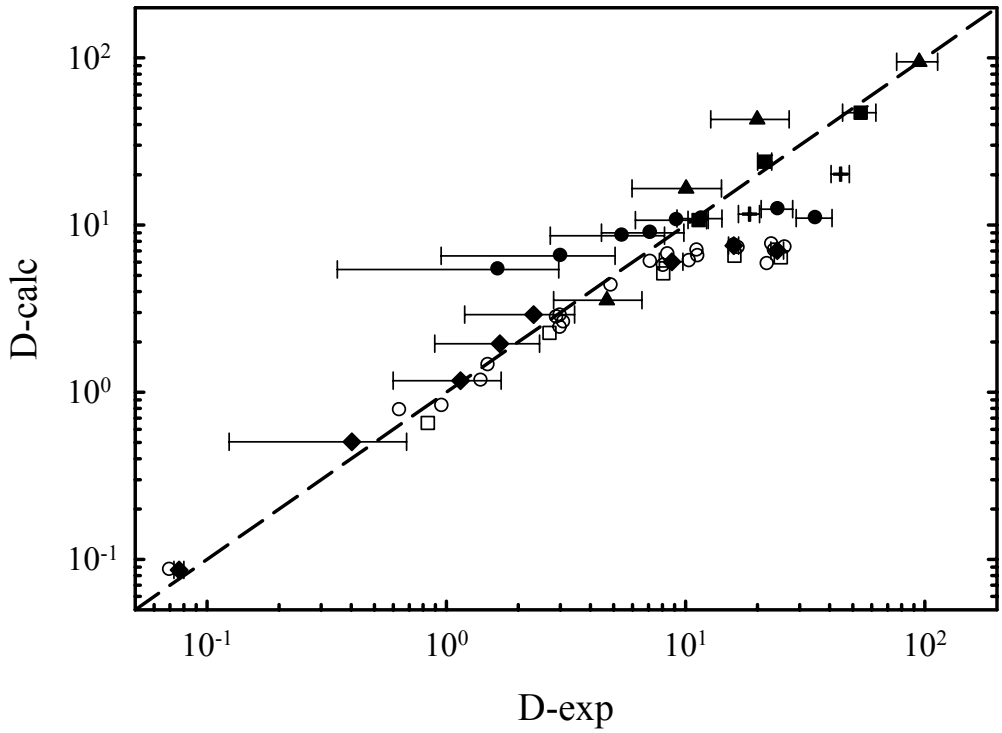

Figure 5.2 Plot of experimental vs. calculated data for Pu(IV) distribution ratio determined using Equation 13 and a value of $K_1=1.77\times10^5$. The line represents theoretical correlation between experimental and calculated data. (◆) 0.2 to 4 mol·L^{-1} HNO_3; (▲) 0.5 mol·L^{-1} HNO_3, various $LiNO_3$; (■) 1 mol·L^{-1} HNO_3, various $LiNO_3$; (+) 2 mol·L^{-1} HNO_3, various $LiNO_3$; (●) 1 mol·L^{-1} $LiNO_3$, various HNO_3; (○) 0.2 to 4.2 mol·L^{-1} HNO_3, [Petrich & Kolarik, 1981]; (□) 0.5 to 4 mol·L^{-1} HNO_3, [Karraker, 2001].

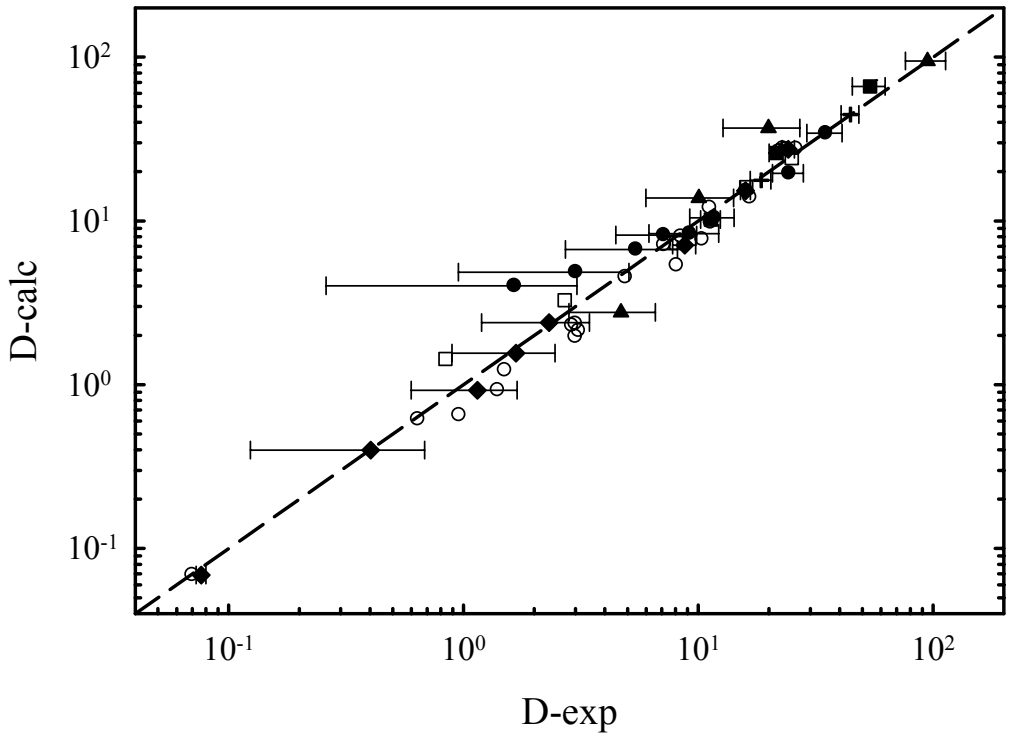

Figure 5.3 Plot of experimental vs. calculated data for Pu(IV) distribution ratio determined using Equation 15 and values of $K_1=1.06\times10^5$ and $K_2=2.12\times10^4$. The line represents theoretical correlation between experimental and calculated data. (◆) 0.2 to 4 mol·L^{-1} HNO_3; (▲) 0.5 mol·L^{-1} HNO_3, various $LiNO_3$; (■) 1 mol·L^{-1} HNO_3, various $LiNO_3$; (+) 2 mol·L^{-1} HNO_3, various $LiNO_3$; (●) 1 mol·L^{-1} $LiNO_3$, various HNO_3; (○) 0.2 to 4.2 mol·L^{-1} HNO_3, [Petrich & Kolarik, 1981]; (□) 0.5 to 4 mol·L^{-1} HNO_3, [Karraker, 2001].

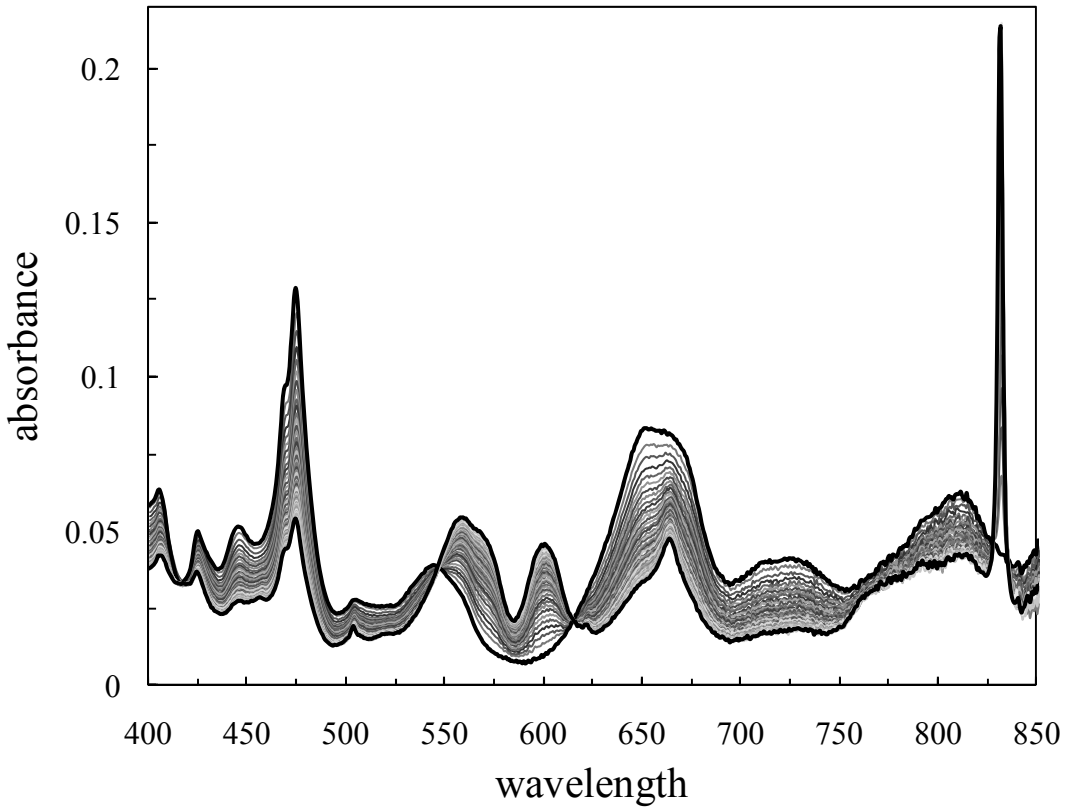

Figure 6.1 ViS-NIR spectra showing the disproportionation of Pu(IV) (2.64×10^{-3} M) in 0.1 M HNO_3 within 4 hours in 5 minutes intervals. Initial spectrum of Pu(IV) (top line, peak maximum at ~ 475 nm) changes continuously with formation of Pu(III) (~ 558 and ~ 600 nm), and Pu(VI) (~ 830 nm).

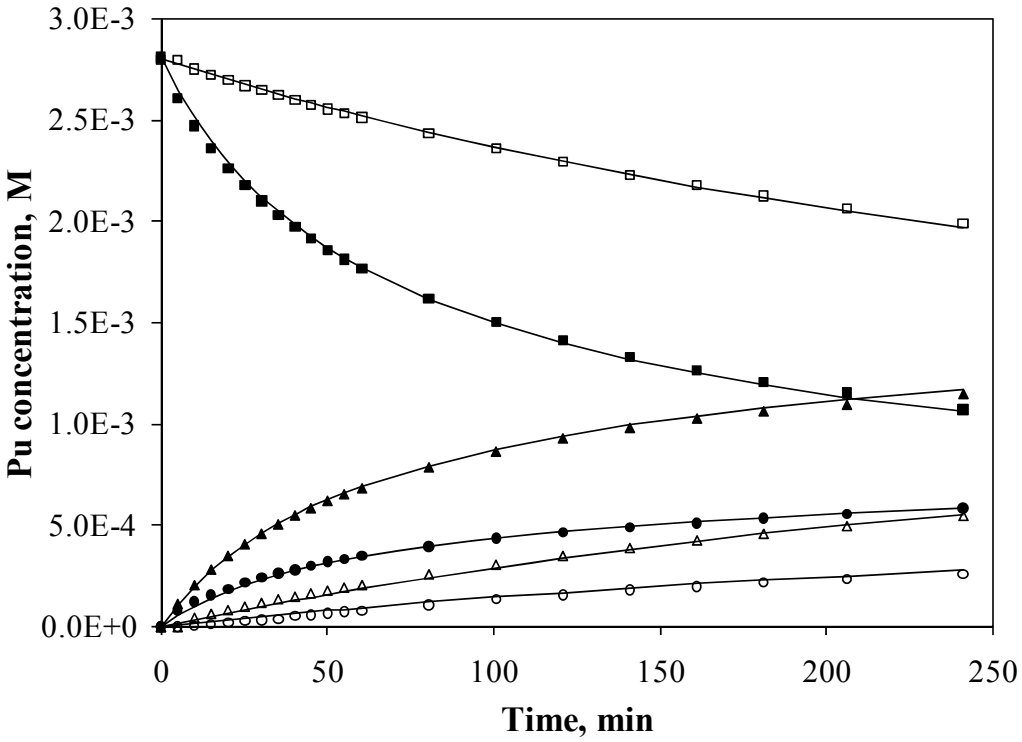

Figure 6.2 Experimental (symbols) and calculated (lines) concentration profiles of Pu species occurring by disproportionation reaction of Pu(IV). The calculated data were obtained by fitting the experimental results with third order reaction kinetics. 0.1 M HNO_3 – full symbols; 0.2 M HNO_3 – open symbols. Pu(IV) – squares; Pu(III) – triangles; Pu(VI) – circles. Initial conditions: 2.8×10^{-3} M Pu(IV), T=22°C. The calculated concentrations were obtained using k'=529 and k'=85 $mol^{-2}\cdot L^{2}\cdot min^{-1}$ for 0.1 and 0.2 M HNO_3, respectively.

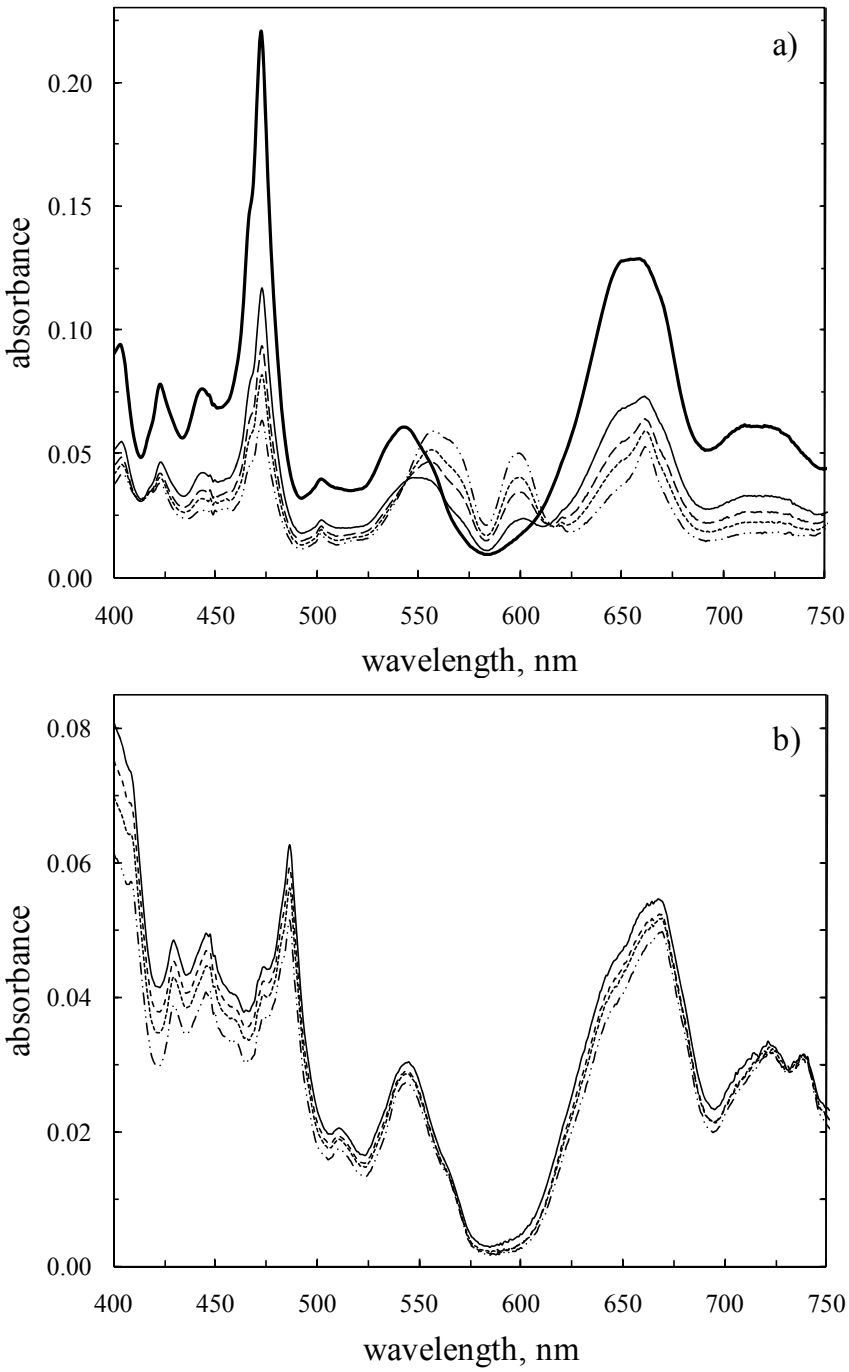

Figure 6.3 Comparison of ViS-NIR spectra of Pu in: (a) 0.1 M HNO_3, and (b) TBP after extraction from 0.1 M HNO_3. ── freshly prepared Pu(IV) in 0.1 M HNO_3; and after: ── 2 min; - - - 5 min; ···· 10 min; – ·· – 20 min extraction.

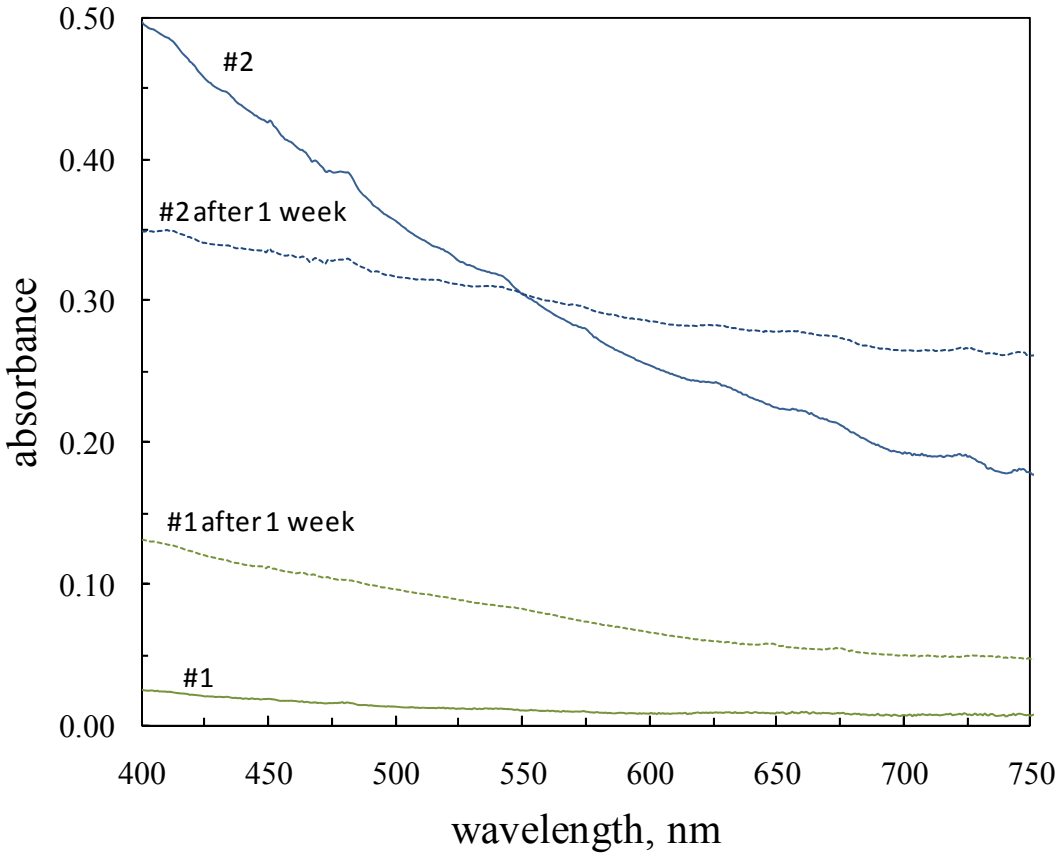

Figure 6.4 Comparison of Vis-NIR spectra of 2 samples of colloidal Pu in TBP taken shortly after the extraction from 0.1 M HNO_3, and after a one week with no contact with the aqueous phase

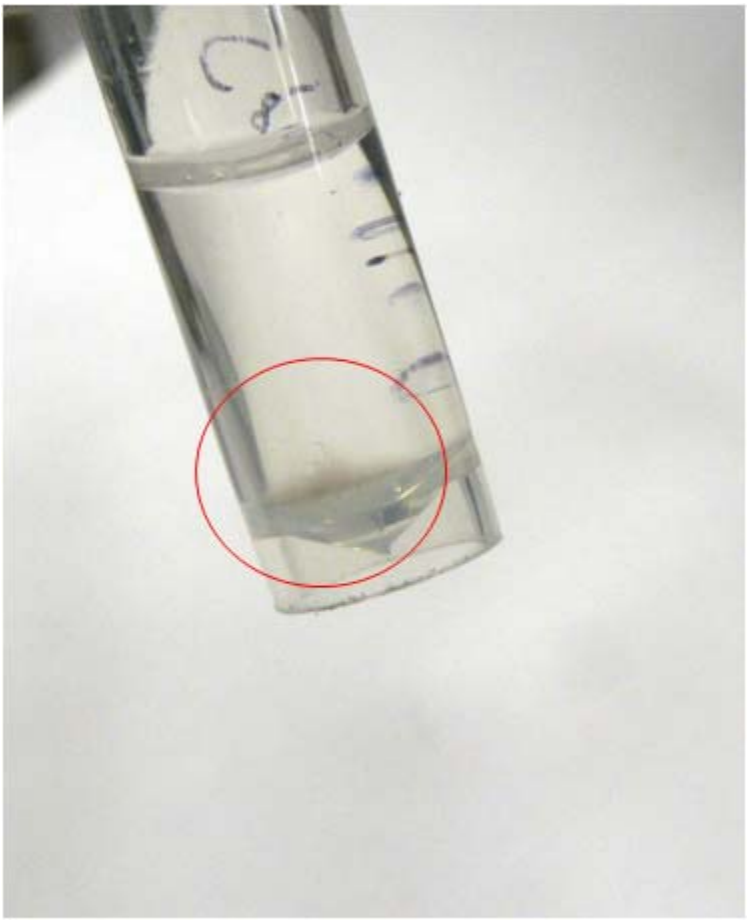

Figure 6.5 Picture of Pu colloid in TBP formed after extraction from 0.1 M HNO_3 and centrifugation of the organic phase.

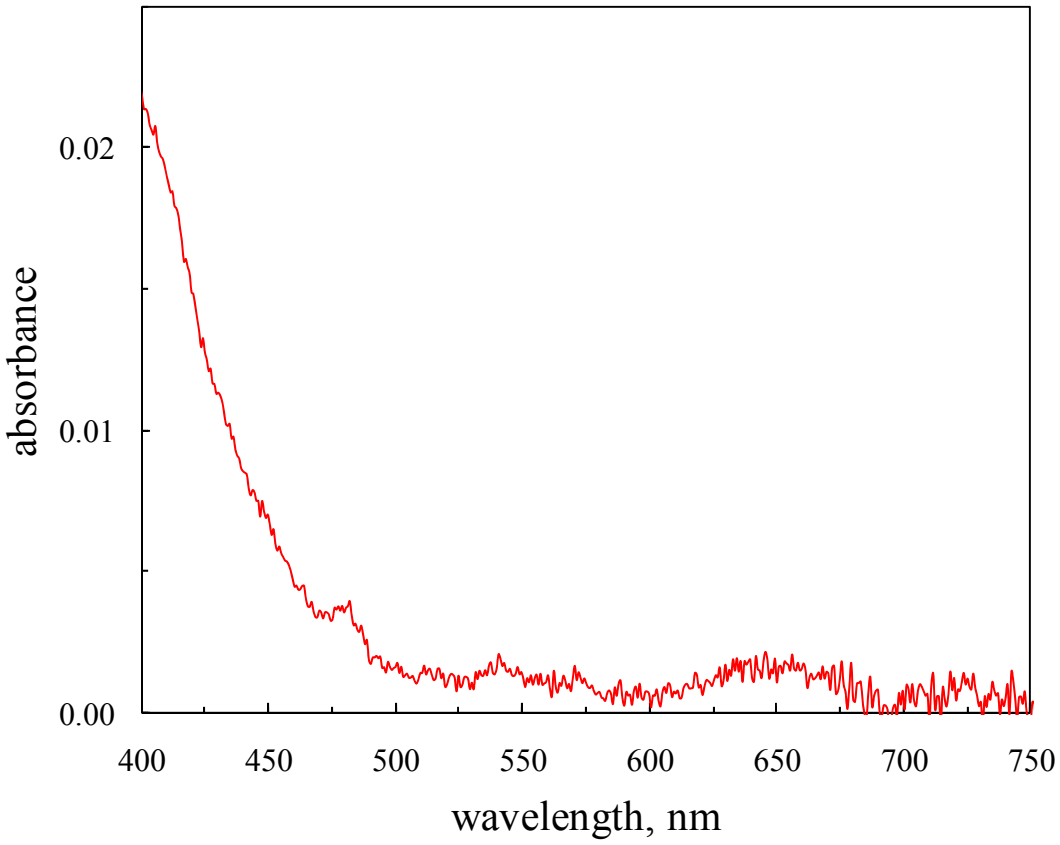

Figure 6.6 Vis-NIR spectrum of dissolved Pu colloid in TBP after centrifugation at 17 500 rpm for 10 minutes.

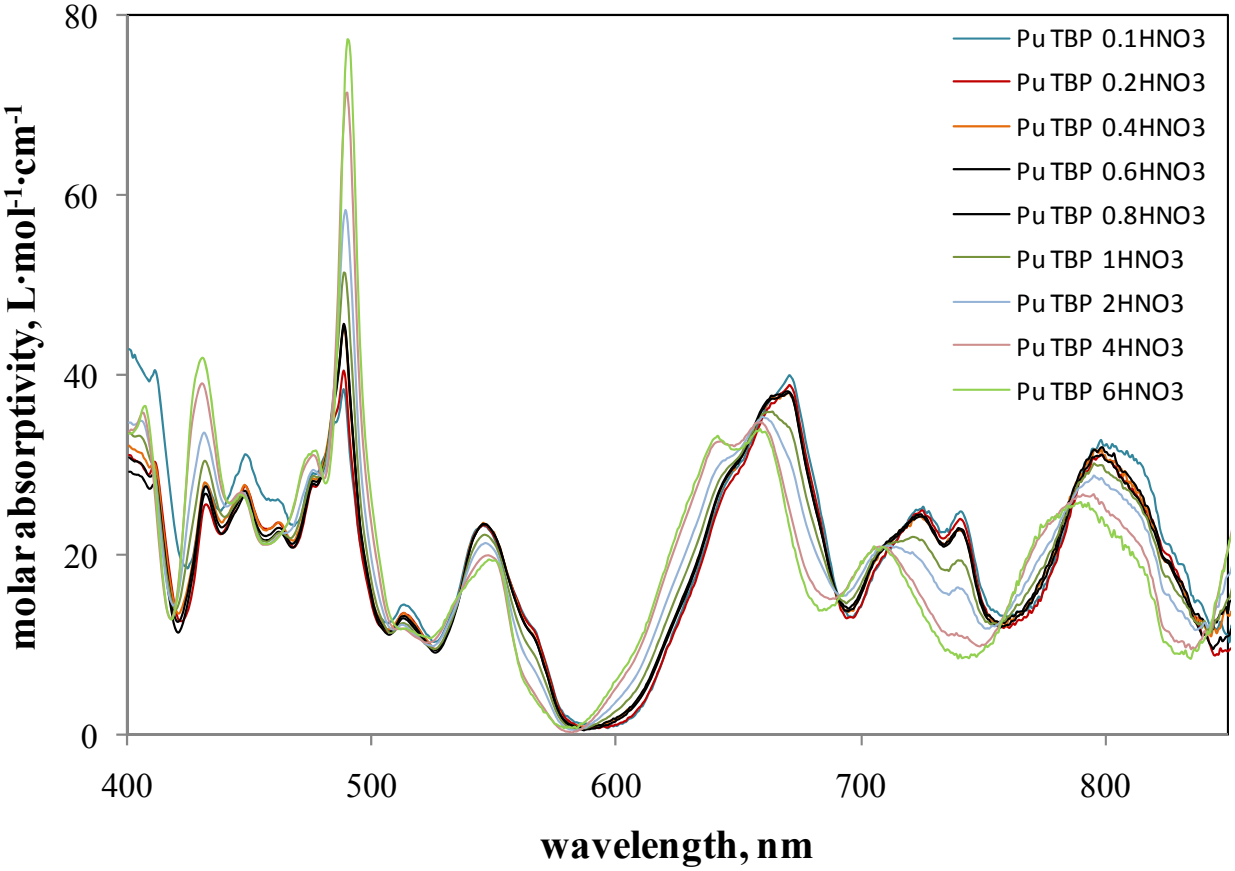

Figure 6.7 Vis-NIR spectrum of Pu(IV) in TBP after extraction from 0.1-6 M HNO_3.

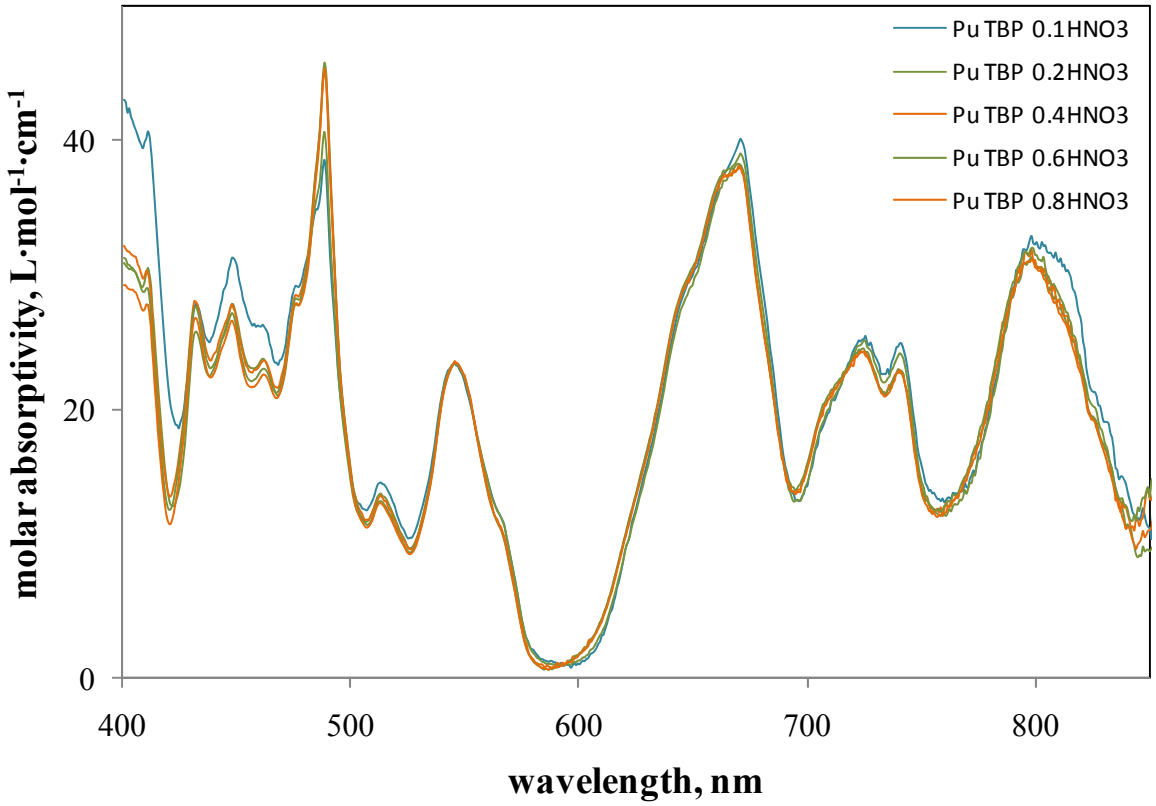

Figure 6.8 Vis-NIR spectrum of Pu(IV) in TBP after extraction from 0.1-0.8 M HNO_3.

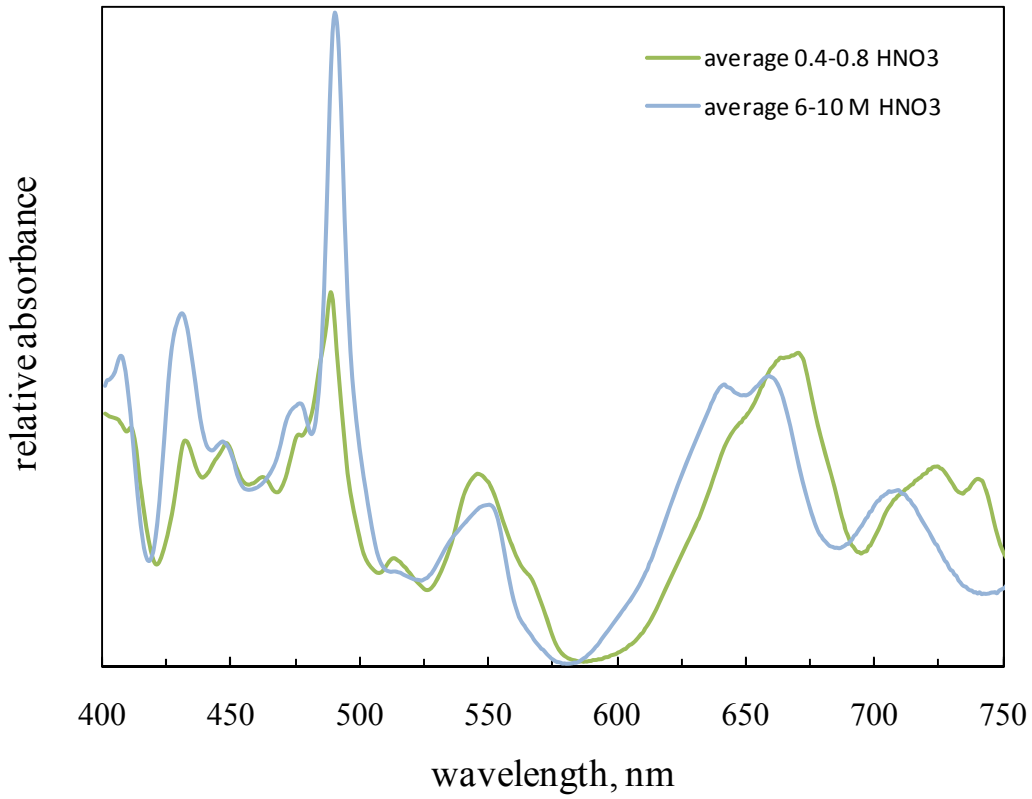

Figure 6.9 Comparison of averaged Vis-NIR spectra of Pu(IV) in 30 % TBP extracted from different regions of initial nitric acid concentration.

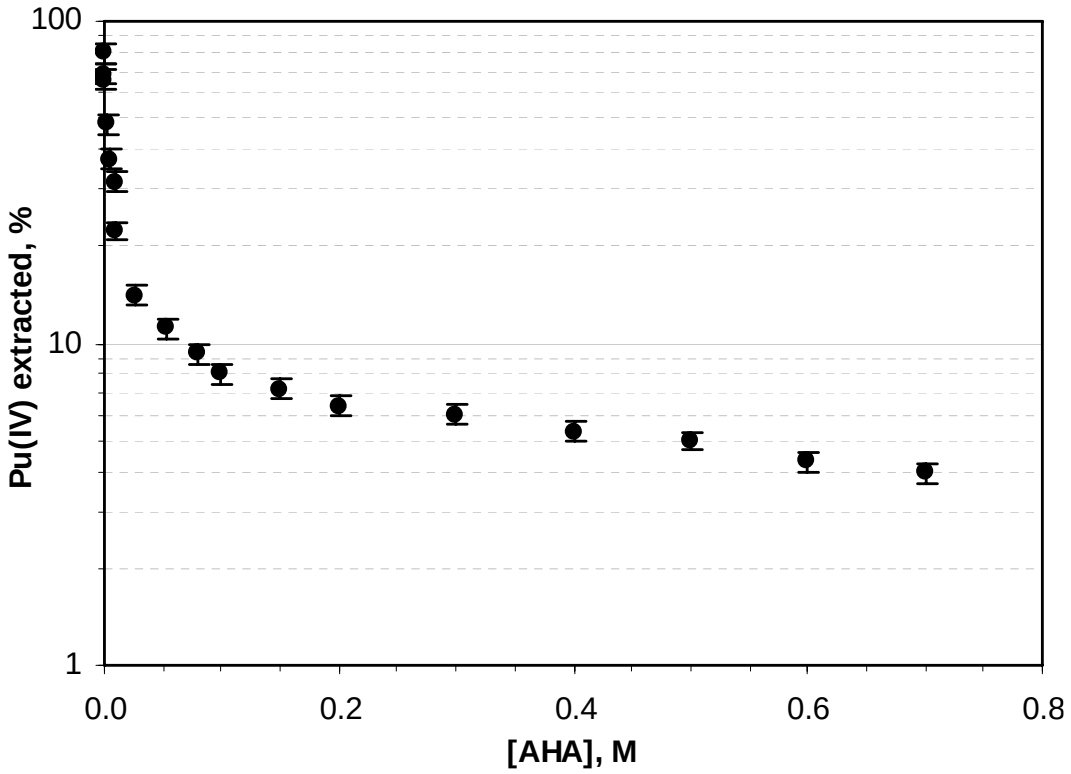

Figure 7.1 Dependence of extraction yield of Pu(IV) by 30% TBP from 1M HNO_3 on concentration of AHA.

Figure 7.2 Characteristic brownish-red color of Pu(IV)-AHA complex suggest its presence in TBP after extraction of Pu(IV) from HNO_3 in the presence of AHA.

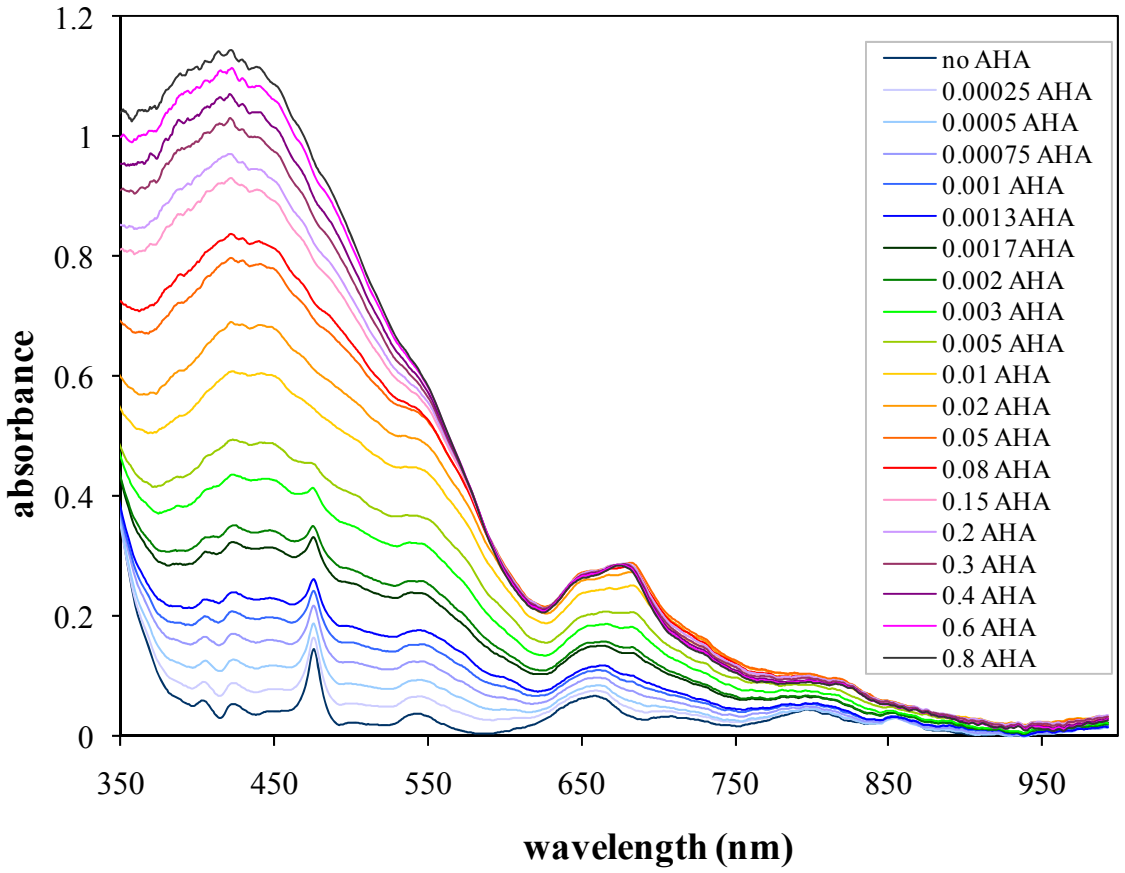

Figure 7.3 Changes in the Vis-NIR spectra of Pu(IV) due to formation of Pu-acetohydroxamate complexes in 1M HNO_3. Pu(IV) concentration: 1.87×10^{-3} M.

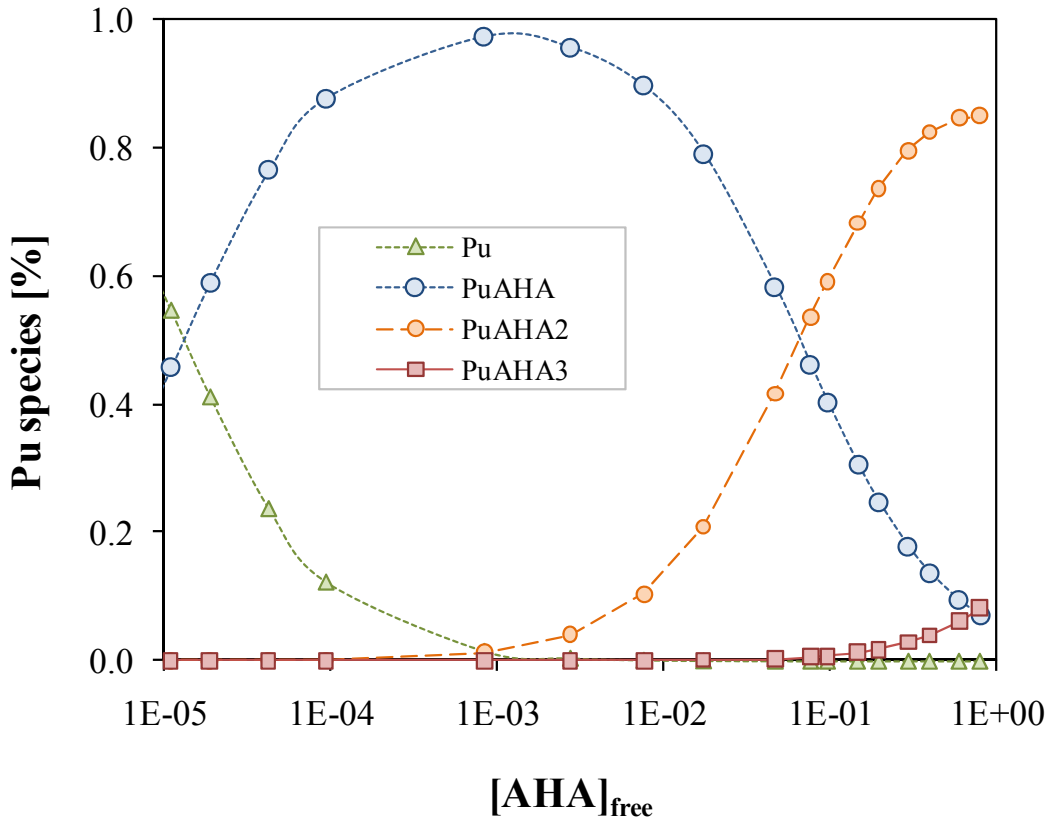

Figure 7.4 Speciation diagram for Pu(IV)–AHA system calculated for total [Pu(IV)]=2.26x10^{-3}M, 1M HNO_3 and various concentration of AHA ($[AHA]_{free}$ denotes AHA non-complexed with Pu).

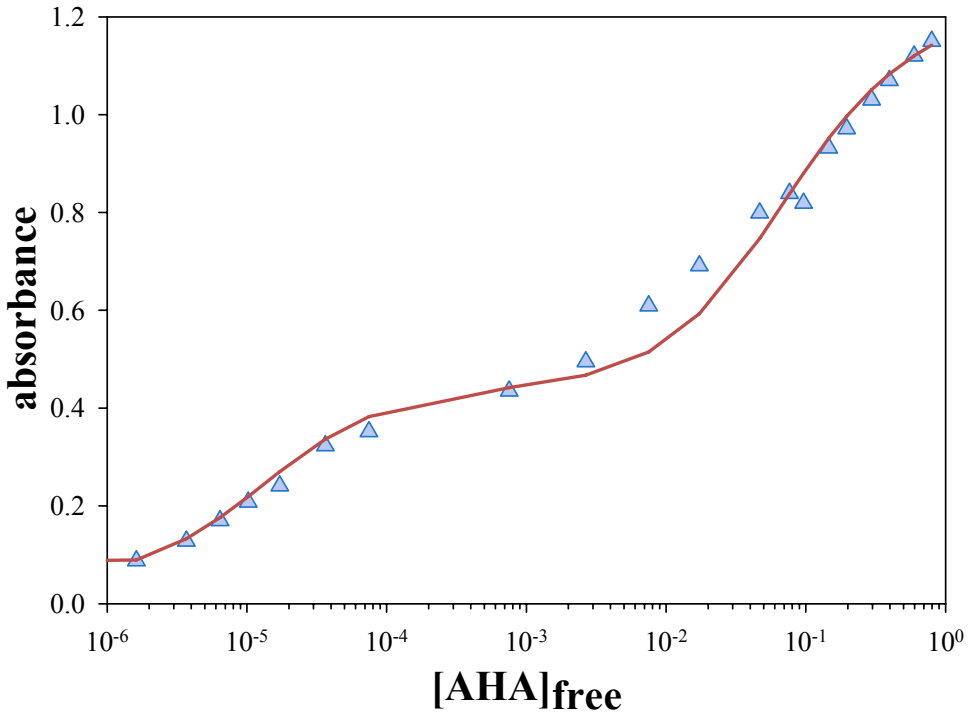

Figure 7.5 Experimental and calculated absorbance of aqueous solution of Pu(IV) at λ=423 nm as a function of free concentration of AHA (non-complexed with Pu); experimental data (▲), calculated data (line)

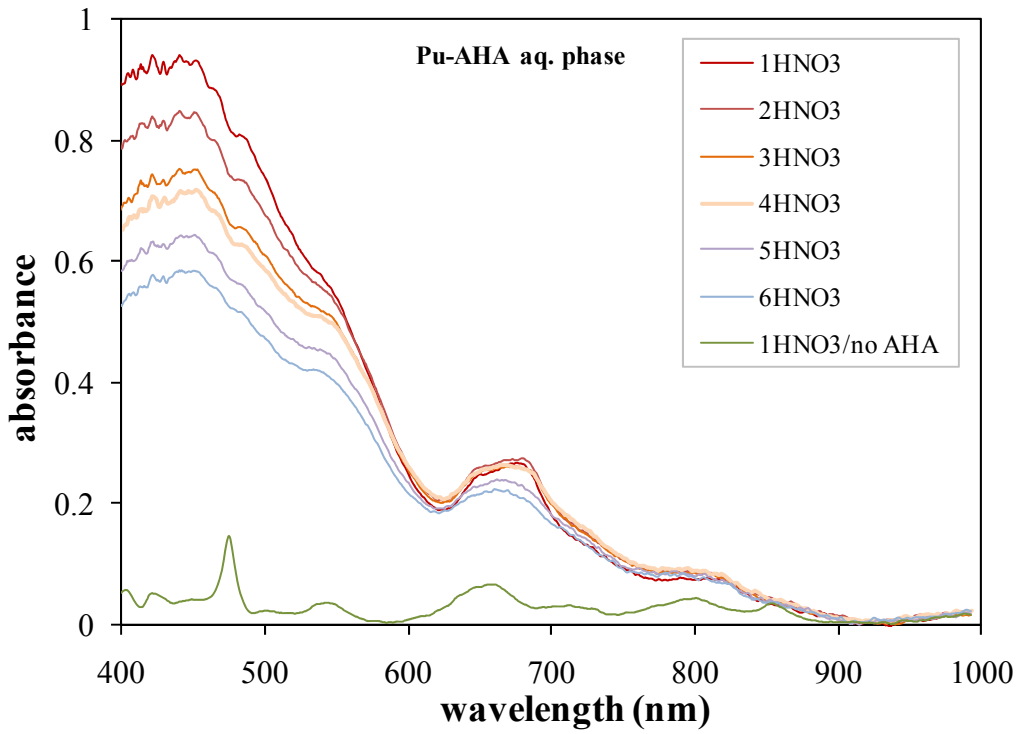

Figure 7.6 Absorption spectra of Pu(IV)-acetohydroxamate complexes for 1 (spectrum on the top); 2; 3; 4; 5; and 6M HNO_3 (spectrum on the bottom) and 0.4M initial concentration of AHA. Spectrum on very bottom belongs to Pu(IV) in 1M HNO_3 without presence of AHA.

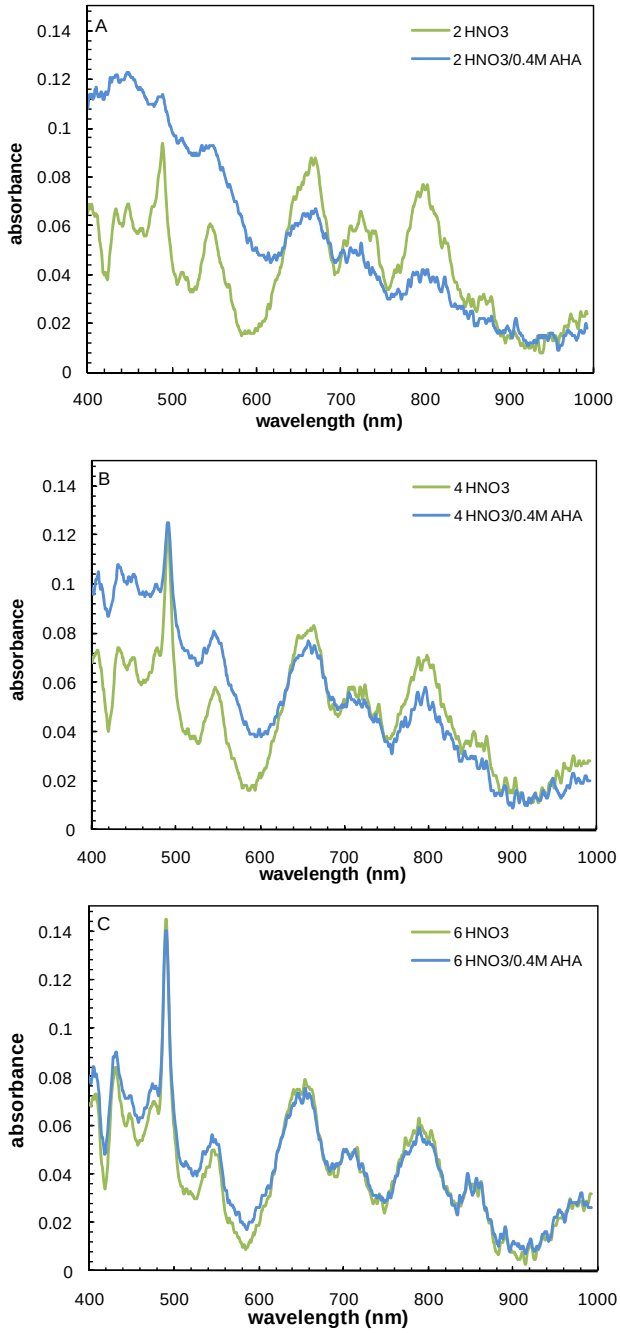

Figure 7.7 Absorption spectra of Pu(IV) in 30% TBP after extraction from aqueous phase containing: A) 2M HNO_3; B) 4M HNO_3; C) 6M HNO_3 in the absence and presence of 0.4 M AHA.

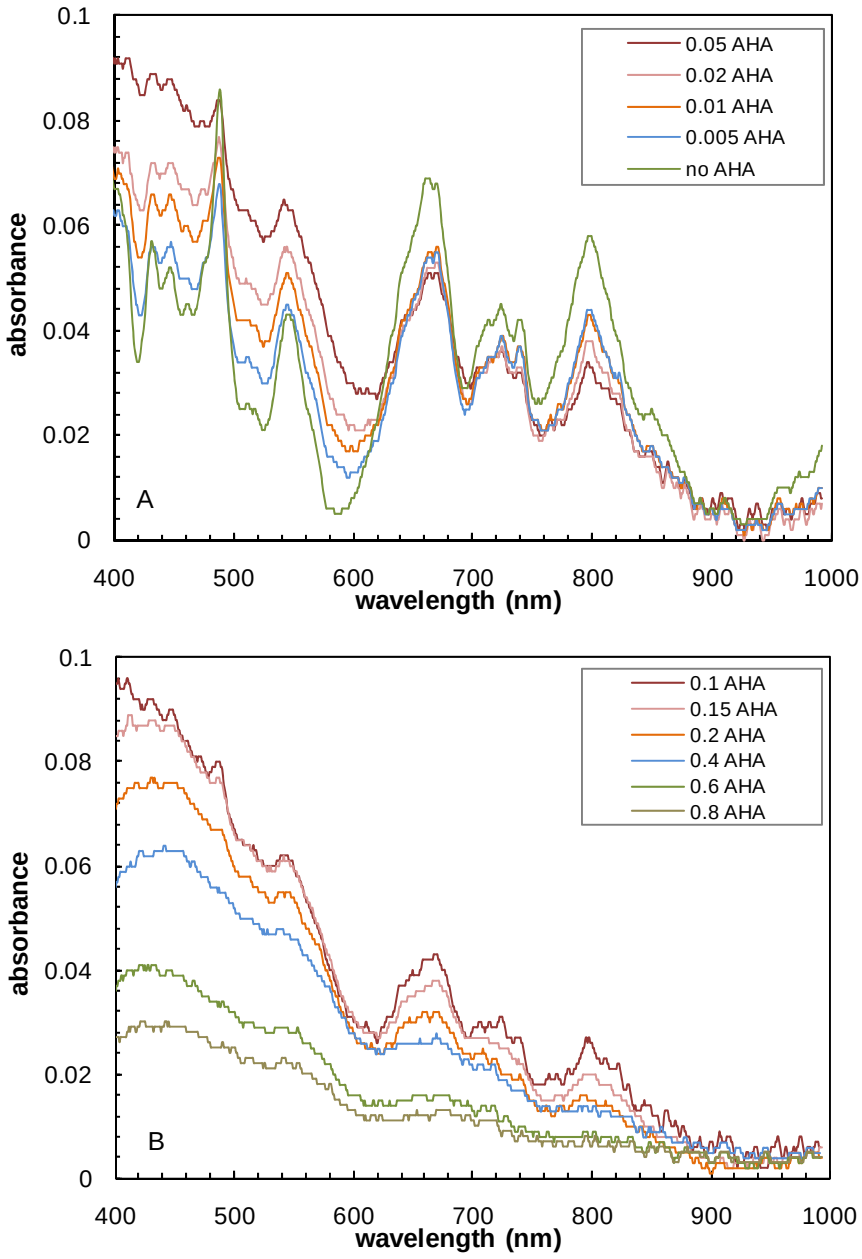

Figure 7.8 Absorption spectra of Pu(IV) in 30% TBP after extraction from aqueous phase containing 1M HNO_3 and various concentration of AHA